

博士論文

Grasping-Type Haptic Devices to Expand Visual Media

(映像メディアを拡張する把持型触覚デバイス)

半田 拓也

Abstract

In this thesis, we propose two methods for adding haptic information to visual media provided by broadcasting and communications and providing universal information services that anyone can use. We first propose a method for conveying the shape, size, and the differences of partial hardness/softness of a three-dimensional object. We then propose a method for directly converting the timing, magnitude, and direction of impact between moving objects into haptic stimulation. These two methods are not only useful for visually impaired individuals but can also be applied to improving realism through virtual reality technology.

To evaluate the effectiveness of our first haptic presentation method, we investigated the fundamental characteristics of human haptic sensation, conducted basic design, prototyping, and preliminary evaluation. We then developed a grasping-type haptic device based on the requirements from the preliminary findings. This device presents four haptic stimuli on a finger pad of the index finger, two points on the palm, and one point on the thumb. As the results of user studies, the difference in the side surfaces of the 3D shapes could be identified, and the effectiveness of the haptic presentation method was clarified.

The hardness of an object is detected through the index finger and thumb when holding our haptic device by controlling the actuator based on the spring constant that is considered to reflect the hardness (elasticity) of the target object. We developed a pulse width modulation control method for the actuator output in accordance with the hardness data set for each voxel of a computer graphics object. The results of an experiment comparing the difference between the hardness presented on the haptic device and that of a real spring suggests that the user can sufficiently distinguish the difference in relative hardness.

To evaluate the effectiveness of our second haptic presentation method, we developed a novel grasping-type haptic device that physically dents the surface of elastic ball grasped by user for directly transmitting the sense of the magnitude and direction of the impact on human haptic sensation. We clarified that this grasping-type device can present the direction of an impact more intuitively compared to vibration alone. In addition, the masking effect when simultaneously presenting concave and vibration stimuli to the palm was verified from the relationship with the spatial resolution of the haptic sense of the palm. Furthermore, the method for simultaneously presenting vibration and concave stimuli can be applied for explicitly presenting the target object. This greatly affects the sense of self-attribution, which is one of the issues when applying haptic stimuli to visual media.

Finally, we clarified some guidelines of haptic technology that contributes to the expansion of visual media to universal service.

Contents

Chapter 1	Introduction	1
1.1	Background	1
1.2	Nature of human haptic perception	3
1.3	Fundamental principle of haptic information conveyance.....	8
1.4	Our approach and goal of thesis.....	11
1.5	Organization of thesis	11
Chapter 2	Number of haptic stimulation points on finger pad necessary for recognizing 3D shapes	12
2.1	Potential of multipoint force feedback to finger pad	12
2.2	Multipoint force feedback system	14
2.3	Recognition of 3D geometry using multipoint force feedback to finger pad	16
2.4	Conclusion.....	20
Chapter 3	Grasping-type haptic device to present 3D shape and Hardness of virtual objects	21
3.1	Integration between multi-finger and multipoint haptic feedbacks	21
3.2	Potential of using internal forces to present virtual surface	27
3.3	Development of a grasping-type haptic device “GraspForm”	31
3.4	Conclusion	42
Chapter 4	Grasping-type haptic devices to present impact sensation between moving objects	43
4.1	Method to present direction of impact force applied to an object	43
4.2	Grasping-type haptic device to present impact points with vibrations.....	47
4.3	Method to evoke the sense of self-attribution in visual content	57
4.4	Conclusion.....	61
Chapter 5	Applications and feedback from field tests	62
5.1	Haptic display system to transmit shape and hardness of remote object	62
5.2	Haptic interface system for physically experiencing sports games	64

Chapter 6 Conclusion	74
6.1 Summary of results	74
6.2 Design guidelines of haptic devices to expand visual media.....	75
6.3 Conclusion and future perspective.....	76
Acknowledgement	77
Bibliography.....	78
Publications	82
Appendix A.....	84
Appendix B.....	90

Chapter 1

Introduction

In this thesis, we propose two methods for adding haptic information to visual media through broadcasting and communications and providing universal information services that anyone can use. The aim with this research was to enable the presentation of information that can be recognized only by touching an object, such as rare animals and artwork, or transmitting vibrations and impact during sports games to the haptic sense of viewers to provide a sense of reality.

1.1 Background

1.1.1. Visual media

The visual image originated from the kinetograph and kinetoscope at the end of the 19th century, and the history of visual media is said to have started with the invention of the cinematograph [1]. When television broadcasting started in the 20th century, visual media developed and spread rapidly. Today, smartphones have become popular, and the number of visual contents distributed through broadcast and the Internet is immeasurable. In addition, media that handle images beyond the conventional screen view are becoming widespread with the progress of augmented reality (AR) and virtual reality (VR) technologies.

There are various video formats, and visual media have been broadly divided into passive mass media, represented by movies and television, and interactive media represented by video games. However, social networking services (SNS) and online multiplayer video games have recently become widespread, and it is difficult to simply distinguish between passive or interactive and multiplayer or personal experiences.

1.1.2. Haptic-information conveyance for visual media

Movie theaters and attractions where people can experience not only images and sounds but also haptic stimuli such as vibration and wind have become popular. In addition, three-dimensional (3D) TV and AR/VR, which are expected as next-generation media, are thought to further improve the user experience (UX) with haptic information. However, general-purpose input/output devices that can transmit various haptic information of objects, such as cameras and displays for visual information and microphones and speakers for auditory information, have not been put into practical use.

As shown in Fig. 1.1, when transmitting haptic information of a real object, such as artwork to a remote person, it is necessary to sense the haptic information of the real world then transmit and reproduce it on the user side. The reproduced object is called a virtual object for the reason that it is virtually identical to that perceived by humans and feels genuine. Haptic sensations are interactive sensations between the surface of an object and the cutaneous surface of a human. Therefore, it is necessary to simulate transformation of the object due to human touch when presenting a virtual object.

In a one-to-one (1:1) relationship between a target object and user, a robot arm equipped with a haptic sensor can be operated from a remote location through a haptic device attached to the operator's hand. This concept is called tele-existence [2], which can convey the response of the object to the operator as reaction forces and vibrations. The practical possibility of tele-existence is increasing due to the rapid progress in ultra-low-latency communication technology such as fifth-generation (5G) mobile communication. However, it is difficult to apply this method to one-to-many (1:N)-type mass media such as broadcasting.

The following research problems arise assuming 1:N broadcasting/communication services that transmit haptic information of an object to many users simultaneously: 1) measuring the physical characteristics of the target object, 2) modeling and simulation, 3) transmitting, and 4) representing haptic information according to the user's environment.

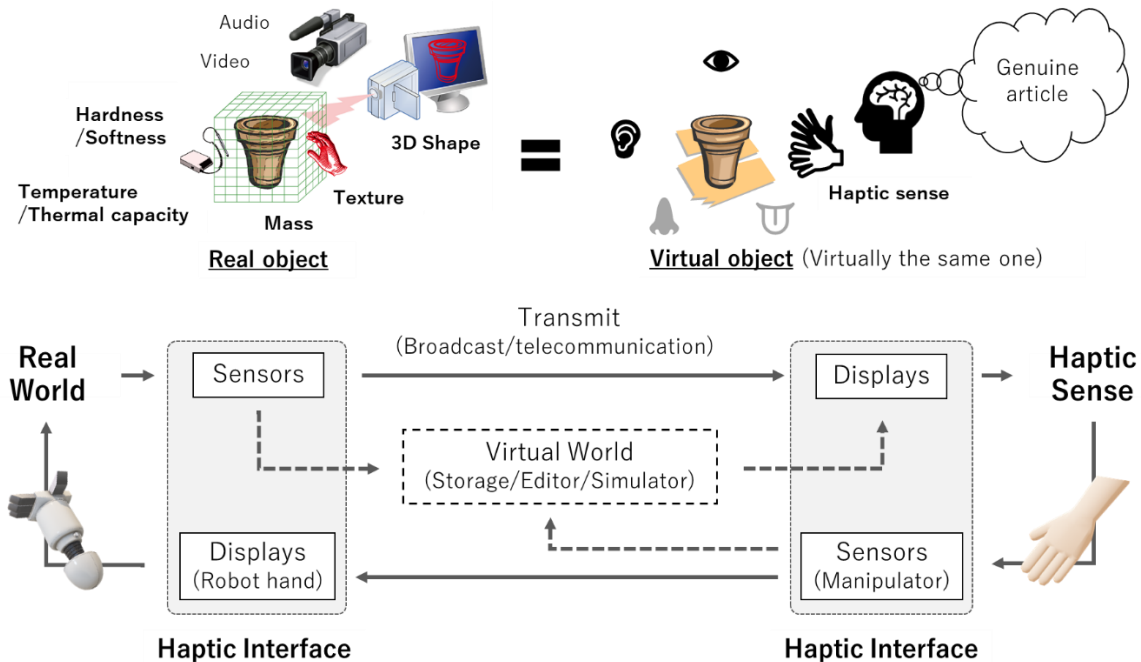


Fig. 1.1. Concept of haptic-information conveyance for visual media.

If the haptic information can be transmitted as one more sense that complements vision and audio, such new media can convey the material, hardness/softness, warmth, and so forth to the viewers. It is also possible to touch information of the target that a person with visual impairment could not know before. Furthermore, it will be possible to provide powerful and realistic feeling by conveying movements and impacts of content, such as that of dramas and sports.

1.2 Nature of human haptic perception

1.2.1. Human hand

The basic structure of the human hand can be considered in terms of its bones and associated joints, muscles, and skin. Standard terminology is used to refer to the various digits and parts of the hand, as shown in Fig. 1.2. The palm of the hand is divided into three regions: the thenar eminence that overlies the thumb metacarpal, mid palm area, and hypothenar eminence that overlies the metacarpal of the little finger [3].

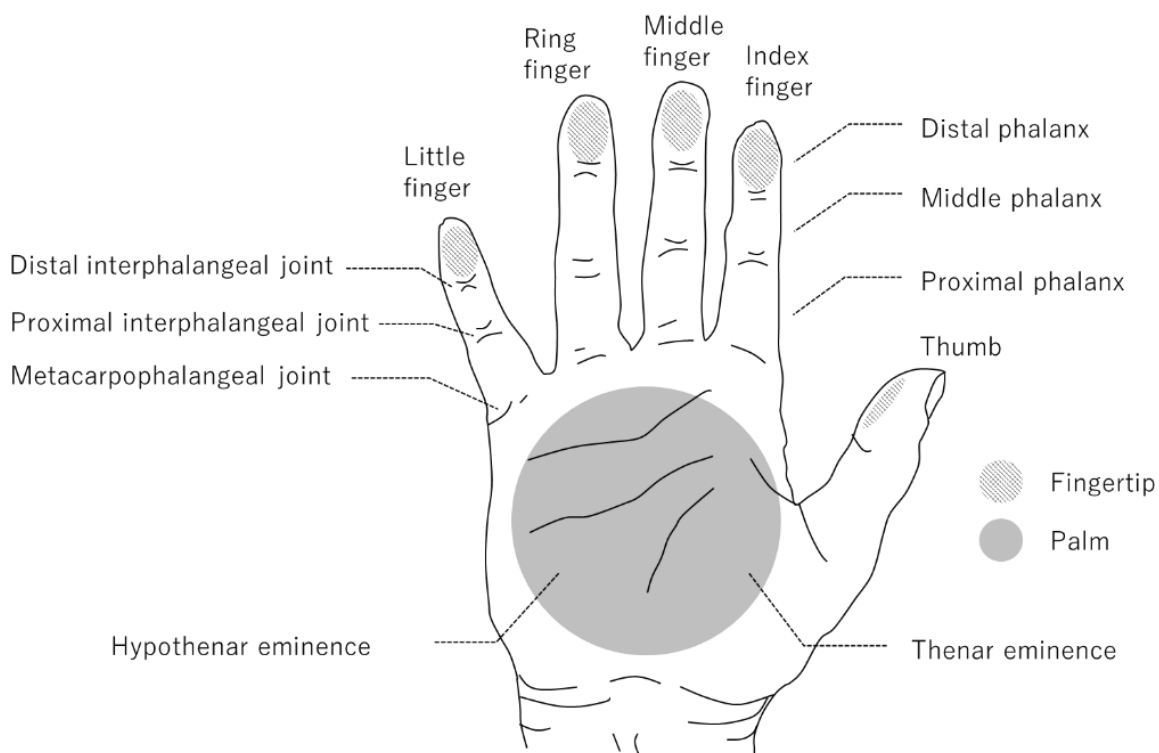


Fig. 1.2. Volar aspect of hand and standard anatomical terminology. Reconstructed and modified from [3].

1.2.2. Haptic perception and sensation

Human haptic perception is enabled through haptic sensation. Haptic sensation is categorized in somatic sensations. Somatic sensations do not have differentiated special sensory organs. Haptic sensations felt through the skin are called cutaneous/tactile sensations, and those felt through the muscles, tendons, and joints are called deep/proprietary sensations.

Cutaneous/tactile sensations include temperature sensations (thermoreceptors) and pain sensations (nociceptors). Deep/proprietary sensations are necessary for self-recognition of body posture. The shape and hardness of objects are perceived through haptic sensations. This means that we recognize the shape and hardness of an object from the cues of both cutaneous/tactile sensations and deep/proprietary sensations. These aspects are discussed in detail in Chapter 3.

1.2.3. Mechanoreceptors in human glabrous skin

Human skin consists of two major subdivisions: epidermis and dermis. The skin of the hand contains numerous eccrine sweat glands that keep the skin damp and assist in controlling body temperature through evaporative heat loss [4]. Fig. 1.3 shows the structure of glabrous skin and the location of the four types of mechanoreceptors (Meissner corpuscles, Merkel cells, Ruffini endings, and Pacinian corpuscles) [4]

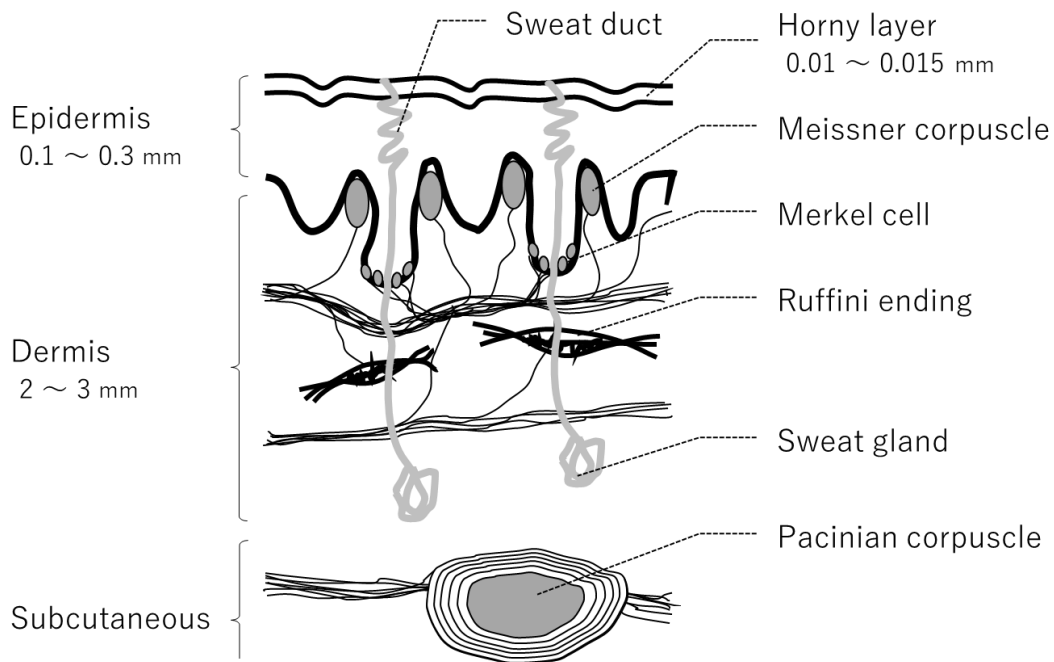


Fig. 1.3. Structure of glabrous skin of human hand illustrating locations of four types of mechanoreceptors. Reconstructed and modified from [4].

The mechanoreceptors react to mechanical stimuli, which are converted into centripetal electric signal pulses, as shown in Fig. 1.4 [4]. The response types are classified into four characteristics (FA I, FA II, SA I, and SA II). FA stands for fast adapting, which indicates the receptors stop firing impulses soon after the mechanical stimulation. In contrast, SA stands for slowly adapting, which indicates the receptors emit intermittent nerve impulses for several minutes after the first mechanical stimulation [4]. SA mechanoreceptors respond to deformation as almost static pressure imposed on the skin. The type I mechanoreceptors cover small regions around them that have sharp borders, and the type II ones cover large regions with obscure borders. It is understood that FA I respond to the velocity of deformation and FA II responses to the acceleration of deformation.

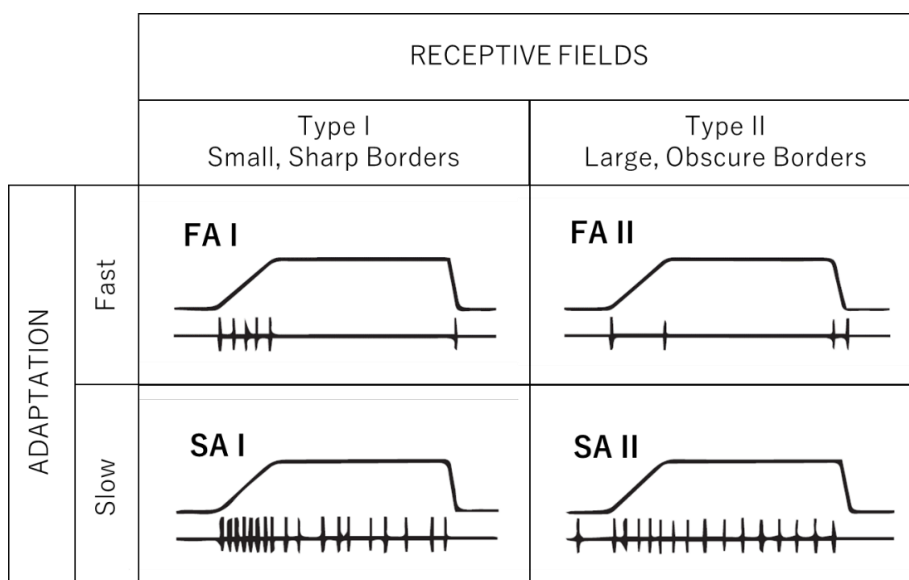


Fig. 1.4. Types of mechanoreceptive unit in glabrous skin of human hand. Graphs show impulse discharge (lower trace) to perpendicular ramp indentation of skin (upper trace) for each unit type. Reconstructed and modified from [4].

The resolutions and spatial density of each mechanoreceptive unit are shown in Fig. 1.5. FA I and SA I are dense in the fingertip. This is the reason that the spatial resolution in a psychophysical test of the fingertip is significantly higher than those of the other finger areas and palm [5]. Fig. 1.6 shows the vibrational displacement threshold of the four mechanoreceptive units. For vibratory stimuli [6] [7] [8], FA I sensitive to the frequency of around 80 Hz, FA II sensitive to frequencies of around 250 Hz, and SA I and SA II are sensitive to frequencies around 30 and 250 Hz, respectively.

Considering the above characteristics of each mechanoreceptive unit, it is assumed that Meissner corpuscles correspond to FA I, Pacinian corpuscles correspond to FA II, Merkel cells correspond to SA I, and Ruffini endings correspond to SA II [4]. From the above neurophysiological knowledge, each of the four mechanoreceptors have a specialized role in detecting temporal and spatial frequencies. These aspects are discussed in detail in Chapter 4.

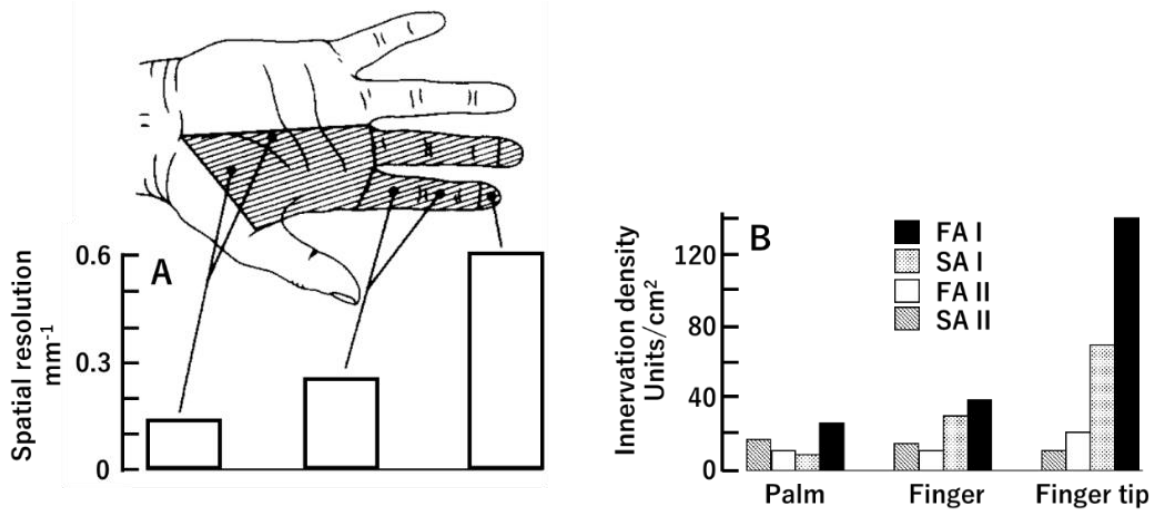


Fig. 1.5. A) Spatial resolution in psychophysical test of two-point discrimination. Height of columns shows inverse of two-point three holding units of mm^{-1} . B) Histogram showing density of innervation of four mechanoreceptive units in different regions of glabrous in area of human hand. Reconstructed and modified from [5].

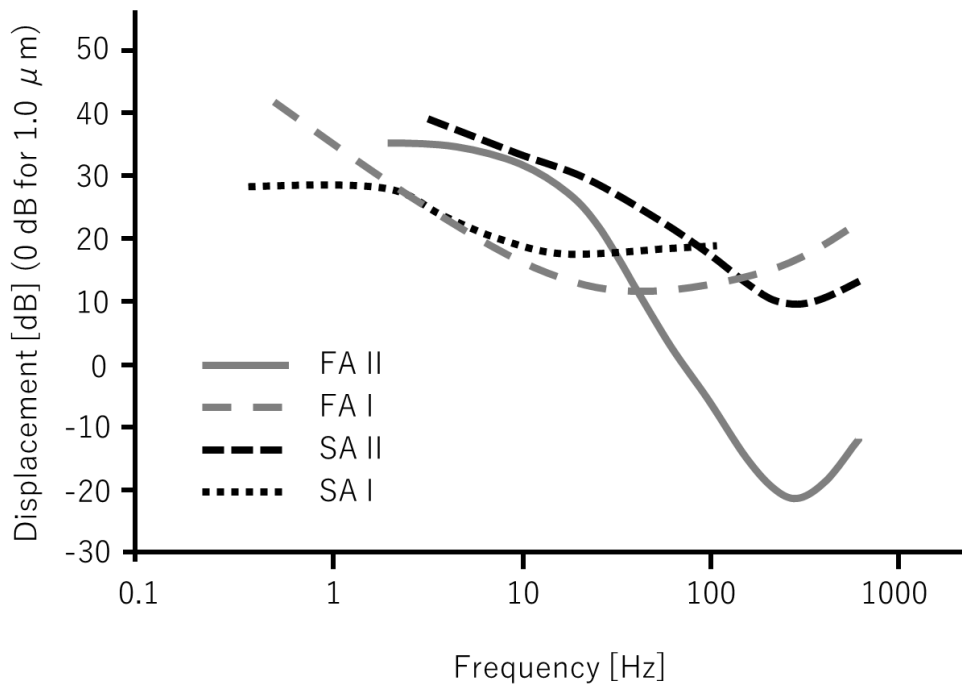


Fig. 1.6. Displacement thresholds of four mechanoreceptive afferent units in glabrous skin with respect to vibration frequencies. Reconstructed and modified from [6].

1.2.4. Deep / Proprietary sensation

Deep sensation, also called proprioception is related to position, movement, and force sensations in human's body or part of the body. Figure 1.7 shows a schematic diagram of the internal structure of the human arm. Here, the outline is explained focusing on the perception in the skeletal muscles, tendons, and joints related to deep sensation.

Muscle spindle is a kind of elongation sensor distributed in skeletal muscle, and is related to perception of changes in muscle length. The Golgi tendon organ is a kind of tension sensor in the tendons at both ends of the skeletal muscle, and responds when the tendon is pulled by external force or contraction of the muscle itself. Both the muscle spindle and the Golgi tendon organ are known to respond to vibrational stimuli, and there have been reports of illusions of joint angles by applying vibrational stimuli [9]. As joint receptors, Ruffini endings and Pacinian corpuscles are distributed in the joints, and some organs similar to the Golgi tendon organs are distributed in the ligaments. In addition, it is known that the mechanoreceptors of the skin described above are involved in the perception of finger position and movement.

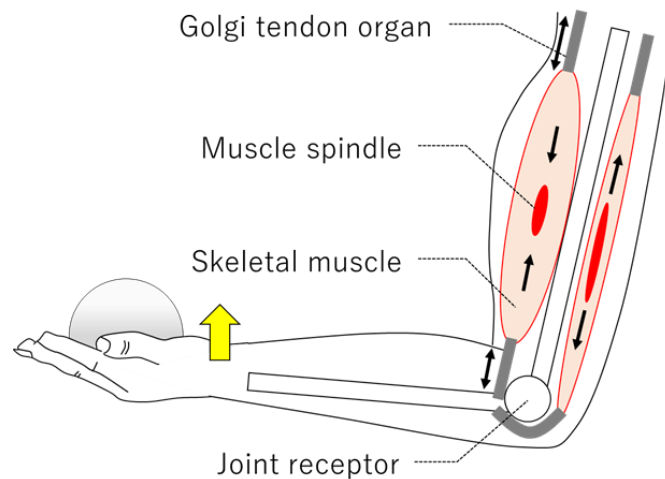


Fig. 1.7. Schematic diagram of the inner structure of a human hand.

1.2.5. Cross-modal perception

Cross-modal perception is a phenomenon in which a certain sensation is perceived differently from the actual input stimuli due to the interaction between the sensations. In recent years, many effective information presentation systems using cross-modal perception have been proposed, especially in AR/VR environments. Pseudo-haptics [10][11] is a representative example of cross-modal perception between visual and haptic sensation. This is a technique that allows the user to perceive a pseudo haptic sensation by appropriately changing the visual movement of the pointer or avatar that reflects the user's physical movements from the actual movement. In particular, it is known that deep senses (positional sense, motor sense, force sense) are influenced by visual information presented at the same time.

1.3 Fundamental principle of haptic information conveyance

1.3.1. Haptic primary color model

Tachi et al. [12] proposed the hypothesis that cutaneous sensation has a many-to-one correspondence from physical to psychophysical perceptual space, via physiological space. As an analogy of the three primary visual colors, they named these haptic information bases the “haptic primary color model” [12]. They defined three spaces, i.e., physical, physiological, and psychophysical or perception, as shown in Fig. 1.8. In the physical space, cutaneous phenomena can be resolved into the following three components: pressure, vibration, and temperature. In the physiological space, cutaneous perception is created through a combination of nerve signals from several types of tactile receptors located in the skin.

As described in Section 1.2, the Merkel cells, Ruffini endings, Meissner corpuscles, and Pacinian corpuscles are known to be activated by pressure, tangential force, low-frequency vibration, and high-frequency vibration, respectively. Some tele-existence projects have attempted to transmit haptic sensation from an avatar robot’s fingers to a human user’s fingers using this theory [12][13][14].

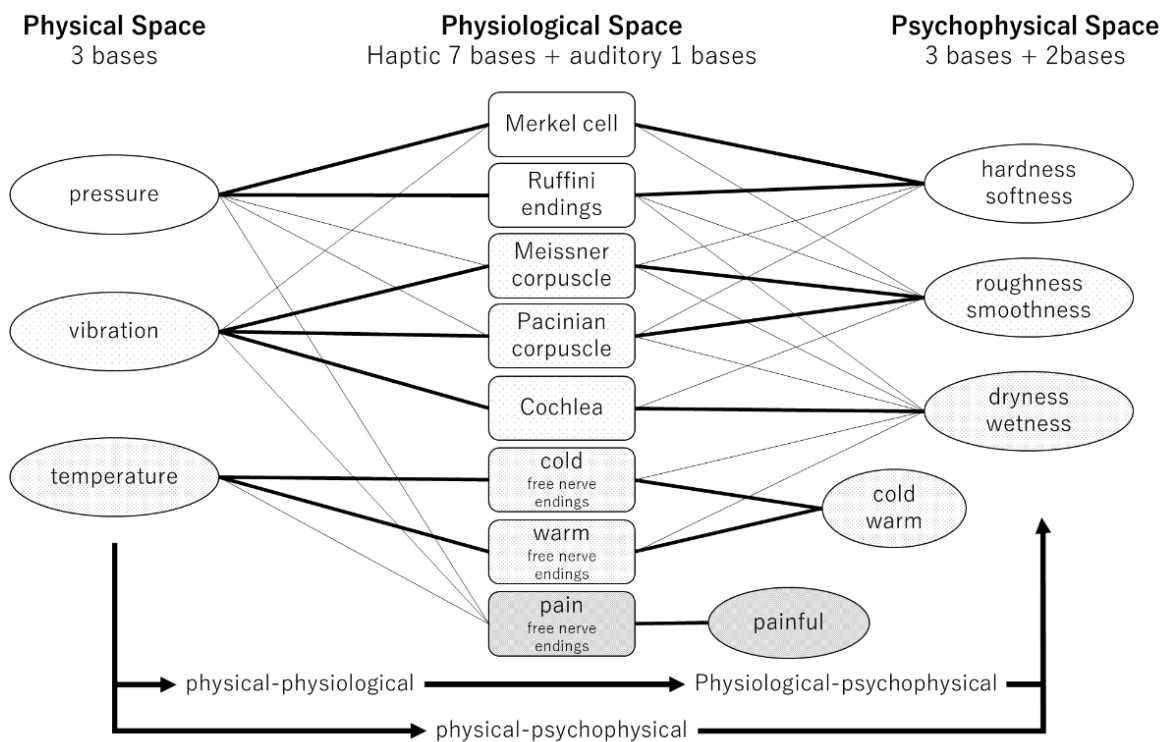


Fig. 1.8. Haptic primary color model. Reconstructed from [12].

1.3.2. Sensing methods for transmitting haptic information

Human hands mainly detect the following information from skin deformations [15]:

- Contact location, force and force direction
- Curvature, distinction among surface, line, and point
- Sliding, prediction of sliding, friction
- Hardness/Softness
- Viscosity and stickiness
- Texture and fine structure such as cloth
- Macroscopic shape of skin deformation

A versatile haptic sensor, which is equal to human skin, is also being investigated imparting tactile sensations to robots. Tele-existence system uses haptic sensors based on the haptic primary color model [12]. However, for creating 1:N haptic media, the following method for obtaining the physical information of an object will be effective.

(1) 3D shape sensing

The 3D shape of a real object can be obtained from a 3D digitizer using laser, and an image-processing technology from multi-view camera images [16]. It has recently become possible to easily model the 3D shape of an object using CG from several images taken with a smartphone camera.

(2) Hardness/Softness sensing

There are various methods for hardness/softness sensing that are used in material hardness tests. Generally, a measuring system applies force to the surface of the object to be measured and acquires displacement of the surface. A contact probe incorporating a force sensor or a fluid noncontact probe is used as a force application system. A camera, laser-displacement meter, potentiometer, and encoder are used as such a system for obtaining displacement.

For integrated sensing of the 3D shape and hardness of an object, Fujiwara et al. [17] developed a noncontact sensing system for hardness/softness distribution using ultrasound as noncontact probes. Fig. 1.9 shows an image of this system, which obtain hardness distribution data with a visual image and coordinate data for point clouds representing a 3D shape.

When the target object (the egg sunny side up in Fig. 1.9) is placed on the measuring stage, the camera takes an image, and the laser-displacement meter scan the point cloud coordinate data (x , y , z coordinate value sets) of the 3D shape of the object. Next, while scanning the focal point of the ultrasound focused on the object surface from the ultrasonic array via the reflector, the laser beam from the laser-displacement meter scanned the amount of vertical displacement of the object surface at the same time when the object surface is sequentially pressurized with acoustic radiation pressure. The hardness of the measurement point is estimated from the ratio of acoustic radiation pressure and displacement at that point, to the hardness distribution data [N/mm] of the surface of the target object.

In the study described in Chapter 5, this noncontact sensing system [17] was used as an input for our application system.

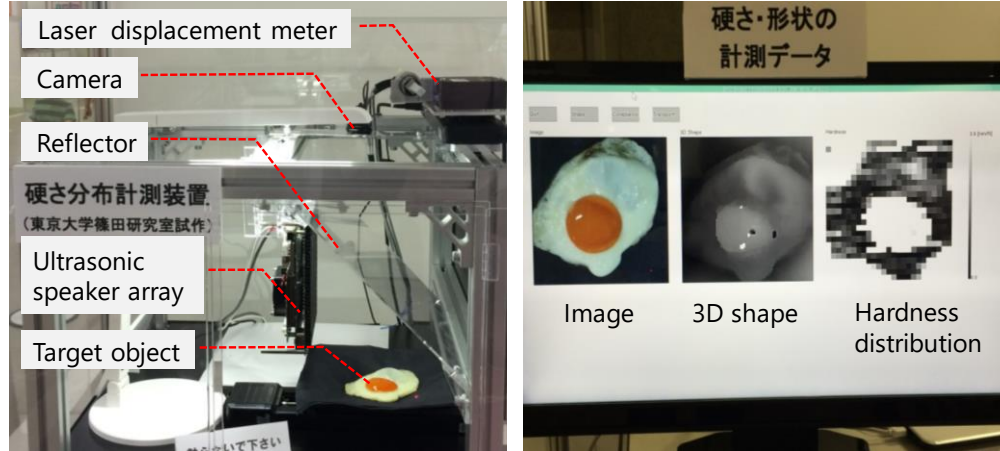


Fig.1.9. Noncontact sensing device for 3D shape and hardness/softness distribution.

1.3.3. Display methods for representing haptic information

To generate haptic sensations in the human hand, a method for representing haptic information is required. According to the haptic primary color mode [12] described in Section 1.3.1, pressure, vibration and temperature play important roles in physical space. In addition, humans detect various information from skin deformation [15]. However, such a haptic-display method for presenting all of information in an integrated manner has not been developed.

(1) Force feedback and 3D shape display

As a haptic display that presents the 3D of a virtual object, pins arranged in an array that are driven up and down to represent the 3D shape of an object has been studied [18][19][20]. However, there are technologic difficulties against improving spatial resolution.

There are several types of force-feedback devices that reproduce reaction forces from a virtual surface to the user's stylus (pen-type input device) or fingertip [21][22][23]. These are devices with higher spatial and temporal resolution than that for driving pins in the above-mentioned array form. There is also an exoskeleton haptic display [24][25][26].

(2) Hardness/Softness display

Materiable [27] is an interactive system that presents the physical properties of objects such as hardness using pins arranged in an array. Same as the point-contact-type device described above, the most simplified hardness simulation model is Hooke's law ($F = kD$, F : force [N], D : displacement [mm], k : spring constant [N/mm]). Such devices can display hardness by presenting the force F [N] calculated by the spring constant set according to the hardness of the virtual object.

For presenting the hardness changes with hysteresis characteristics and nonlinear hardness, it is necessary to control the force to be presented based on simulations such as that using the finite element method [28]. Humans perceive elasticity from the relationship between the amount of displacement and reaction force using the deep sensation. The cutaneous sensation of the finger pad also plays important roles in the perception mechanism of softness when touching a soft object. The

amount of contact area of the finger pad and the pressure distribution are key factors for perceiving the softness of the object surface [29]. In fact, a method of presenting a sense of softness by reproducing the relationship between the indentation force and contact area has been proposed [30].

(3) Vibro-tactile display

Eccentric rotating mass (ERM) has been used as a vibrator in mobile phones and game console controllers. ERM can vibrate the entire device using rotate motion of an eccentric weight attached to the shaft of a motor. However, in the context of the sensitivity of the human mechanoreceptors described in Section 1.2, the vibration of the ERM is in a manner of a symbolic expression as a rhythm pattern by turning vibration ON and OFF.

Haptic technology is one of the most appealing aspects of the latest smart-phones, game consoles, and VR controllers. Linear resonant actuators (LRAs) are used to develop such devices to present vibro-tactile sensation. LRAs can vibrate in the frequency band where human mechanoreceptors are sensitive [6]. LRAs generate an electromagnetic force by passing a current through a coil to vibrate the coil. The principle is basically the same as that of the voice coil motor, but more than two resonance frequencies are provided. The use of piezo elements, which are relatively expensive but have a quick response time of about 1 ms, is also becoming widespread as vibrator for the touch screens on smart-phones and tablets.

1.4 Our approach and goal of thesis

This thesis focuses on 1:N-type visual and haptic media. Among the four issues in adding haptic information to visual media described in Section 1.1, we focused on representing haptic information according to the user's environment. We evaluated the effectiveness of our haptic presentation method that conveys the difference in shape, size, and partial hardness of a 3D object. Next, we developed a method to directly transmit the sense of impact magnitude and direction of the contact between moving objects and verify the effectiveness through evaluation experiments. Finally, we discuss the results and requirements for creating haptic technology that contributes to the expansion of visual media to universal information services.

1.5 Organization of thesis

The organization of the remainder of this thesis is as follow. In Chapter II, we present the basic design, prototyping, and a preliminary evaluation revealing requirements relevant to the number of haptic stimulation points on a finger pad necessary for recognizing 3D shapes. In Chapter III, we describe the concept and evaluation results of grasping-type haptic devices to present 3D shape and hardness distributions of an object. In Chapter IV, we present a method for transmitting the timing and impact of haptic sensation when moving objects come into contact and verify the effectiveness of this method through evaluation experiments. We also argue that concave haptic stimuli can be applied to control the sense of self-attribution. In Chapter V, we describe some useful application systems of our proposed methods. We finally conclude the thesis in Chapter VI.

Chapter 2

Number of haptic stimulation points on finger pad necessary for recognizing 3D shapes

We investigated the fundamental characteristics of human haptic sensations, and conducted basic design, prototyping, and preliminary evaluations. We conducted a subjective assessment with the cooperation of six visually impaired individuals on the ease of exploring an object's edges as a function of the number of force-feedback points. The evaluation results suggested that the ease of recognizing edges improved significantly with two or more force-feedback points compared with a conventional point-contact method. This could be most easily recognized when using four force-feedback points under the experimental conditions.

2.1 Potential of multipoint force feedback to finger pad

As described in Section 1.3, our finger pads can detect various information from skin deformation [15]. Fig. 2.1 shows typical human haptic explorations for recognizing the characteristics of an object such as texture, temperature, weight, exact shape, volume, and hardness [31]. However, in conventional point-contact-type force feedback devices [22], it has been difficult to tactily explore edges and vertices, which are important to recognize exact 3D geometry. Fig. 2.2 illustrates the following four types of force feedback methods for representing the surface of a virtual object through a human finger:

- (a) Three degrees of freedom (3-DoF) force applied to a fingertip via a thimble.
- (b) 3-DoF force applied to a finger pad via a plate.
- (c) 3-DoF force applied to a finger pad via a plate with 1 DoF pin arrays.
- (d) Multi-3-DoF force applied to a finger pad via multi-3-DoF points.

Methods (a) and (b) are conventional point-contact-type force feedback methods [22]. We attempted to use these methods to recognize the 3D shape of a virtual object [32]. However, it is difficult to trace the sudden gradient change of the surface especially at the corner (vertex) of the object. Method (c), which uses 1-DoF pin arrays, is also a conventional method of representing the geometry of the surface of an object. Pin arrays are often mounted using piezo actuators, which displacement is less than 1 mm.

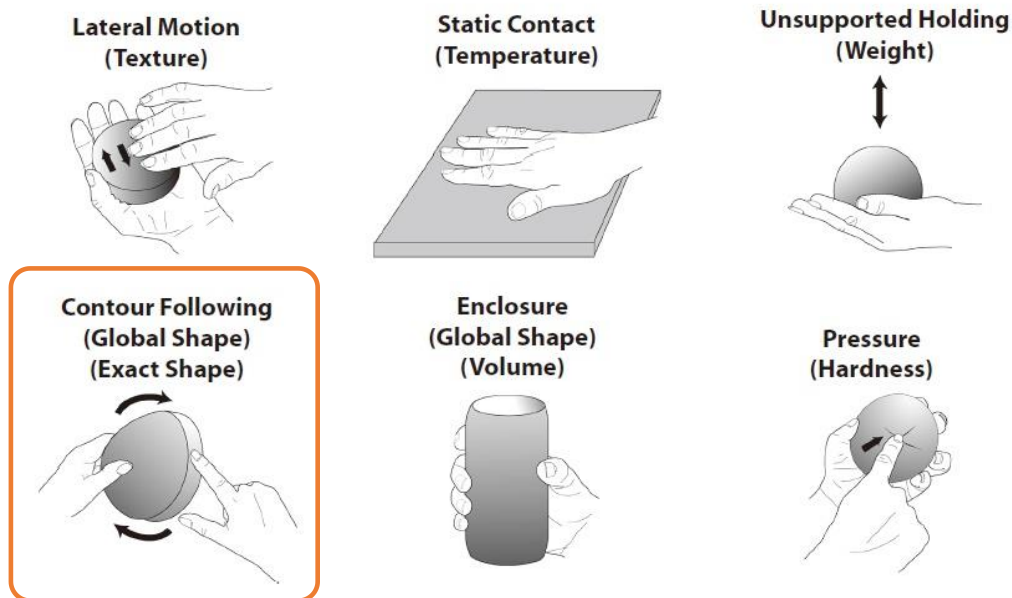


Fig. 2.1. Haptic explorations for recognizing each characteristic of object. Reconstructed from [31].

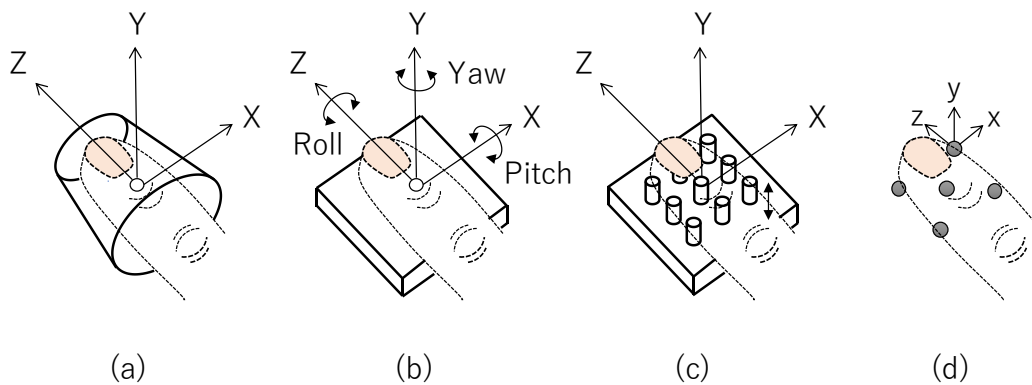


Fig. 2.2. Force-feedback methods for representing surface of object to finger pad. (a) 3-DoF force applied to fingertip via thimble, (b) 6-DoF force applied to finger pad via plate, (c) 3-DoF force applied to finger pad via plate with 1-DoF pin arrays, (d) multi 3-DoF force applied to finger pad via multi 3-DoF points.

Consider a case in which a finger pad touches a quadric surface without moving the finger laterally. Fig. 2.3 is a schematic diagram of a quadric surface pattern (flat, cap, cup, ridge, and rut) and the variations to express each quadric surface using a 1-DoF pin array (five or nine) and 3-DoF force point array (three to five). The 1-DoF pin array requires at least a 3×3 pin array to represent the difference between the cap and ridge and the cup and rut. The 3-DoF force point array can present a 3 DoF force at each point independently, so it is theoretically possible to express the difference in the five quadric surfaces at least using three force points.

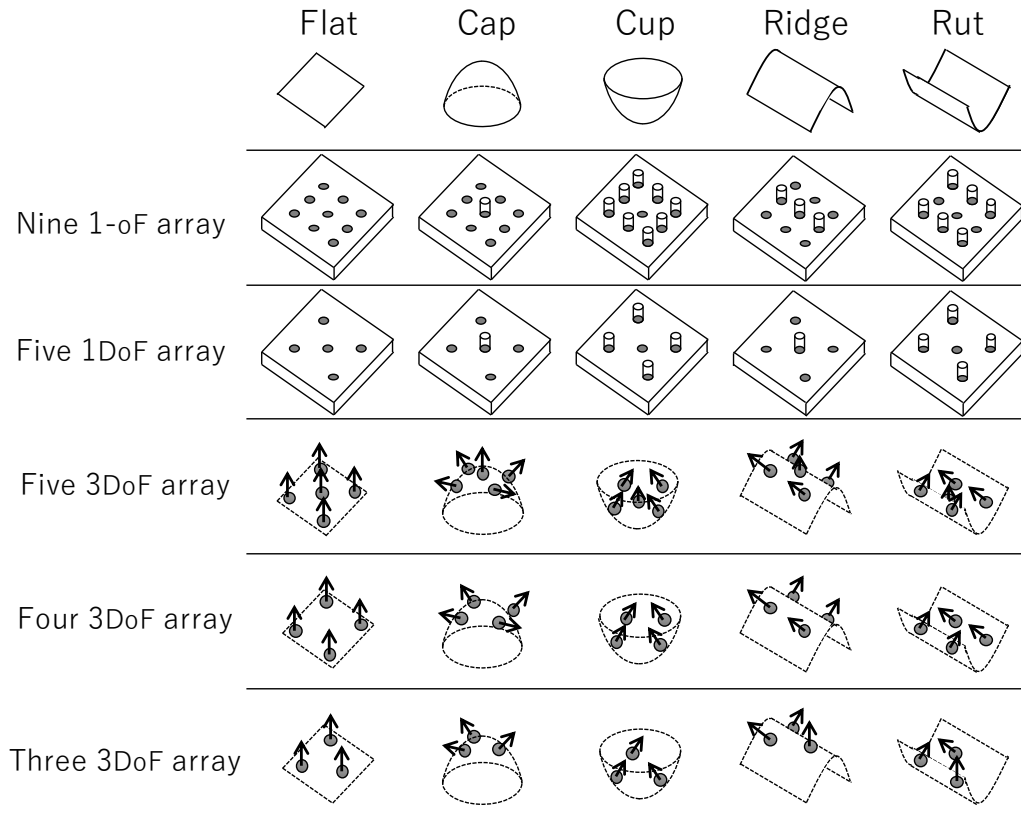


Fig. 2.3. Schematic diagram of quadratic surface pattern (flat, cap, cup, ridge, and rut) expressed by 1-DoF pin array (five or nine pins) and 3-DoF force point array (three to five points)

2.2 Multipoint force feedback system

To clarify requirements for improving the recognition of edges and vertices, we constructed a prototype system that uses five conventional force feedback devices. This system can provide 3-DoF force feedback to each of the five points on a finger pad [33]. Fig. 2.4 shows this multipoint force feedback system, which consists of five force feedback components (3D system, Phantom Premium 1.5 3-DoF [34]) with a 4-mm diameter iron sphere at the tip of the mechanical linkage.

As shown in Figs. 2.4 and 2.5, the five force-feedback points are connected via the fabric surface fastener so that when the distance between them is maximum, it is placed at the vertex of a 10mm square and its center. It is also possible for the spheres to be adjacent to each other. The force-feedback point is reproduced as a virtual pointer in the virtual space on the computer, and a reaction force proportional to the interference depth vector is output to each point according to the contact between the virtual pointer and virtual object (refresh rate 1 kHz).

The presence or absence of force feedback for each point and the magnitude of output force can be individually controlled. The user can touch the upper and side surfaces of a virtual object that fits in a hemisphere with a diameter of about 20 cm.

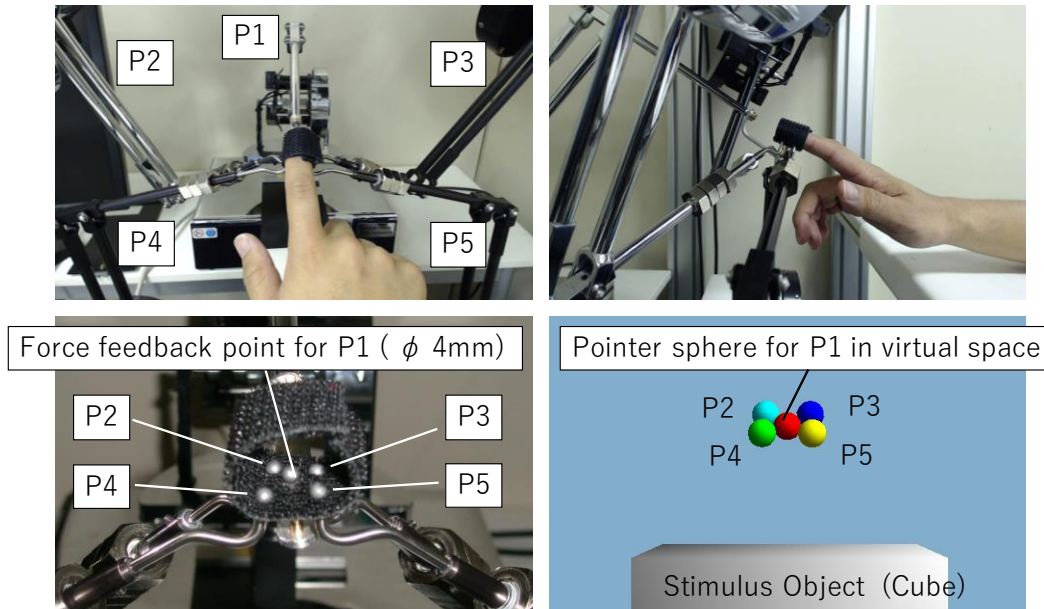


Fig.2.4. Multipoint force-feedback system. P1 to P5 indicates each force feedback point and related PHANToM device

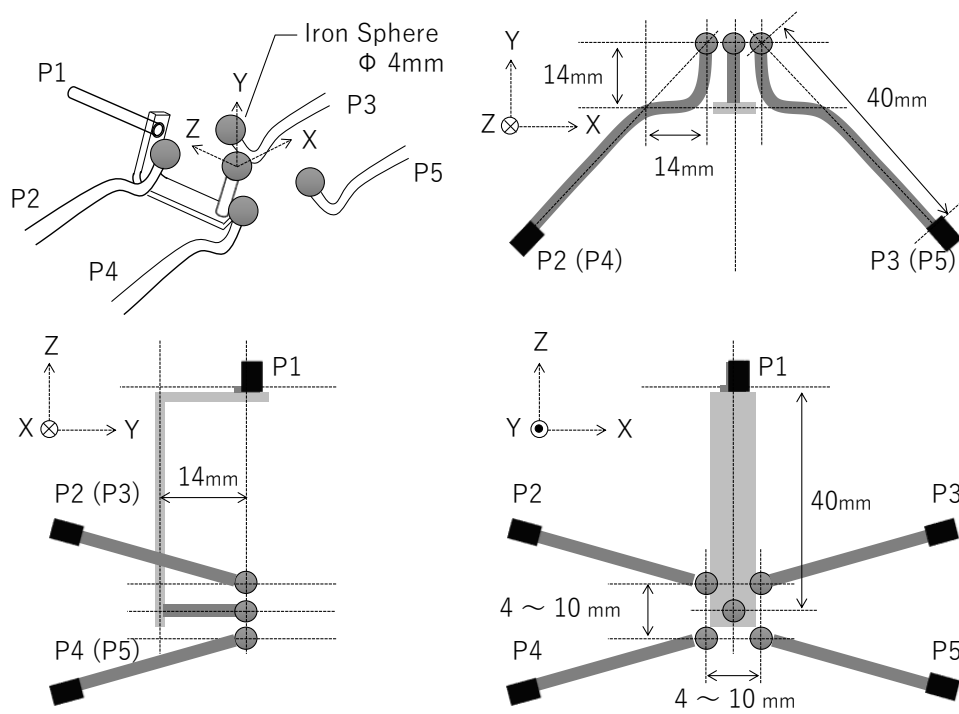


Fig. 2.5. Placement relationship of five force-feedback points touched with finger pad of user

2.3 Recognition of 3D geometry using multipoint force feedback to finger pad

We conducted a subjective assessment with the cooperation of six visually impaired individuals on the ease of recognizing an object's ridgeline as a function of the number of force-feedback points.

2.3.1. Method

A participant was seated in front of the apparatus described in Section 2.2, and the fabric fastener was attached in a thimble so that the five points touched the index finger-pad of his/her right hand. The height of the chair was adjusted so that the arm from wrist to elbow could be placed freely on the desk. Participants touched the ridgeline around the upper surface of the presented virtual object in a clockwise direction starting from the ridgeline on the front side. They then evaluated the ease of recognizing the ridgeline according to the evaluation criteria shown in Fig.2.6.

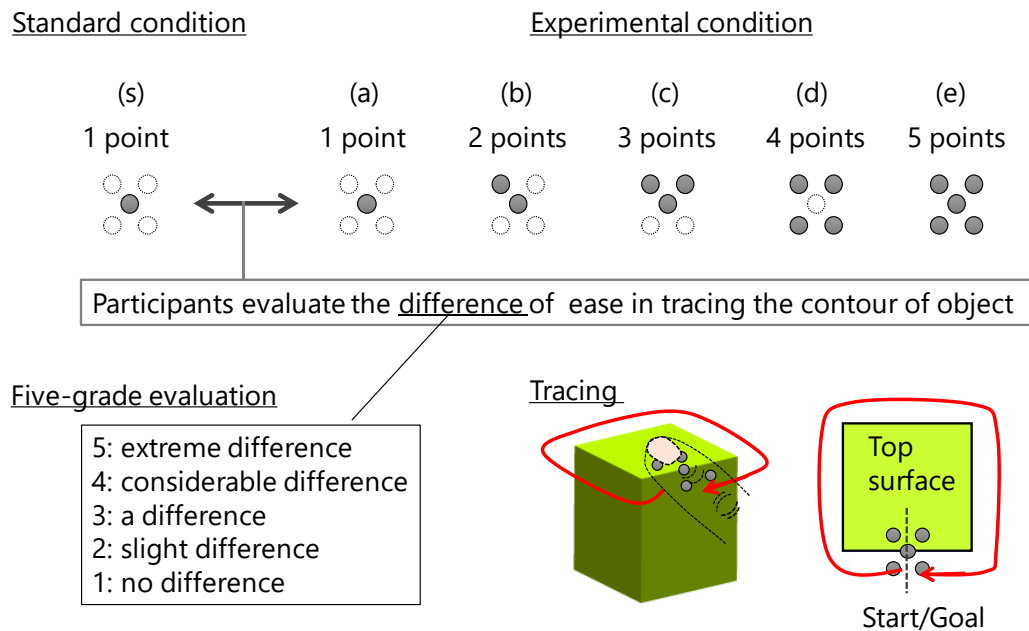


Fig. 2.6. Experimental conditions and criteria of subjective evaluation.

Fig. 2.7 shows the 3D objects used in the experiment. The objects were three types of polygonal columns in which the inner angle of the top surface at each vertex was 60° , 90° , 120° , and a cylinder with no vertex. The perimeter of the solid shape was 360 mm. The number of haptic stimulation points was controlled by the presence or absence of applying force-feedback for points. Therefore, only the presence or absence of the reaction force from the virtual object was changed while five points were always touching the participant's finger pad.

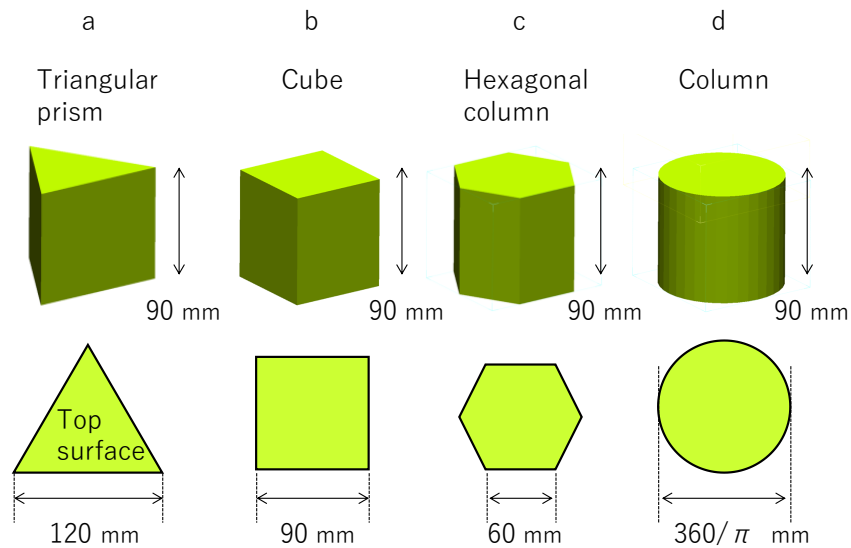


Fig. 2.7. Four 3D shapes presented as experimental stimuli.

Participants were asked to explore the ridge of the object, which were presented in random order. For each trial, participants evaluated the difference in the ease of tracing the ridgeline/ contour of the object on a five-grade scale compared to the standard condition (one-point haptic stimulation). In addition, the exploration time and trace of each stimulus point during the task were recorded without notifying the participants. Each participant conducted 20 trials (4 objects \times 5 conditions) in 30 minutes and repeated it 5 times with a 30-minutes break (total 100 trials).

There were six visually impaired participants (two males and four females, 20's – 50's). Informed consent was obtained from all individual participants included in this study. All procedures we carried out involving human participants were in accordance with the ethical standards of the institutional committee and with the 1964 Helsinki declaration and its later amendments or comparable ethical standards.

2.3.2. Results

The results are shown in Fig. 2.8. Fig. 2.8a shows that the main effect was significant as a result of one-way analysis of variance (ANOVA) based on the number of haptic stimulation points ($F(4, 476) = 79.227, p < 0.01$). Fig. 2.8b shows the mean exploration time for the ridgeline of the cube. A one-way ANOVA based on the number of haptic stimulation points showed a significant main effect ($F(4, 116) = 3.557, p < 0.05$). When the number of haptic stimulation points was four, the exploration time seemed to be shortened however, there was no significant differences from the Bonferroni's multiple comparison.

Fig. 2.8c shows the total trace length of the central stimulation point while the participant's finger was exploring the ridgeline of the cube. The dotted line in the figure indicates the length of one ridgeline, i.e., 360 mm. As a result of one-way ANOVA based on the number of haptic stimulation points, the main effect was significant ($F(4, 116) = 7.085, p < 0.01$). As a result of multiple comparison, significant difference was observed between the one-to-three point and four-point conditions.

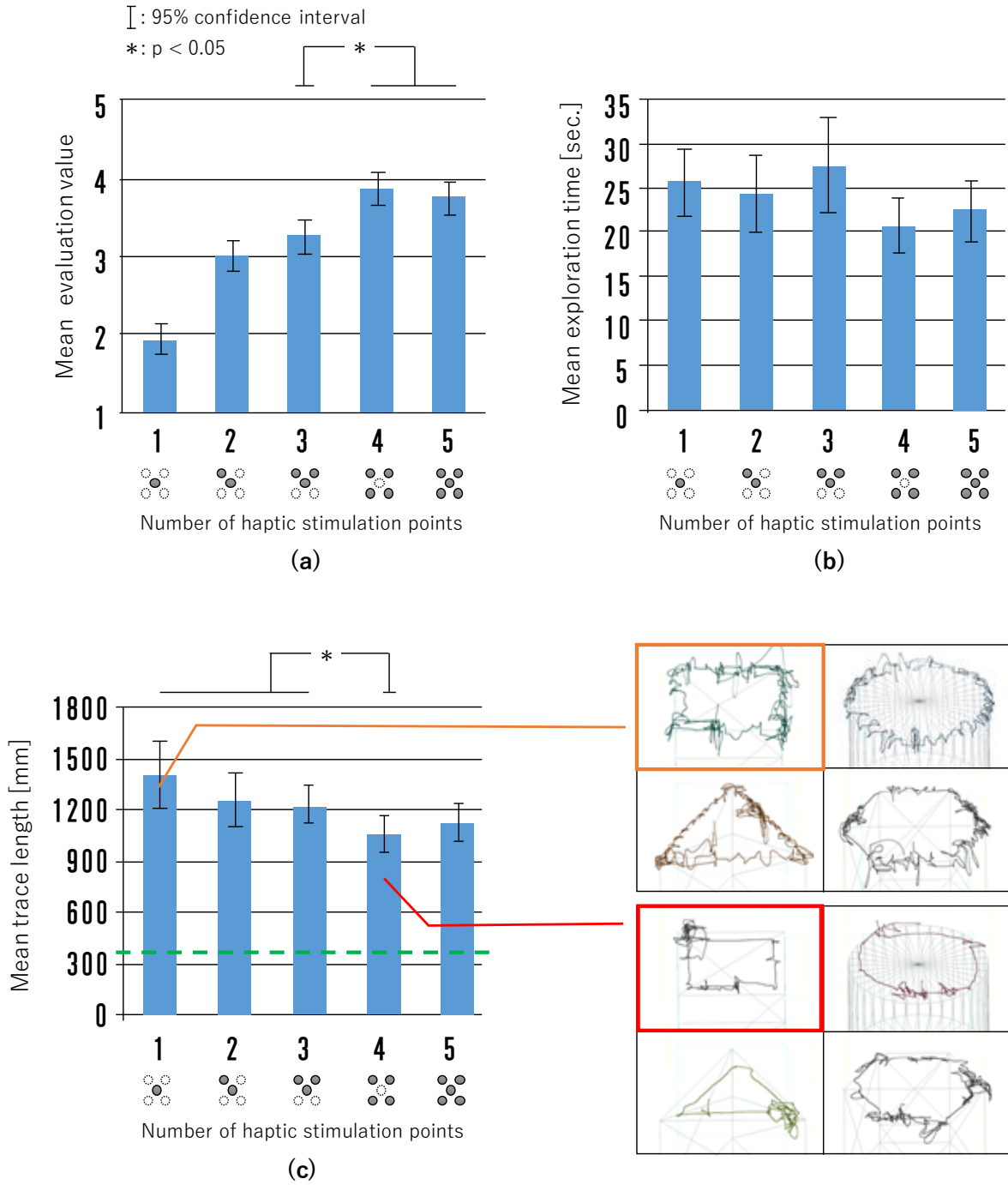


Fig. 2.8. Experimental results. (a) Mean subjective evaluation value evaluated the difference in the ease of tracing the contour/ridgeline of the object on a five-grade scale, (b) mean exploration time for ridgeline of cube, (c) total trace length of central stimulation point while participant's finger was exploring contour of cube.

2.3.3. Discussion

From the results of subjective evaluation (Fig. 2.8a), there was a significant improvement when the participants explored the contour of an object with four haptic stimulation points on the finger pad. There was no significant difference between the four-point and five-point conditions. From the trace logging data (Fig. 2.8c), it can be seen that participants moved their finger pad in a fine reciprocating motion and repeated deviation at the ridgeline under the one-point condition. However, when the participants explored the contour of an object with four haptic stimulation points, the ratio of the trace line which was nearly parallel to the ridge line increased. In addition, the pattern of motion trace showed how the whole finger drops out at the corner of the object. As shown in Fig. 2.9, when the number of haptic stimulation points was three, the drop out of the whole finger occurred frequently at the corners. For four haptic stimulation points, at least one point remained on the surface of the object.

Fig.2.9. Image of dropout at corner of object for force feedback for three points (left) and four points (right).

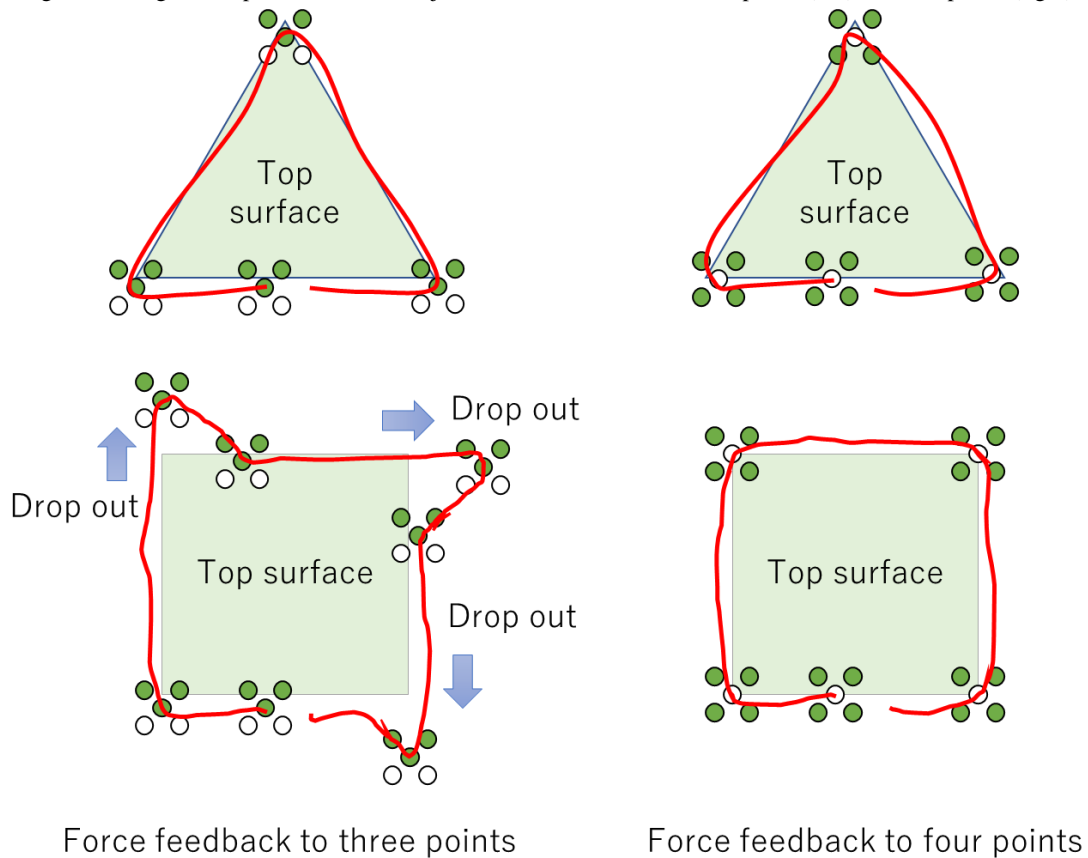


Fig.2.9. Image of dropout at corner of object for force feedback for three points (left) and four points (right).

2.4 Conclusion

We conducted basic design, prototyping, and preliminary evaluations. In conventional point-contact-type force feedback devices, it has been difficult to tactilely explore contours, which are important in recognizing 3D shapes. To improve the ease of tactilely exploring contours, we constructed a prototype system that can provide force feedback with 3-DoFs to each of the five points on a finger pad. Using this system, we conducted a subjective evaluation with the cooperation of six visually impaired individuals on the ease of recognizing an object's edges as a function of the number of force-feedback points. The results indicate that the ease of recognizing edges improved significantly with two or more haptic stimulation points, and the most easily explore condition was four haptic stimulation points. However, from the hypothesis illustrated in Fig. 2.3, three is a minimum number of 3-DoF haptic stimulation points on a finger pad for representing quadric surfaces. It is necessary to verify that three haptic stimuli points will be sufficient when visual information can be used.

Chapter 3

Grasping-type haptic device to present 3D shape and Hardness of virtual objects

In this research, we developed a grasping-type haptic device for representing 3D shape and harness distributions of virtual objects based on the requirements from the preliminary findings described in Chapter 2. From the results of user experiments, it was confirmed that the difference in the side surfaces of the virtual 3D shapes could be identified, and the effectiveness of the proposed method was clarified. In addition, the results of experiments comparing the difference between the hardness presented on the haptic device and the hardness of a real spring suggests that the subject can sufficiently distinguish the difference in relative hardness.

3.1 Grasping-type haptic device to investigate the potential of integration between multi-finger and multipoint haptic feedbacks

3.1.1. Grasping action to recognize the global shape of object

For presenting 3D shapes, there are at least two historical approaches as introduced in section 1.3. One is to represent 3D shapes physically using displays comprising pins and rods [18][19][20] and the other is to represent reaction forces from the surface of an object using force feedback technologies [21][22][23]. The former is advantageous in that it enables wider ranges of objects to be rendered, thus enabling users to obtain shapes with their hands. However, it is difficult to improve resolution and to render whole 360-degree views of objects (so called "2.5D"). The latter is able to render whole 360-degree views of objects but cannot do so at one time because the contact surface cannot be rendered unless the fingertips are moved continuously (refer to Appendix A for more details about preliminary experiment using force feedback devices).

Fig. 3.1 shows again the typical human haptic explorations for recognizing the characteristics of an object [31]. Human tends to be grasping the object when he/she is recognizing the global shape and volume of it. In this research, we have tried to investigate the potential of integration between multi-finger and multipoint haptic feedbacks and developed a mechanically-actuated grasping-type haptic device that renders stable 3D shapes and volume of a virtual object.

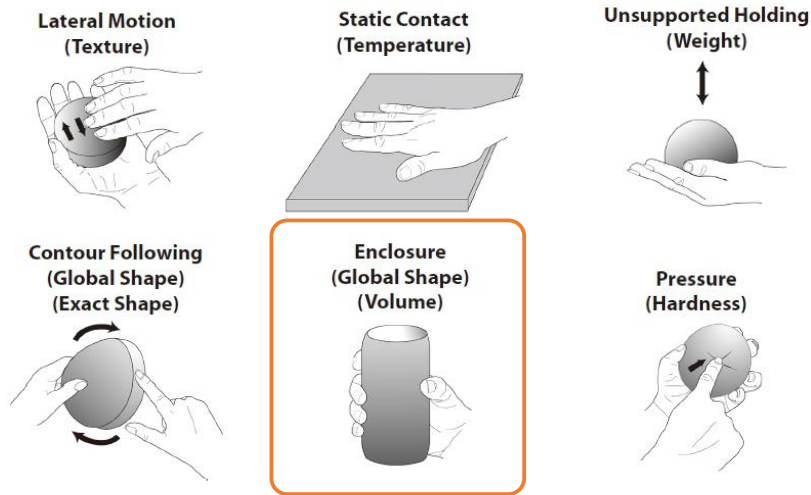


Fig. 3.1. Haptic explorations for recognizing each characteristics of an object. Reconstructed from [31].

3.1.2. Integration between multi-finger method and multipoint haptic feedbacks

We have designed a multi-fingered haptic device that can simulate the condition in which a user is grasping an object with three fingers (thumb, index finger, middle finger) of the right or left hand [35]. As shown in Fig. 3.2, this apparatus has three 5 mm diameter 1 DoF actuating spheres arranged in triangular geometry on the contact area of each of three finger pads.

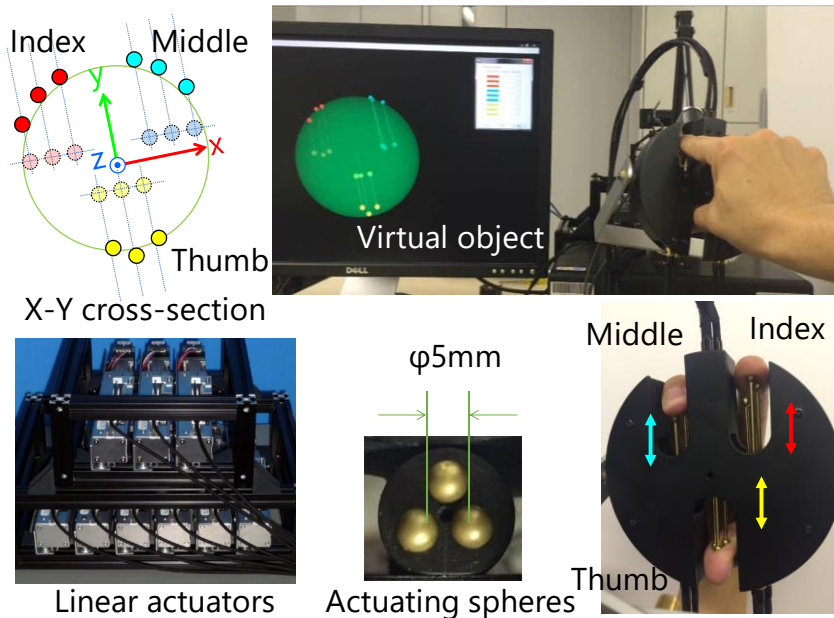


Fig. 3.2. Multi-fingered haptic device.

Fig. 3.3 shows a schematic diagram of the apparatus. Nine actuating spheres in total are connected to linear actuators (Orientalmotor, EAS2X-E005-ARAKD) through each of nine cable releases (HAKUBA KLE-0910). A handheld black circular body (the “Gripper”) packs pairs of an actuating sphere and a brass bar of 40 mm length. This Gripper is attached to a force feedback device (3D systems Phantom Premium 1.5) equipped with a 6DOF encoder.

The Phantom works for the following two patterns. 1. Only for detecting spatial coordinates (x, y, z) and rotation (roll, pitch, yaw) of the Gripper. This mode fully simulates as a mobile handheld device. 2. Outputs forces in a way so as to prevent three fingertips from penetrating to the surface of an object. When users move their hand while holding the Gripper toward the virtual object, the nine actuating spheres move so as to represent the respective surface positions of the object, with control accuracy of less than 1 mm. The maximum force and action speed of the actuating spheres are respectively 40 N and 300 mm/s.

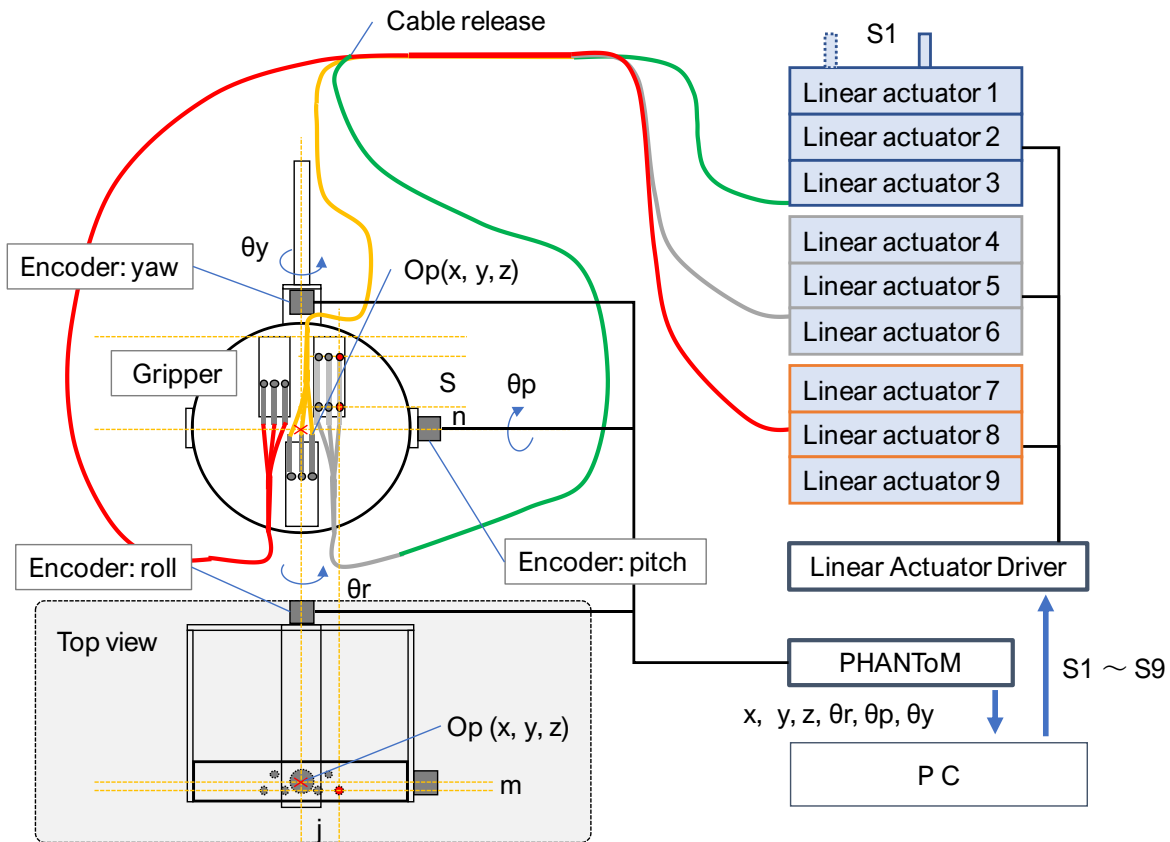


Fig. 3.3. Schematic diagram of the prototype multi-fingered haptic device.

Fig. 3.4 shows the schematic diagram to measure the trajectory of an actuating sphere that should be representing the surface of 80 mm diameter virtual sphere. We measured the displacement of one sphere that actuated according to 12 mm/s horizontal movement using a laser displacement meter (Keyence, IL-300) and a x-z stage. The control frequency of an actuator was 15 Hz and the actuating speed of an actuator was 10, 20, 30, 40, 50, and 100 mm/s. The measurement results (Fig. 3.5) shows that the actuating speed should be more than 30 mm/s to represent an 80 mm diameter virtual sphere.

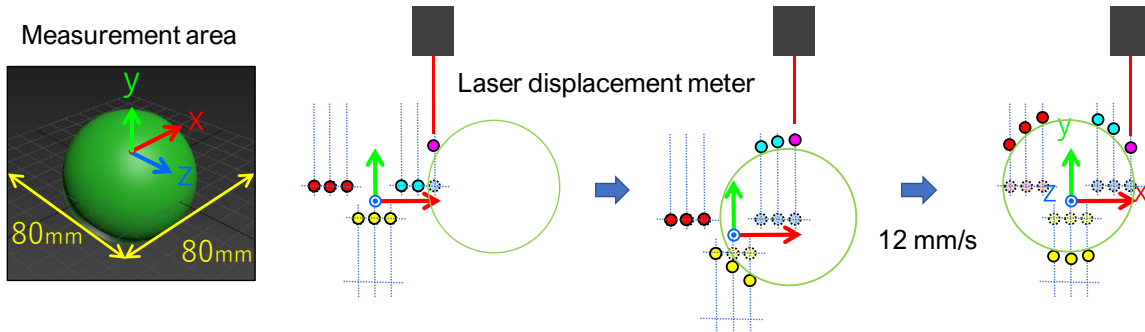


Fig. 3.4. Schematic diagram to measure the trajectory of an actuating sphere.

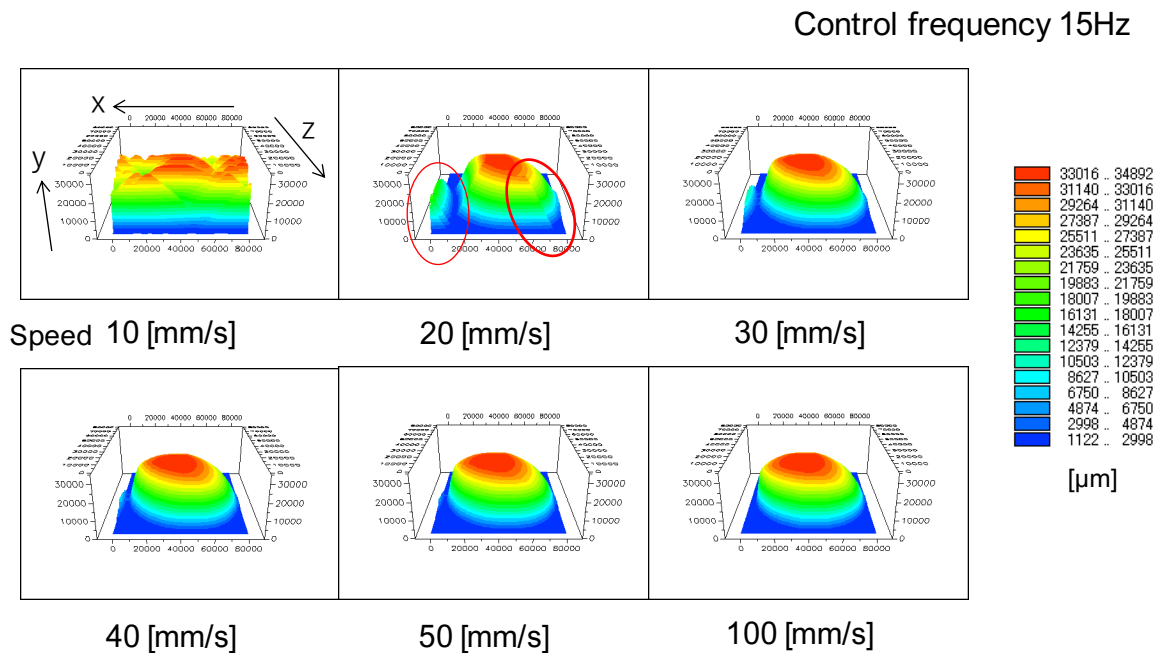


Fig. 3.5. Measurement results of the trajectory of an actuating sphere with the actuating speed of 10, 20, 30, 40, 50, 100 mm/s in the condition of 15 Hz control frequency.

3.1.3. Preliminary experiments

We conducted a two-part user evaluation to test our design concepts and the specifications of a prototype. In the first experiment (Exp1), participants were asked to answer forced choice questions whether the size of the virtual cylinder (comparison stimulus) in their right hand was greater than the real steel cylinder (65 mm diameter) in their left hand. The comparison stimuli were presented in random order with diameters of 50, 55, 60, 65, 70, 75, and 80 mm. Participants tried the method of constant stimuli 140 times. As shown in Fig. 3.6, the x-y stage moved the Gripper with linear reciprocating uniform motion on the short axis of the cylinder at a speed of 24 mm/s. Before the experiment, we measured the physical trajectories of the actuating spheres with a laser displacement meter and confirmed what the rendering surface was with an accuracy of less than 1 mm.

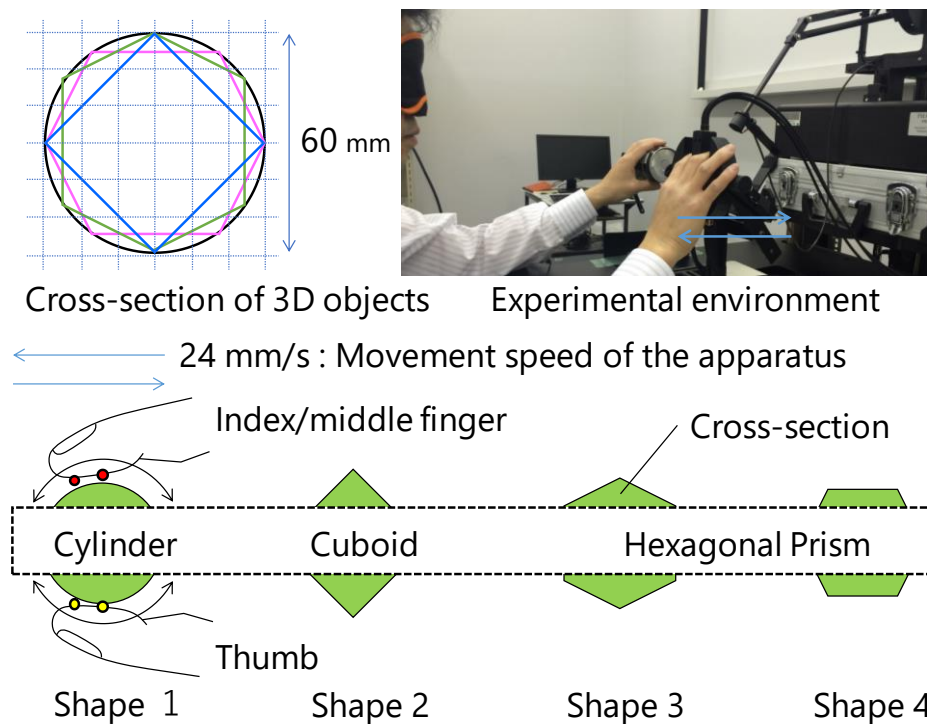


Fig. 3.6. Experimental settings.

In the second experiment (Exp2), participants were asked to answer verbally the number of shape types presented by the Gripper using only their right hand. The stimuli were the four types of shapes shown in Fig. 3.6. Shape 1 was a 60 mm diameter cylinder, and Shapes 2, 3, and 4 were sized so that they could be inscribed in Shape 1. Each shape was presented 10 times in random order, so each participant tried a total of 40 times. The other experimental conditions were the same as those in Exp1.

Participants wore eye masks and heard random mechanical noise sound during the trials. They sat

on a chair propping their elbows on the table in front of the apparatus and grasped the Gripper with their right hand. Because of the limitation of the minimum size of the Gripper, the object was not rendered less than 15 mm from the center horizontal plane of the Gripper (the dotted frame area shown in Fig. 3.6). We recruited 12 righthanded participants (3 males, 9 females) aged 24 - 45. None of them had ever tried using any VR system before. All of them gave their written consent to the experimental protocol that had been approved by the institutional review board.

3.1.4. Potentials and limitations of prototype multi-fingered haptic device

Fig. 3.7 shows the results of the preliminary experiments (Exp1 and Exp2). The left graph (a) is a fitting curb for the mean proportion of bigger responses in which participants felt the comparison stimulus was bigger than the standard stimulus. Error bars indicate a 95% confidence interval. The right table (b) shows the confusion matrix in which participants felt the stimuli in the rows matched the shapes in the columns.

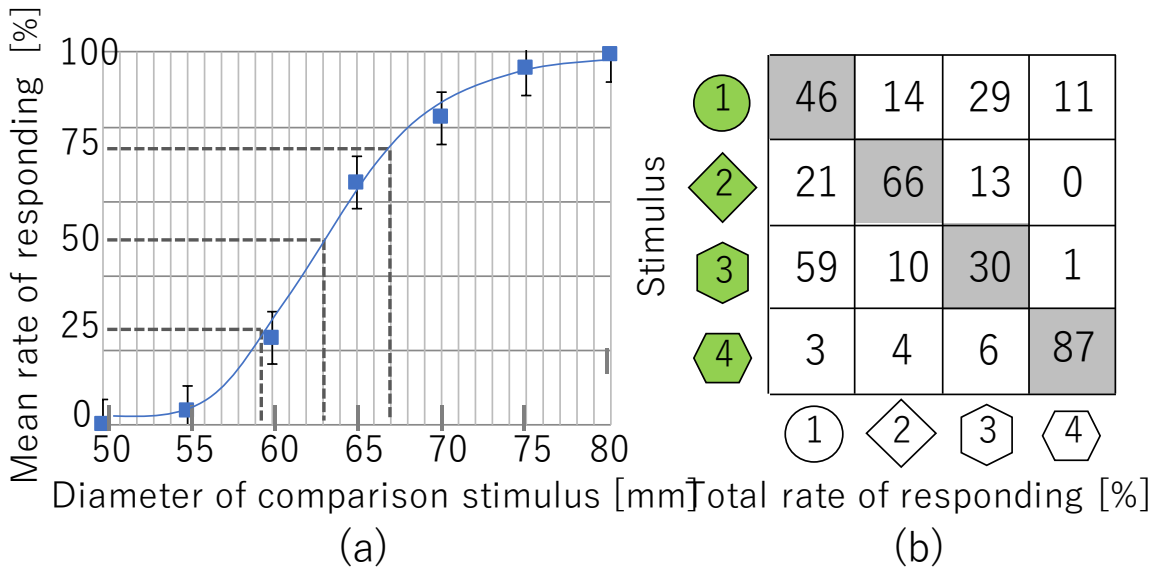


Fig. 3.7. Results of preliminary experiments. (a) Mean proportion of the case in which participants felt the comparison stimulus was bigger than the standard stimulus. (b) Confusion matrix in which participants felt the stimuli in the rows matched the shapes in the columns.

The Exp1 results suggest that this apparatus enables users to ascertain size differences between objects. In this study, participants were able to detect diameter differences of about 5 mm and volume differences of about 1.17 percent. Most participants tended to feel that virtual objects were somewhat bigger than real objects of the same size. This might be because they used only three fingertips to recognize virtual objects and so did not feel anything in their palm or other parts of their hands.

The Exp2 results indicate our proposed shape display makes it possible for users to ascertain shape differences between objects without visual information. In the experiment, the participants were able to identify the trapezoidal surface (Shape 4) and right-angle corner (Shape 2) correctly for the most part. However, the shape with 120-degree corners (Shape 3) was identified as a curved surface (Shape 1) 59 % of the time. This suggests that obtuse angle corners are difficult to recognize under these experiment conditions, and that the apparatus specifications and settings are not able to represent a seamless curved surface well.

The factors behind these difficulties are the apparatus parameters such as the number or size of actuating spheres, the degree of control accuracy, and the frequency of feedback cycles. However, it has the potential to improve operability in virtual environments and enable persons to better appreciate 3D objects by touching them. We confirmed that our approach and apparatus have possibilities to present 3D shapes and sizes of objects virtually, but we also confirmed that there are a number of difficulties and limitations relevant to the apparatus specifications.

3.2 Potential of using internal forces to present virtual surface using grasping-type ungrounded haptic device

The conventional force feedback devices that can present a sufficient force for preventing fingertip from penetration to a virtual surface are categorized as grounded-types. We have used grounded-type devices to clarify the potential of multipoint haptic feedback on a finger pad as described in Chapter 2. However, the method has a critical limitation that the possible explore area is restricted in a hemisphere with a diameter of about 20 cm. To improve this limitation, we consider using internal forces which are generated between fingers and thumb or fingers and a palm when human hand grasp an object. Then, we have prototyped a grasping-type ungrounded haptic device that can present a virtual surface without using external force from a fixture. Fig. 3.8 shows the difference between the grounded-type haptic device and concept of our proposed ungrounded-type haptic device.

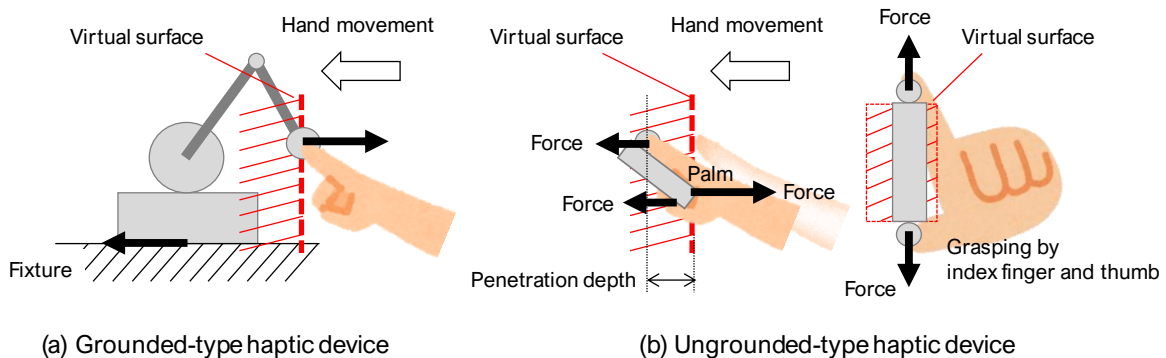


Fig. 3.8. Concept image of grounded-type haptic device and ungrounded-type haptic device.

3.2.1. Preliminary experiment

Fig. 3.9 shows our prototype device as an apparatus for the preliminary experiment. This ungrounded-type haptic device consists of three force feedback actuators (ALPS ALPINE, Haptic trigger) and a VR controller (Facebook, oculus touch R) as a grip body. The maximum output force and displacement of the actuator is 3 N and 7 mm respectively. When a user grasps the grip of the device and moves his/her hand into the virtual surface, the actuators push back the hand of user using the internal force generated between the holding grip and the palm of user's hand.

In the experiment, we evaluate the penetration depth when human hand feels the virtual surface from the applied force generated by the actuator. Although the VR controller has a function to detect 6 DoF motion of the device at 90 Hz, we use a highspeed motion capture system (Detect, L1 Tracker) which can detect 6 DoF motion of the device at 1000 Hz for the preliminary test. This is because the refresh rate of the feedback loop (at least 1000Hz) is another key factor to present a ridged virtual surface in the conventional force feedback device.

The experimental environment and condition are shown in Fig. 3.10. Participants asked to stop their hand when they feel the virtual surface under the one of three output force conditions (0.5 N, 1.5 N, and 2.5 N). To avoid several measurement errors, we prepare different thickness of virtual walls (10 to 100 mm with a 10 mm step) and only judged and recorded whether the participant's hand was stopped in the virtual surface or not as shown in Fig. 3.10. We recruited 8 righthanded participants aged 20 - 50. All of them gave their written consent to the experimental protocol that had been approved by the institutional review board.

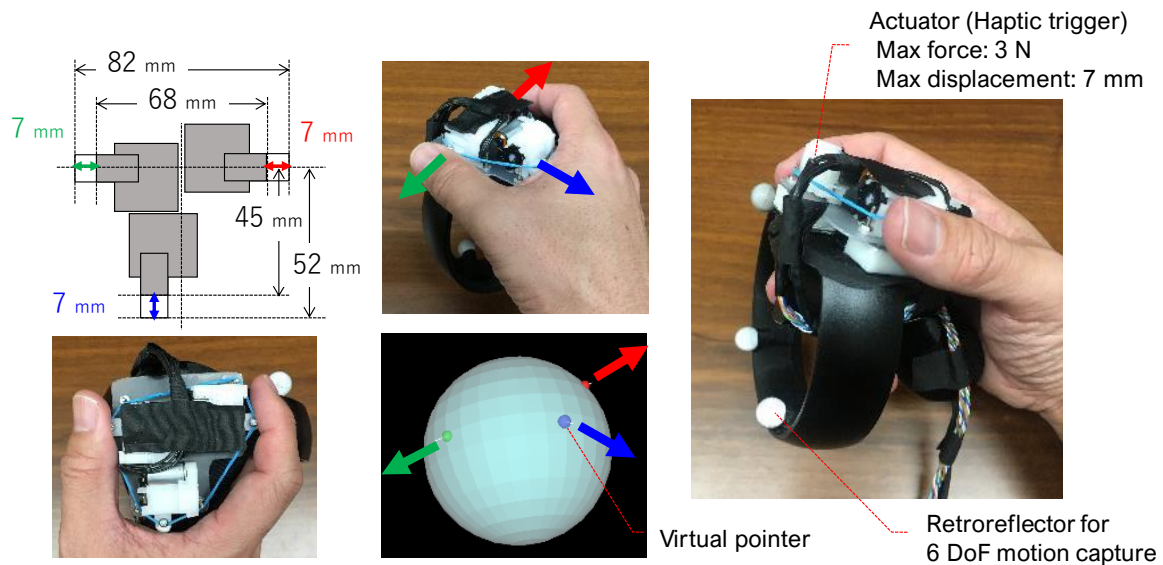


Fig. 3.9. Prototype ungrounded-type haptic device.

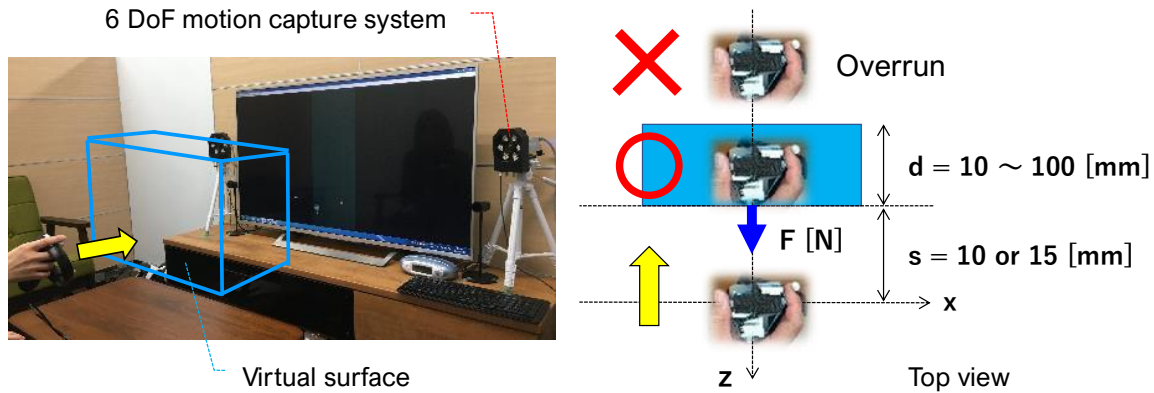


Fig. 3.10. Experimental condition and procedure.

3.2.2. Potentials and limitations of the grasping-type ungrounded haptic device

The experimental result is shown in Fig. 3.11. Fig. 3.11a indicate the mean penetration depth related to the output force of the actuator. From the result, the mean penetration depth at the condition of 0.5 N was larger than that of 1.5 N although the rise time of the force in each condition are same as shown in Fig. 3.11b. It is suggested that participants were not only judging from the momentary cues such as an impact force or vibrations but feeling the virtual resistance area from the consecutive force applied to their palm.

We have hypothesized that the impulse (force \times duration) is a key factor to present virtual surface to the user using inner force method. However, from the result, there was no significant difference between the conditions of 2.5 N and 1.5 N. It is suggested that the method of using inner force can present virtual surface, however, 2.5 N is not sufficient to be feel a rigid surface in this experiment condition. To improve this limitation, we try to investigate the following parameters to present more rigid virtual surface.

- Output force of actuator
- Refresh rate of force feedback loop
- Displacement of actuator

After several trials, we hypothesized that the maximum displacement of the actuator is the most critical factor for presenting the absolute position of virtual surface. This hypothesis will be confirmed using the grasping-type method that can actuate a haptic stimulus up to 40 mm displacement.

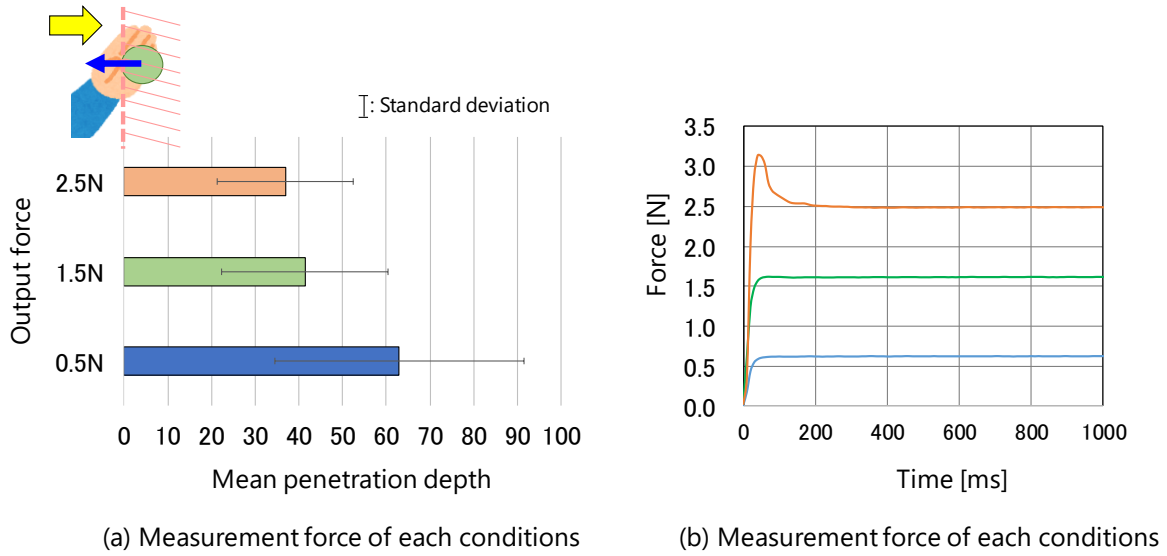


Fig. 3.11. Experimental result. (a) mean penetration depth related to the output force of the actuator, (b) measurement force of each conditions.

3.3 Development of a grasping-type haptic device “GraspForm” to present 3D shape and hardness distribution of virtual objects

3.3.1. Problems and related works

The presentation of haptic information in addition to visual and auditory information can be expected to further enhance user experience in next-generation media such as 3D TV, augmented reality (AR), and virtual reality (VR). Haptic information may make it possible, for example, to convey the hardness or softness and texture of an object, which is difficult when only visual or auditory information is available. The transmission of haptic information is also expected to realize a universal information service that can be simultaneously enjoyed by persons with vision or hearing impairment as described in Chapter 1.

The purpose of this research is to clarify the design guidelines for haptic devices that can be used by more people, including those with disabilities, and to develop haptic devices that enable users to recognize the shape and hardness of virtual objects to expand visual information. Here, we describe our developed grasping-type haptic device in detail, present the results of evaluation experiments, and discuss the results.

A device in which the pins arranged in a rectangular array has been proposed as a means of presenting the 3D shape [18][19][20] and the hardness [27] of a virtual object. These methods enable users to touch the virtual object using both hands, but the structure of the device makes it difficult to improve the spatial resolution. A method that takes a different approach presents the shape and hardness by reproducing the reaction force when the tip of a finger glove or pen is used to trace the surface of a virtual object [22][34]. This is one of the methods that provides the highest spatial and temporal resolution. We have investigated the possibility of recognizing the shape of an object without relying on vision by applying this method of haptic presentation to multiple fingertips and the palms of hands [32]. However, the method of using haptic feedback described above requires a fixture base of appropriate size and weight to serve as a fulcrum for applying the force to be presented.

Other proposals include a device that is attached to the user’s body so that the user’s body provides the reaction force base [36] and the housing of a device held in the hand serves as the reaction force base [12]. All of these proposed devices assume use in an AR or VR environment where visual information is also available. In addition to the issues raised in the previous studies, there is the problem of enabling users to know the shape and hardness of virtual objects, even without visual information. Considering the issues described above, we devised a way to present the reactive force from a virtual object reproduced by computer graphics to opposing fingers of the hand, such as the index finger and thumb or fingers and palm as shown in section 3.2.

When recognizing the shape of a 3D object by touch, it is important to explore the entire object with the hands to understand the overall shape, but to recognize the shape in detail, it is important to use the fingers to sense the contours [31]. We varied the number of haptic stimulation points for the pad of the index finger from one to five and confirmed that there is a significant improvement in understanding the contours of an object when there are four or more stimulation points compared with when there is only one point as described in section 3.1 [33]. We applied this knowledge to develop the GraspForm haptic device for spatially presenting the 3D shape and hardness distributions of a virtual object. In the next subsection, we briefly describe GraspForm and its control method [37][38].

3.3.2. Development of the GraspForm haptic device

The appearance of the GraspForm device and a demonstration system is shown in Fig. 3.10. The configuration of the system is illustrated in Fig. 3.11. The system can present the shape and hardness of a virtual object by controlling the state of a device in real space so as to always match the state of a CG object in a virtual space on a computer. The motion of the device is acquired with six degrees of freedom (6DoF) by a motion capture system (DITECT L1 Tracker) using a high-speed stereo camera at 1000 frames per second (fps). When the user wearing the device moves their hand to a point of contact with a virtual object, the shape of the object is presented to the user's index finger, thumb, and palm (Fig. 3.10).

GraspForm comprises four modules as illustrated in Fig.3.11 and described in Table 3.1. The modules can be used in various combinations according to the application. Module A presents the surface shape of the object to the index finger. It consists of four servomotors (HITEC HS-5035HD) and rack and pinion gears, which drive four touch effectors that are in contact with the pad of the index finger up to a distance of about 7 mm above and below the module to match the surface shape of the virtual object. The effectors are three-axis pressure sensors with a diameter of 6 mm (Touchence SP22-FFC15). A pressure vector is measured for each effector.

Module B uses an actuator (ALPS ALPINE Haptic trigger) to present the hardness of the part gripped by the user via GraspForm. Module C presents the surface position on the object at two points on the palm of the user. Module D is a 14-mm-thick platform on which modules A, B, and C are mounted. Built-in servomotors (HITECHS-5035HD) operate independently 10 mm above and below the module.

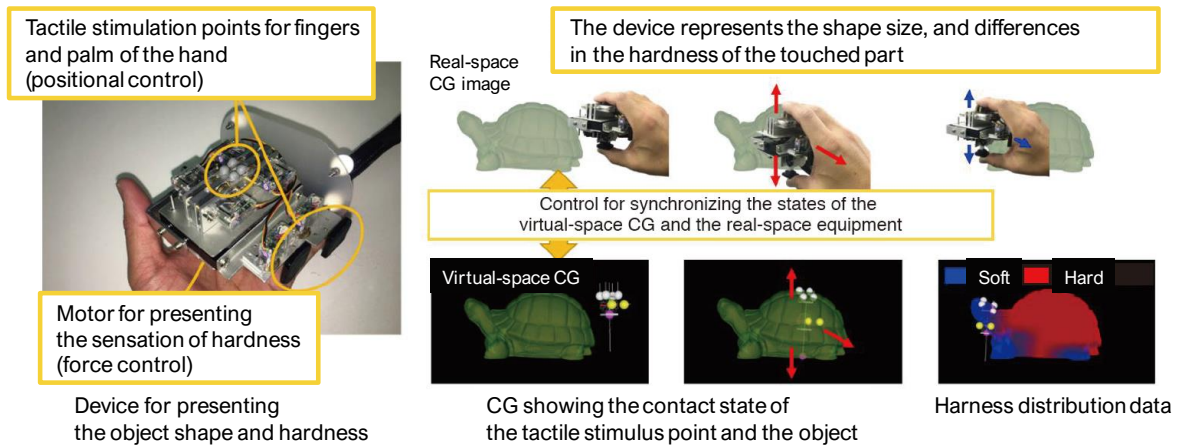


Fig. 3.10. Appearance of the GraspForm haptic device and implementation demo system.

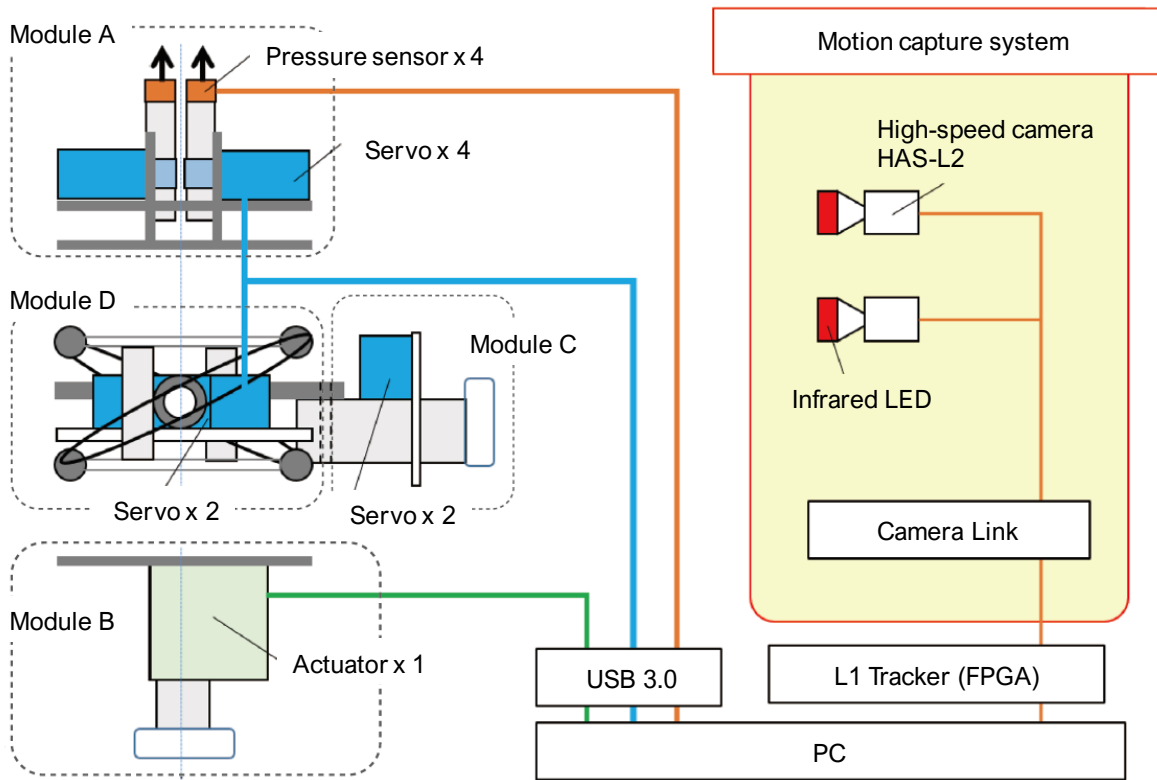


Fig. 3.11. Configuration of the GraspForm demo system.

Table 3.1. Specifications for the GraspForm modules.

	Module A	Module B	Module C	Module D
Control method	Position control	Force control	Position control	Position control
Translation	0.7 cm	0.7 cm	2.0 cm	1.0 cm x 2
Number of stimulus points	2 x 2	1	2	2
Stimulus area	1.3 x 1.3 cm ²	2 x 2 cm ²	2 x 2 cm ²	7 x 5 cm ²
Weight	60 g	30 g	50 g	50 g
Size	3 x 6 x 5 cm	4 x 3 x 2 cm	3 x 7 x 4 cm	2 x 7 x 5 cm

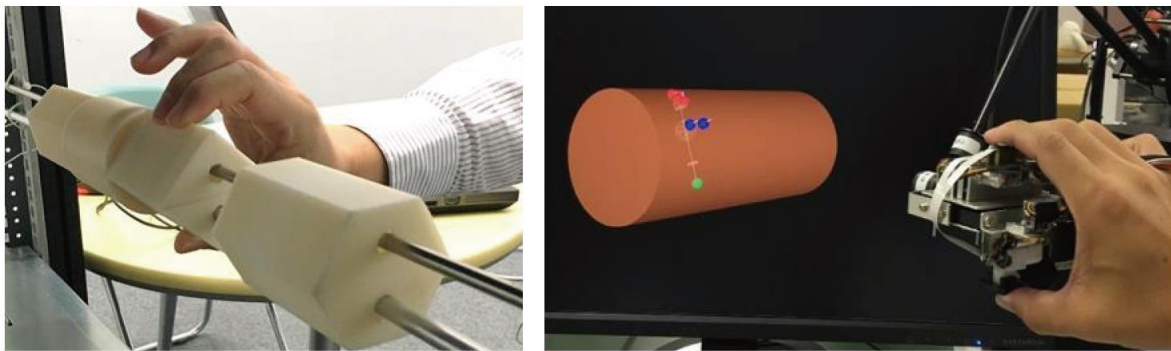
The two types of actuator control that are generally used in haptic devices are force control and position control. In force control, the generated actuator force is controlled according to the depth of haptic stimulation points that penetrate the surface of the virtual object. Most force control methods use encoders and actuators to detect translation or rotation. In position control, the position of the haptic stimulus point is controlled according to the force applied to the stimulus point. In most cases, feedback control with a force sensor and an actuator is used (refer to Appendix B for more details).

It is also possible to control the actuator so that the spatial position of the haptic stimulus point reproduces the absolute coordinates of the virtual object surface without using a force sensor [32][36]. GraspForm uses positional control for the index finger actuator (servomotor) and force control for the thumb actuator (control updating frequency of 60 Hz). Linear actuators based on DC motors are used and driven by pulse width modulation (PWM) control, which can maintain a linear relationship between voltage and output.

3.3.3. Evaluation of 3D shape presentation performance

(1) Experimental setup and method

The experimental setup is shown in Fig. 3.12. The experiment involved touching a real object with bare hands (Fig. 3.12a) and touching a virtual object with GraspForm (Fig. 3.12b). The virtual and real objects have the same size. The test participants were instructed to use the pads of the right index finger and thumb for touching. The cross sections of the four 3D shapes used as experimental stimuli are shown in Fig. 3.13. Shape 1 is a cylinder that is 60 mm in diameter and 80 mm in length. Shapes 2 and 3 are both hexagonal columns with dimensions designed so that they can be inscribed in a cylinder with a diameter of 60 mm, but shape 2 presents a flat surface to the touch and shape 3 presents the apex of an obtuse angle (120°). Shape 4 is a square prism with dimensions designed so that it can be inscribed in a cylinder with a diameter of 60 mm and presents a right angle to the touch.



(a) Bare hand (real object)

(b) GraspForm (virtual object)

Fig. 3.12. Experimental setup for recognition of 3D shape by touching.

For all the experimental conditions, the stimulus shapes were fixed in space, the subjects were blindfolded, and the subject's hand was guided to a position near the shape. The participants were then instructed to begin touching. They first memorized the correspondence between the shapes and their numbers, and then the stimulus shapes were presented to the participant in random order. The participants touched the top and bottom of each object and responded by voice with the number of the shape. The touching method involved placing the index finger on the top of the shape and the thumb on the bottom of the shape, and then moving the entire hand forward and backward once as shown in Fig. 3.13. The participant's eyes were covered with a mask and the noise that masks the sound of the device operation was presented by a speaker so that the operating state of the device could not be known from its sound. Each participant performed 80 trials (4 shapes \times 20 times).

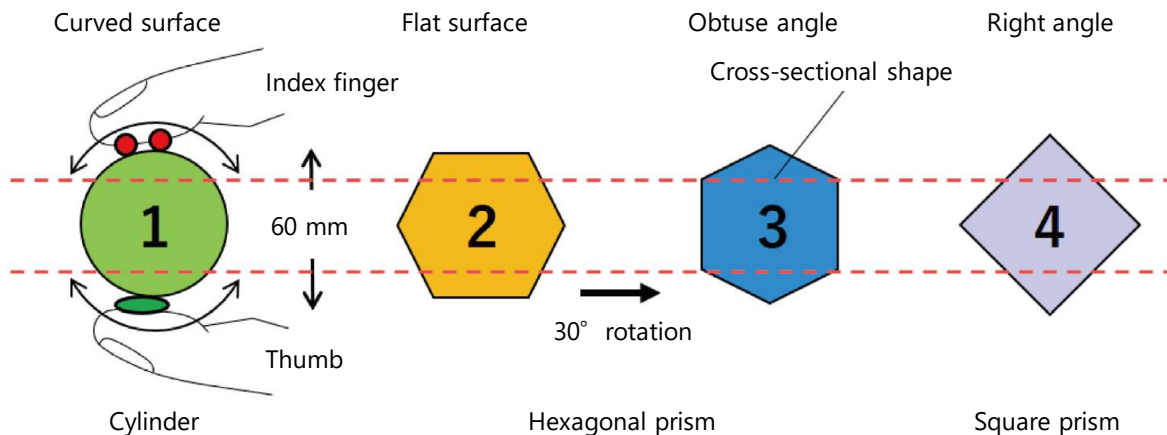


Fig. 3.13. Cross section of the stimulus shapes used for 3D shape recognition experiments.

(2) Results

The confusion matrices for the participant responses are shown in Fig. 3.1.4. Fig. 3.1.4a presents the results for barehand touching. We can see, for example, that the cylindrical shape was distinguished from the other three shapes in 100 % of the trials. Fig. 3.1.4b shows the results for touching a virtual object with GraspForm. We can see that, for example, a cylindrical shape was misrecognized as an obtuse angle of a hexagonal column in about 11 % of the trials. The data from Fig. 3.1.4b is presented as a bar graph in Fig. 3.1.5 for the statistical comparison of the differences in average values. In Fig. 3.1.5, the four shapes are referred to simply as “curved”, “flat”, “obtuse angle”, and “right angle”.

(3) Discussion

We can see from the results presented in Fig. 3.14a that the four stimulus shapes can be identified without visual information when real objects are touched with bare hands. The observation of the experimental situation revealed that there was one case in which a response was made immediately after touching the curved surface, which is the side of the cylinder. For other shapes, however, it is

likely that a few percent of the shape recognition errors can be attributed to the location at which the subject first touched the object and the variation in the speed of moving the hand back and forth.

The results presented in Fig. 3.14b and Fig. 3.15 show that participants were generally able to distinguish the curved surface and the right angle, although this was not the case for the real objects. The results for the flat and obtuse angle stimuli were also significantly higher than the chance level (25 %), revealing that the participants were able to at least identify the approximate shape. For the haptic recognition of the flat and obtuse angle stimuli, however, about half of the responses did not distinguish the two stimuli or confused them with right angles. This is considered to indicate the limit of the presentation performance for the number of haptic stimulation points of GraspForm and the actuator control with an update frequency of 60 Hz.

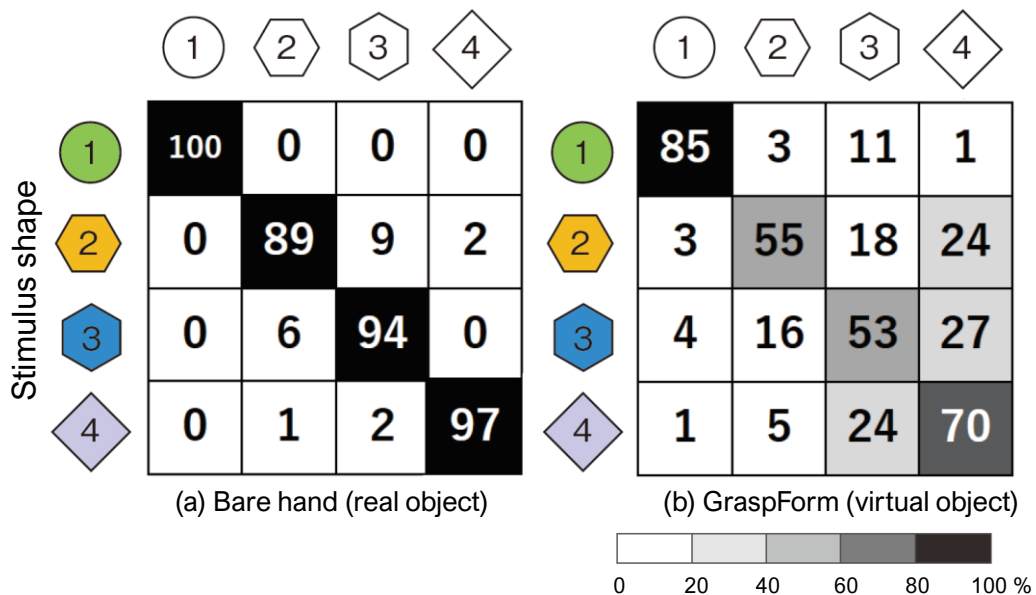


Fig. 3.14. Confusion matrices for subject responses. (Average values for 12 subjects rounded to whole numbers)

To achieve the presentation performance for 3D shapes that is equivalent to touching real objects with bare hands by using the approach described here, the number of stimulation points and the control frequency of the actuator must be increased. It has been reported that, in general, masking the sensation of the skin on the fingers significantly reduces the ability to distinguish concave and convex shapes, and we have also confirmed through preliminary experiments that the rate of correct response dropped to about the chance level when participants were wearing gloves made of 3-mm-thick synthetic leather. We considered the possibility that the shape presentation performance of GraspForm in the experiments presented here would be better than that when touching real objects while wearing a 3-mm-thick glove. In future work, we would like to verify the degree of skin sensation masking to which the shape presentation performance of GraspForm is equivalent or the degree to which the performance approaches the sensation of bare skin.

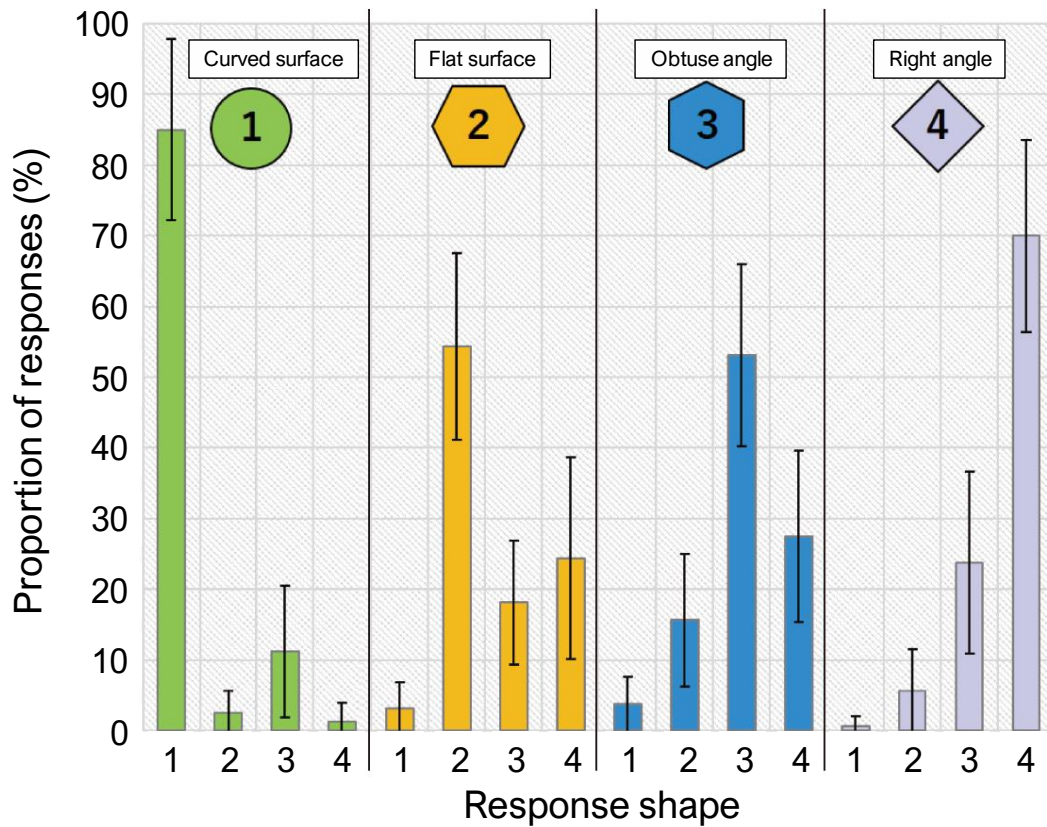


Fig. 3.15. Proportion of subject shape responses for each virtual object stimulus shape (Averages for 12 subjects; the error bars indicate the 95% confidence interval)

3.3.4. Evaluation of presentation performance for object hardness

We performed experiments to evaluate the presentation of hardness when GraspForm is used to handle virtual objects. We then evaluated the presentation of hardness to obtain guidelines for the design of a device that presents hardness.

(1) Experimental setup and method

Humans use deep sensation to perceive the rigidity (elasticity) of an object from the relationship between the amount of depression and the reactive force [29]. The area of contact between the finger pad and the object and the distribution of pressure in that area have also been indicated as a mechanism for perceiving hardness and softness. A method of presenting a sense of softness by reproducing the relationship between the pushing force and the contact area has also been proposed [30]. In the research presented here, the spring constant, which is considered to correspond to the hardness (elasticity) of the virtual object, is taken as a parameter and the hardness is presented by controlling an actuator according to the parameter. The objects were limited to linear elastic bodies

(referred to simply as elastic bodies below). Assuming that humans recognize the hardness of an elastic body by pinching between the thumb and the index finger, hardness was presented to the index finger and thumb of subjects wearing GraspForm.

In the experiments, the hardness of the elastic body was assumed to be recognized by a pinching movement of the index finger and thumb. The hardness presented by GraspForm was compared with that of a real elastic body (compression coil spring). The participants used a pinching movement of the thumb and index finger of the right hand to compare the hardness presented by GraspForm with that of the reference compression coil springs. The hardness of GraspForm, which is the comparison stimulus, was then changed by adjusting the duty ratio (DR, %) of the PWM control so that the subjects felt the same hardness from GraspForm and the coil spring reference stimulus. In this way, the relationship between the reference stimulus hardness and the hardness presented by GraspForm was obtained.

The reference stimuli used in the experiments are shown in Fig. 3.16. The hardness of the contact surface of the standard stimulus and the spring constants (N/mm) of the coil springs are listed in Table 3.2. The material of the contact surface was ABS resin for reference stimulus A and silicone rubber for reference stimulus B. For both stimuli, the dimensions of the contact surface were 16 mm \times 23 mm \times 5mm. Reference stimulus A had a contact surface hardness of 90 as measured using a rubber hardness measurement instrument (JIS K6253 Durometer Shore A). Compression coil springs with seven different spring constants (0.6, 0.8, 1.3, 1.8, 2.1, 2.5, and 2.9) were used for the stimuli. The contact area hardness for reference stimulus B ranged from 10 to 90 in increments of 10 as measured using the rubber hardness tester. The spring constant of the compression coil springs was 2.5 N/mm.

In the experiments, the two reference stimuli (A and B) were presented at random. Informed consent was obtained from the 12 participants, who were right-handed and ranged in age from 30 to their 50s. Each participant performed 32 trials (two trials for each of the 16 reference stimuli).



Fig. 3.16. Reference stimuli A (upper) and B(lower)

Table 3.2. Contact surface hardness and spring constants of compression coil springs (N/mm) for reference stimuli A and B (A is ABS resin and B is Silicone rubber)

A	Contact surface hardness	90	90	90	90	90	90	90	-	-
	Spring constant	0.6	0.8	1.3	1.8	2.1	2.5	2.9	-	-
B	Contact surface hardness	10	20	30	40	50	60	70	80	90
	Spring constant	2.5	2.5	2.5	2.5	2.5	2.5	2.5	2.5	2.5

(2) Results

The DRs for the PWM control when the hardness presented by the GraspForm actuator is judged to be the same as that of reference stimulus A are shown in Fig. 8 (average values for 12 subjects, error bars indicate the standard deviation, and the coefficient of determination¹⁶ R^2 of the regression line¹⁷ is 0.9335). The DRs for which the hardness presented by the actuator is the same as that of reference stimulus B are shown in Fig. 9 ($R^2 = 0.9941$).

We can see from the results presented in Fig. 8 that the hardness of compression coil springs with spring constants from 0.6 to 2.9 N/mm can generally be presented within the DR range from 0 to 100% when PWM control is applied to the actuator (maximum presentation force of 3 N). Although there was a large variation in the absolute value of perceived hardness for the subjects, there were no cases in which the relationship between the DR and the hardness of reference stimulus A was reversed in the data of individual subjects.

From the results presented in Fig. 9, we can see that, for the same spring constant, presentation is possible within the DR range achievable with PWM control, even when the contact surface hardness was varied from 10 to 90. In this case, two of the subjects responded that they were unable to reproduce the hardness of reference stimulus B of 70 or higher, even for a DR of 100% (the presented hardness was limited by the force generated by the actuator). In the same way as for reference stimulus A, however, there was no case in which the relationship between the DR and the hardness was reversed.

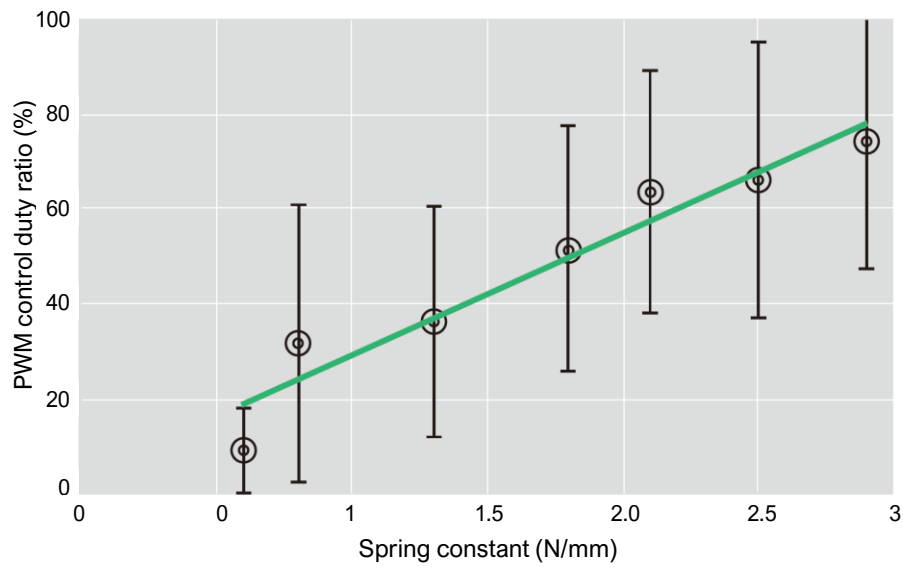


Fig. 3.17. Duty ratio for which the hardness presented by the actuator was felt to be the same as that presented by the reference stimulus A springs (Average values for 12 subjects; error bars indicate standard deviations)

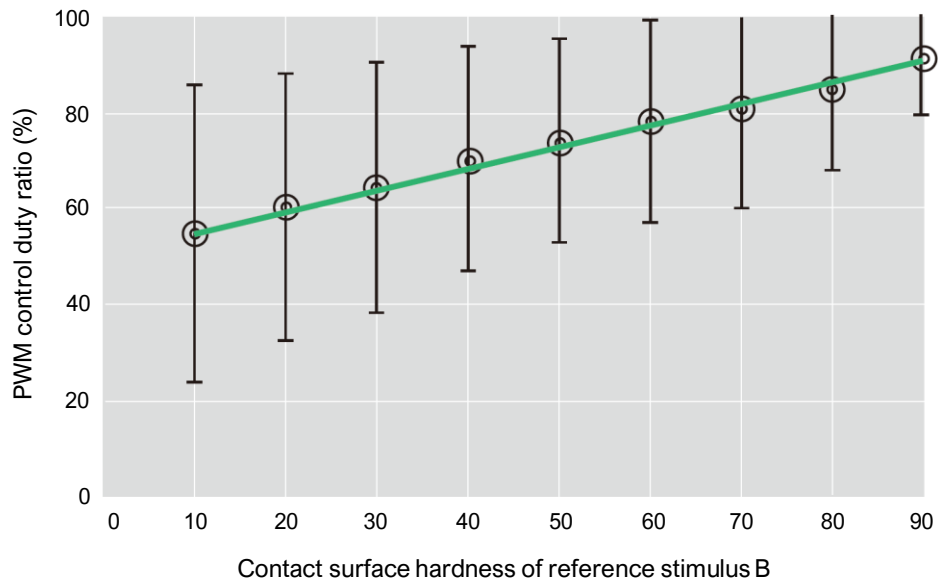


Fig. 3.18. Duty ratios for which the hardness presented by the actuator was felt to be the same as that presented by the reference stimulus B springs (Average values for 12 participants; error bars indicate standard deviations)

(3) Discussion

The results presented above show that the subjects were able to perceive differences in relative hardness for both reference stimulus A and reference stimulus B. The variation in the output of the actuator (DR of the PWM control) perceived as the hardness of the real object was greater than expected. This is considered to result from differences in the characteristics of the actual springs and the actuator. Specifically, differences in finger pressure and the method of determining hardness among the test subjects are considered to be one factor causing the large variation seen in the experiments. The method of determining hardness was not limited in the experiments, and each subject was free to determine hardness by performing the pinching operation.

The comments made by the subjects after the experiments revealed that some subjects, to the extent possible, applied a constant force to the spring and made the determination from the difference in displacement; others made a pinching movement with the same rhythm while keeping the displacement the same, as much as possible, in determining hardness from the magnitude of the pressure on the fingers (load on the fingers).

Investigation of the hardness presentation method on the basis of the results presented above, we have implemented and adopted a new hardness presentation scheme for GraspForm in which the difference in the relative hardness of the parts of virtual objects is presented rather than the absolute hardness of the object. The relative hardness presentation approach is a way of dealing with the variation in hardness perception across users, and we believe that hardness can be presented in a way that the characteristics of the target object can be easily understood, without saturation due to actuator performance.

In this method, the actuator output is controlled by PWM according to data consisting of the set of hardness values for all of the virtual object voxels within a range that does not exceed the maximum presentation force of the actuator. First, the reaction force from the virtual object (F_0 [N]) is calculated as the product of the displacement (d [mm]) of the actuator caused by the pressure of the user's finger and the hardness value set for each voxel (c ; 0 to 1.0 [N/mm]). Then, the actuator is controlled by setting the DR of the PWM control to the value of $(100 \times F_0)/F_{\max}$, where F_{\max} is the preset value for the maximum presentation force of the actuator. This method is considered to improve the reproducibility of the difference between the soft and hard parts of a virtual object. We will test the ability of the control system to present the optimum hardness with respect to the performance of the actuator in future work.

3.4 Conclusion

In this chapter, we have developed a haptic device that can present the 3D shape and hardness of a virtual object in air towards implementing a universal information device. Basic experiments with the device revealed that users are able to understand the shape and hardness of virtual objects, even without visual information. The results of shape recognition experiments show that subjects using this device can distinguish shapes by touching each side of a cylinder, a hexagonal prism, and a square prism, all having a diameter of 60 mm. An experiment was also conducted to present hardness using a real spring with a spring constant between 0.6 and 2.9 N/mm as a reference stimulus, and the results showed that discrimination is possible. In future work, we intend to further improve the presentation performance for shape and hardness, and move forward with the research and development of haptic devices for implementing specific services.

Chapter 4

Grasping-type haptic devices to present impact sensation between moving objects

In order to establish a method for the second purpose, we developed a grasping-type haptic device that converts contact timing between objects in a movie scene into haptic stimulation. We clarified that this method can present the direction of an impact more intuitively compared to the condition of vibration alone. Then, the masking effect when simultaneously presenting a concave stimulus and a vibration stimulus to the palm was verified from the relationship with the spatial resolution of the haptic sense of the palm, and the problems were clarified. In addition, our proposed method for simultaneously presenting vibration and concave stimuli can be applied to a method of explicitly presenting the target object. This is a factor that greatly affects the sense of self-attribution which is one of the issues when applying haptic stimuli to visual media.

4.1 Method to present direction of impact force applied to an object

4.1.1. Problems and related works

Haptic devices have become increasingly popular, since many interesting research results have been revealed [40]. We have developed ball-type haptic devices to present intensity and momentum, which provide the real thrill of sports. Haptic information will also be helpful for intuitive expression of speedy game at sporting event that are difficult to convey in words for visually impaired people. However, our previous method could not present the direction of impact force applied to the ball.

Vibration is commonly used to present impact force in AR/VR environments [41][42][43]. For presenting direction, there are wearable vibrotactile interfaces for aiding the visually impaired to navigate through their surroundings [44][45][46]. Kim et.al, show clear impact stimuli using a 2 degrees of freedom (DoF) haptic actuator with a permanent magnet and direction-controlling solenoids [47]. However, these methods could not present the rich impact vibration. In this section, we make the following contributions. 1. User study evaluating directional recognition using our four types proposed device without visual cues. 2. Haptic device that presents 1 DoF impact direction with vibrations applied to a ball.

4.1.2. Prototype methods and apparatus

We developed four types of haptic interface to clarify key factors that make users feel the direction of impact sensations (Fig. 4.1). Figure 1a is a sponge ball ($\varnothing = 70$ mm) with built-in one vibrator that presents rich vibrations as a standard for comparison. Figure 2a is a sponge ball with built-in two vibrators that can vibrate each side of the ball independently. Figure 2c is a sponge ball with built-in one vibrator and two servo motors that can stick out each side of the ball independently. Figure 2d is our proposed haptic display that can pull in each side of the ball independently with rich vibrations.

We hypothesized that pulling in or denting mechanism has following two advantages compared to sticking out or convex mechanism. 1. The force required to dent the surface of the ball is mainly depends on the elasticity of the sponge ball. This allows us to design a mechanical denting structure without having to examine user's varied grasping power. 2. The denting stimuli can present passive perception that is similar to the real phenomenon when a ball is hit by something.

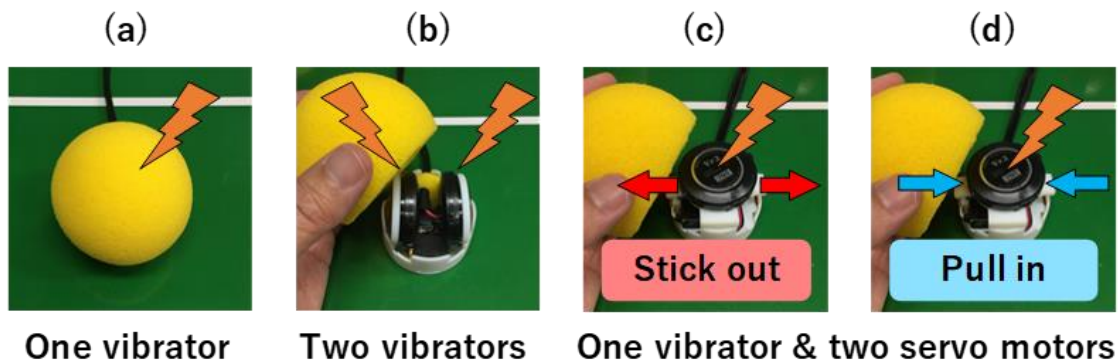


Fig. 4.1. Four types of ball-type haptic display with built-in (a) one vibrator, (b) two vibrators, (c)(d) one vibrator and two servo motors. All vibrators are same device (Acouve, Vp210).

4.1.3. Preliminary experiment

We confirmed whether the user could feel the impact direction of the ball using our proposed haptic displays. Participants were asked to sit on a chair in front of the experimental apparatus and grasp a ball-type display in their right hand. They were also asked to wear noise-canceling headphones producing white noise during an experimental sequence. A blindfold box was used to cover their right hand so that participants could not visually determine the haptic cues. Seven (one male and six females) right-handed participants having an average age of 36.7 (22 – 50) took part in the experiment.

Hb1 means impact vibration stimuli using the device showed in Fig. 4.1a. Hb2L/R mean impact vibration stimuli side L/R respectively. Hb3L/R mean impact vibration with convex stimuli on the side L/R respectively. Hb4L/R indicate impact vibration with dent stimuli on the side L/R respectively. Then, two different tasks of experiments were conducted in the completely same apparatus and

conditions. In the experiment 1, participants were asked to respond the question of “Which side of the grasping ball was stimulated?”. On the other hand, they were asked to respond the question of “Which direction the grasping ball will be flying?”.

Participants were asked to verbally respond with the three alternatives (left, neither left nor right, right) for each of two experiment. Each participant performed 84 trials (7 conditions × 12 times) in pseudo random order. Informed consent was obtained from all individual participants included in this study. All procedures performed in studies involving human participants were in accordance with the ethical standards of the institutional committee and with the 1964 Helsinki declaration and its later amendments or comparable ethical standards.

Experimental conditions



Three alternatives



Fig. 4.2 shows the experimental conditions and three alternatives for the response of participants.

4.1.4. Results and Discussion

Fig. 4.3. and Fig. 4.4. show the mean proportion of answers of experiment 1 and experiment 2, respectively. Note that participants answered whether the ball will move to their left or right after the impact cues in the experiment 2 (Fig. 4.4). The results indicate that the participants seem to feel vibrating side (Hb2L/R) and convex side (Hb3L/R) as the moving direction, however, there are considerable variation between individuals.

On the other hand, participants feel denting stimuli (Hb4L/R) as the moving direction that is opposite to the denting side of the ball. We use this significant effect to design our application demo system (see detail in Chapter 5). Our proposed method has been experimentally confirmed to be effective in making the user perceive the direction of the impact applied to the ball.

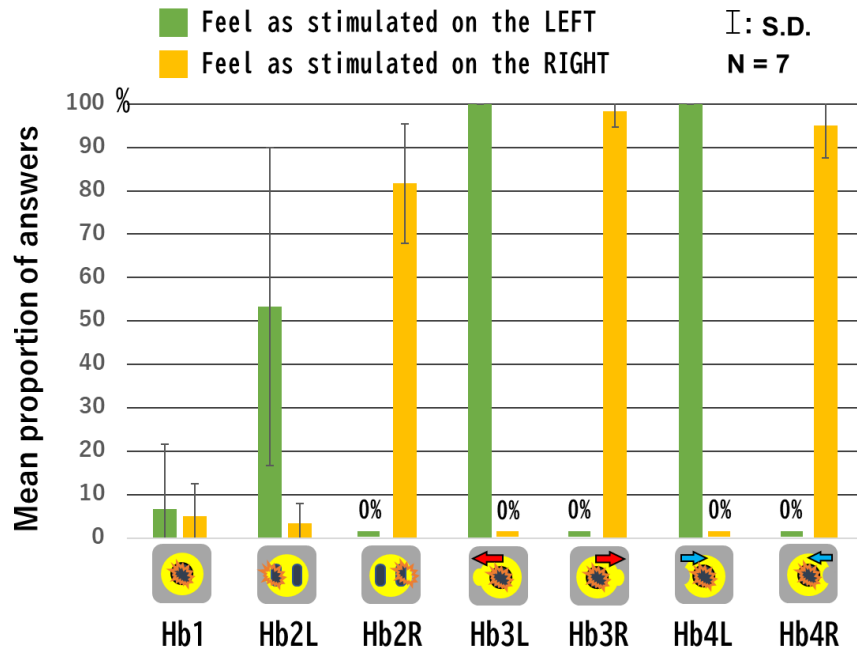


Fig. 4.3. Mean proportion of answers of experiment 1.

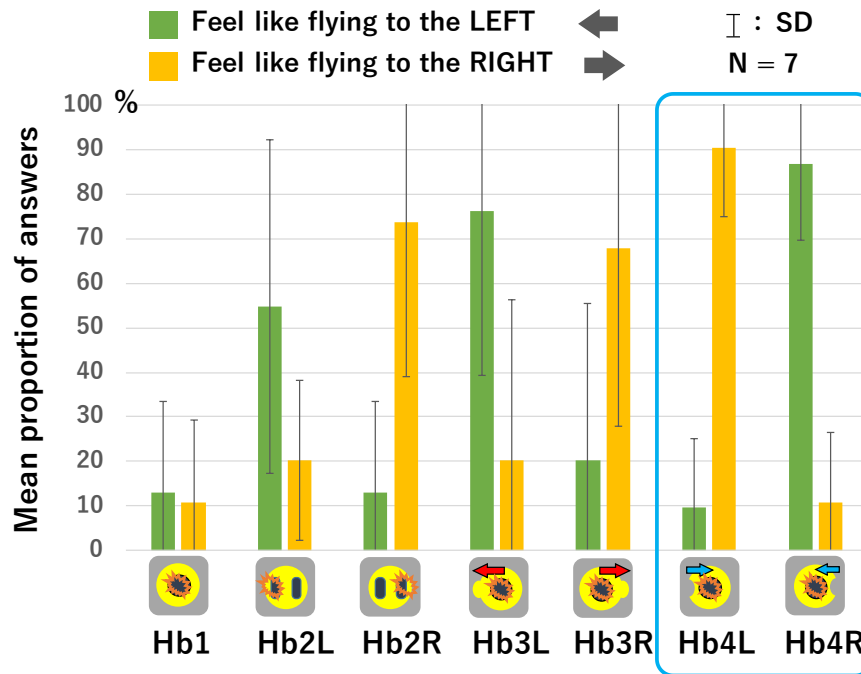


Fig. 4.4. Mean proportion of answers of experiment 2.

4.2 Grasping-type haptic device to present impact points with vibrations

4.2.1. Related Works

For presenting direction, there are wearable vibrotactile interfaces for aiding the visually impaired to navigate through their surroundings. Most uses four or eight cardinal positions around the human back, torso, and wrist to present direction information using vibrators [44][45][46]. There are also handheld direction interface systems that do not use vibrations. Amemiya et al. [48] proposed a method to navigate users in eight cardinal directions with pseudo-attraction force. Antolini et al. [49] proposed direction indicator using the gyro effect.

The following two types of direction displays are suitable for use in combination with impact vibration. One is a skin stretch feedback interface system for fingertip [50], and the other is a 2 degrees of freedom (DoF) haptic actuator using a permanent magnet and direction-controlling solenoids [47]. Azuma developed a vibration cube to intuitively convey various pieces of information such as ball direction in sports programs [51]. This cube-shaped device is sized to fit in the user's hands, and each face can be vibrated independently. However, it could not present the intense impact. This research suggested that the information of impact position plays an important role to present impact direction.

4.2.2. Development of Grasping-type haptic device "Hapto-ball" to present impact points with vibrations

We previously developed a grasping-type haptic device to present impact vibrations that depend on the amount of a ball's estimated acceleration during real sports events (see details in Chapter 5). As stated above, we assumed that the information of impact position plays an important role to present impact direction. Therefore, the grasping-type haptic device "Hapto-ball" which we propose in this section, is equipped with denting surface mechanism to present the impact points as well as the impact vibration.

Hapto-ball is made of elastic material so that the spherical surface elastically comes into contact the human hand and the force required to concave (not convex) is mainly depends on the elasticity of the ball. This allows us to design a mechanical denting structure without having to examine user's varied grasping power.

(1) Device design

Fig. 4.5 illustrates the structure of Hapto-ball. Four servo motors (Kyoritsu, WR-EC155) and one vibro-transducer (Acouve, Vp408) are covered with a 90-mm sponge ball with a polyurethane surface. The green (or right gray in B/W print) dots and lines in Fig. 4.5 indicate nylon strings connecting the servo horns to polyurethane surface. The dent points are arranged in eight positions. All dent points are arranged in 35 mm from the central axis of the ball so that most people will be able to touch all eight dent points in one hand.

The distance between the adjacent dent points are 30 mm. As shown in Fig. 4.5, the dent displacement (d) mainly depends on the length of the horn (w) and the rotation angle (θ) of the servo motor. In addition, the elasticity of the ball is an important factor. we measured the elasticity of the

ball as Young's modulus using a softness measurement system (Tec Gihan, Yawasa MSES-0512). The Young's modulus of the dent point is approximately 96.3 kPa (mean value of ten measured data, SD: 0.94).

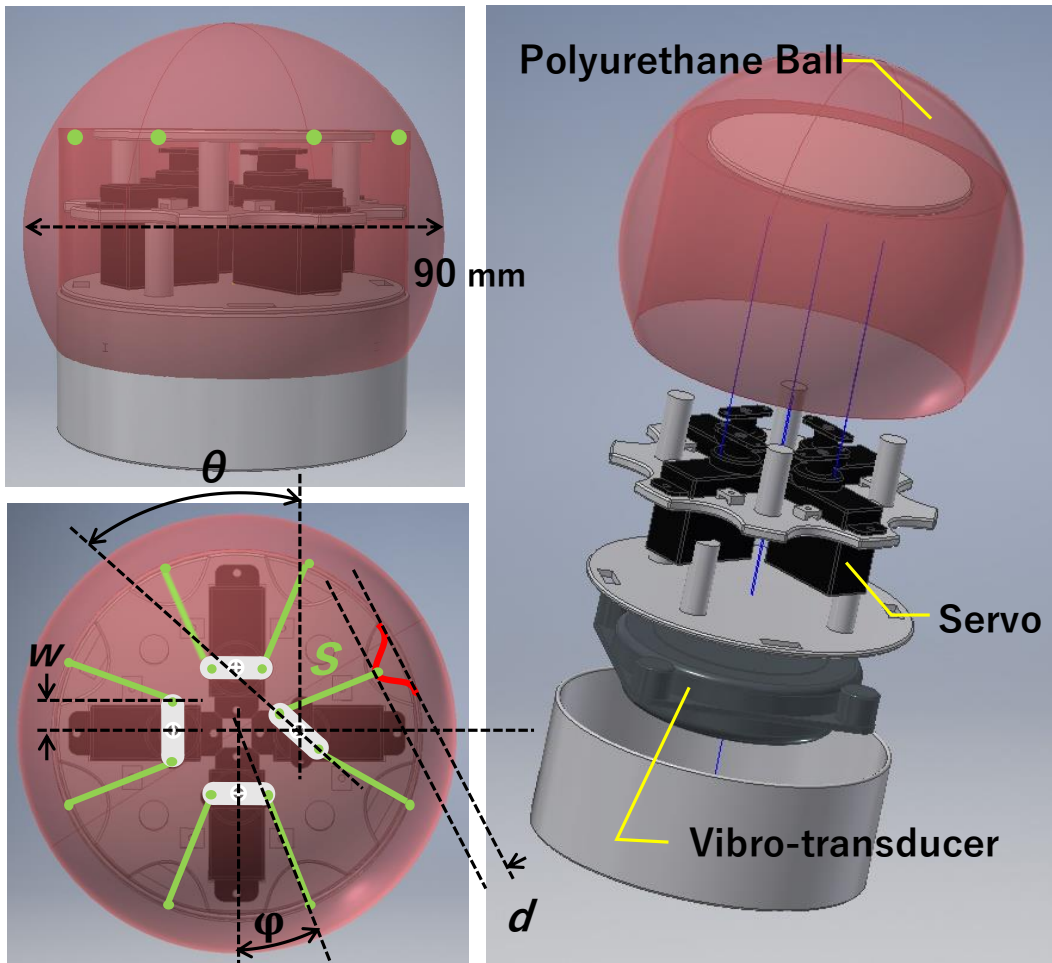


Fig. 4.5. Structure of proposed grasping-type haptic device Hapto-ball.

Fig. 4.6 shows the mechanism that the surface of the ball is dented by a servo motor with a nylon string. The torque (τ) of a servo motor is 0.98 N·mm. Therefore, the calculated value of a tensile force that is generated by a servo motor to the surface of the ball is approximately 2.09 N ($= \tau / w \cos \phi$, $\tau = 0.98$ N·mm, $w = 0.5$ mm, $\phi = 20^\circ$, see Fig. 4.5). This tensile force is sufficient for the elasticity of the ball (96.3 kPa = 0.0963 N/mm²) to dent the surface at least 3 mm.

The surface of the ball pushes back the user's skin by elastomeric restoring force when the servo horn return to the default angle ($\theta = 0^\circ$). The four servo motors are controlled using a microcontroller (Arduino SRL, Arduino Nano), and the input signal from a PC (Apple, MacBook pro, mac OS X) to the vibro-transducer is amplified by an audio amplifier (Rasteme Systems, RSDA202), as shown in Fig. 4.7.

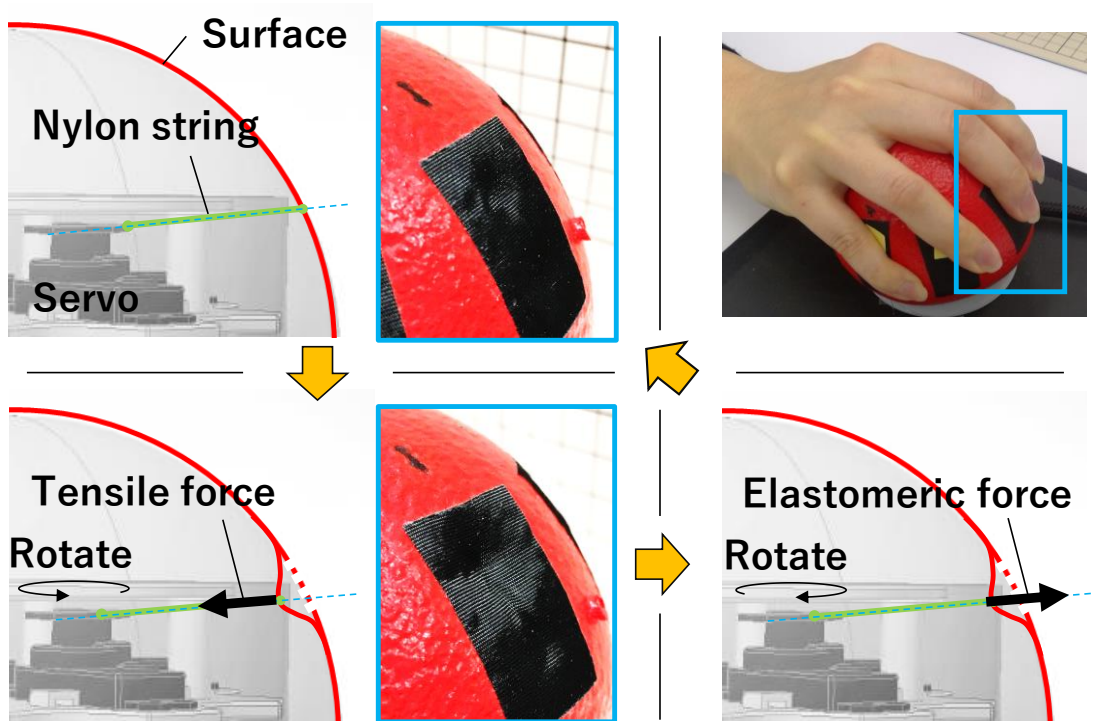


Fig. 4.6. Surface denting mechanism

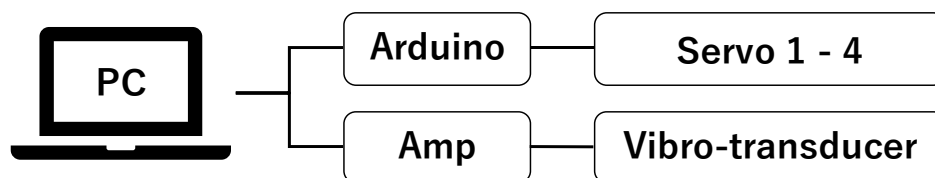


Fig. 4.7. System schematic diagram

(2) Basic performance

It is possible to calibrate the variation in displacement to adjust the tension of the nylon strings and rotation angle of the servo motors. Fig. 4.7 shows the measured displacement data of each dent point using a laser displacement meter (Keyence, IL-300) when each servo was driven by a pulse width modulation (PWM) signal, after displacement calibration.

To present impact vibration during sporting events, the dynamic range of vibration intensity is important. Therefore, amplitude-frequency characteristics which stimulate user's hand should be obtained. In this work, we conducted a measurement of the maximum acceleration of the surface of ball-type device using a digital vibration meter (Showa Sokki, 1332B). Fig. 4.8 shows the acceleration measured at the top of the ball-type device when 10-V_{pp} sinusoidal vibration frequencies of 30, 80, and 250 Hz were input to the vibro-transducer. These frequencies were selected by referencing previous studies [4][5][6] for the sake of discussing the vibrotactile masking effect, which is described in Sections 4.2.3 and 4.2.4.

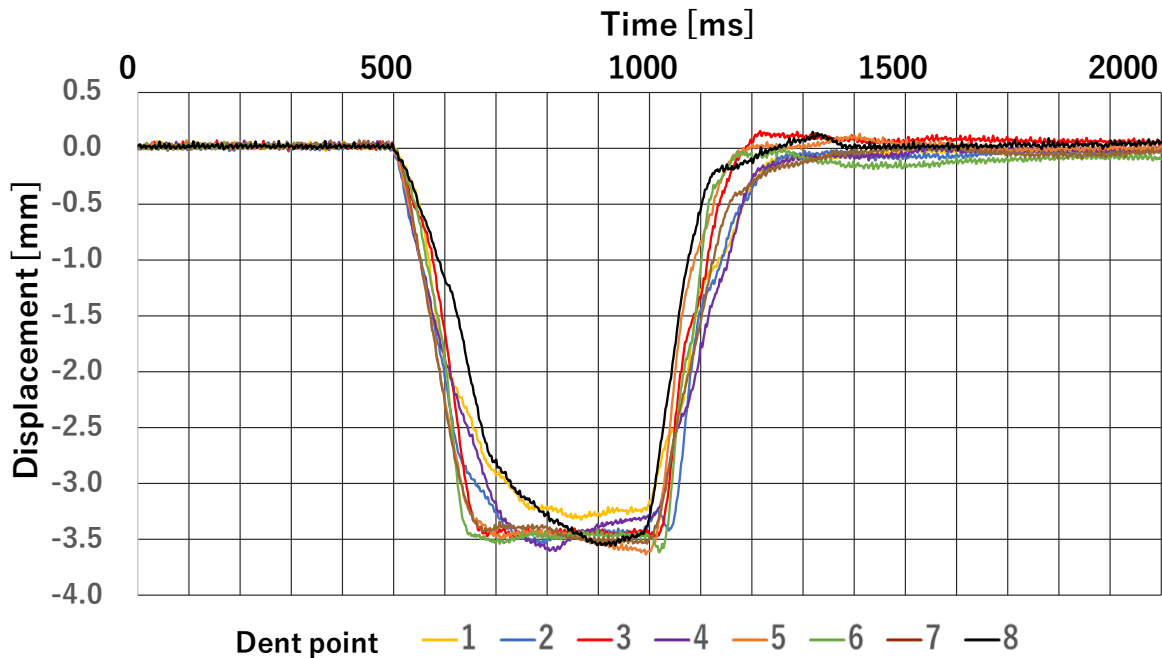


Fig. 4.8. Measured displacement of each dent point after manual adjustment of rotation angle for each servo motors.

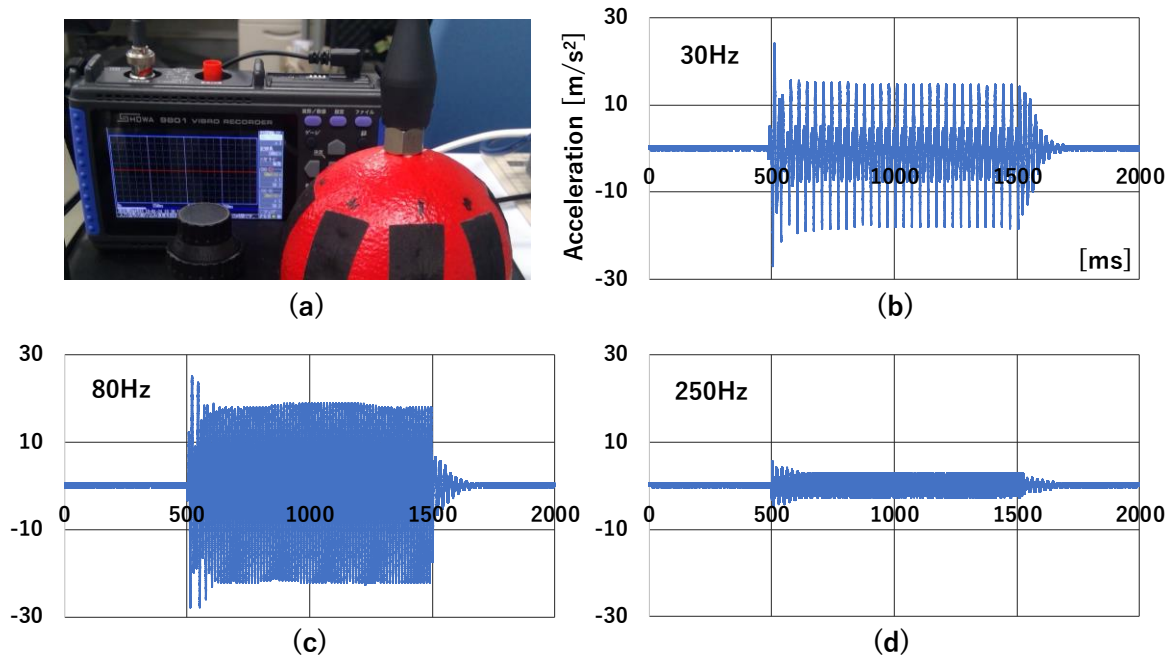


Fig. 4.9. Acceleration measured at top surface of ball-type haptic interface when 10-V_{pp} sinusoidal pedestal signals of 30 (a), 80 (b), and 250 Hz (c) were input to vibro-transducer.

4.2.3. Experiment

In this experiment, we assumed that a reduced pressure sensation produced by the dented surface is perceived independently from vibrotactile sensations. There are many parameters to consider for clarifying a series of tactile sensation masking effects, i.e., time gap, intensity, and frequency. As a first step, we confirmed whether the user could detect the dent points with the vibro-transducer's maximum amplitude of the continuous vibration.

(1) Experimental setup

As shown in Fig. 4.10, participants were asked to sit on a chair in front of the experimental apparatus and grasp the ball-type interface in their right hand to touch all eight dent points. They were also asked to wear noise-canceling headphones producing white noise during an experimental sequence. A blindfold box was used to cover their right hand so that participants could not visually determine the dented points. To avoid influence of a participant's memory, there was an indicator to represent the eight dent points.

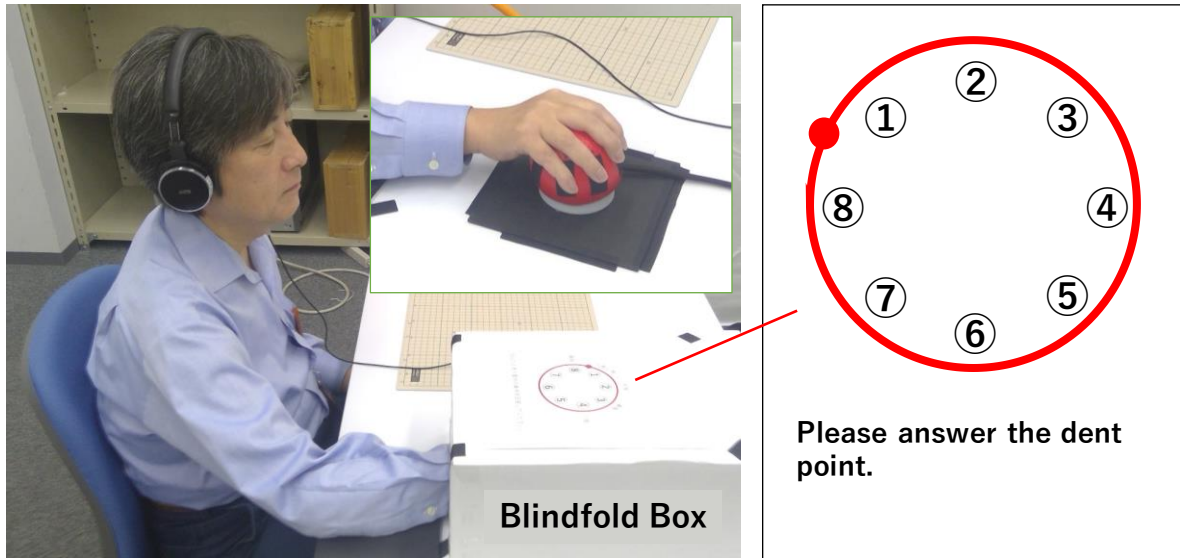


Fig. 4.10. Experimental setup

(2) Participants and procedure

Fourteen (two males and twelve females) right-handed participants having an average age of 43.1 (22 – 50, SD: 7.63) took part in the experiment. Fig. 4.11 shows the timing chart of the source signals in this experiment. White noise was first played through the headphones. Pedestal vibration was then presented through the vibro-transducer from 300 to 1200 ms. One of the points was then dented from 500 to 1000 ms. Participants were asked to verbally respond with the dented point number whenever they perceived the surface was dented. As stated above, the pedestal vibration frequencies were 0 (no vibration, to represent as 0 Hz for the purpose of convenience), 30, 80, and 250 Hz for discussing the vibrotactile masking effect on the different mechanoreceptor types (Merkel's discs: SA-I, Meissner's corpuscle: FA-I, Pacinian corpuscle: FA-II).

Each participant performed 320 trials (4 frequencies × 8 dent points × 10 times) in pseudo random order. Finally, we captured the correspondence relation between the dent points on the ball and touch points of each participant's hand using double-sided tapes. Informed consent was obtained from all individual participants included in this study. All procedures performed in studies involving human participants were in accordance with the ethical standards of the institutional committee and with the 1964 Helsinki declaration and its later amendments or comparable ethical standards.

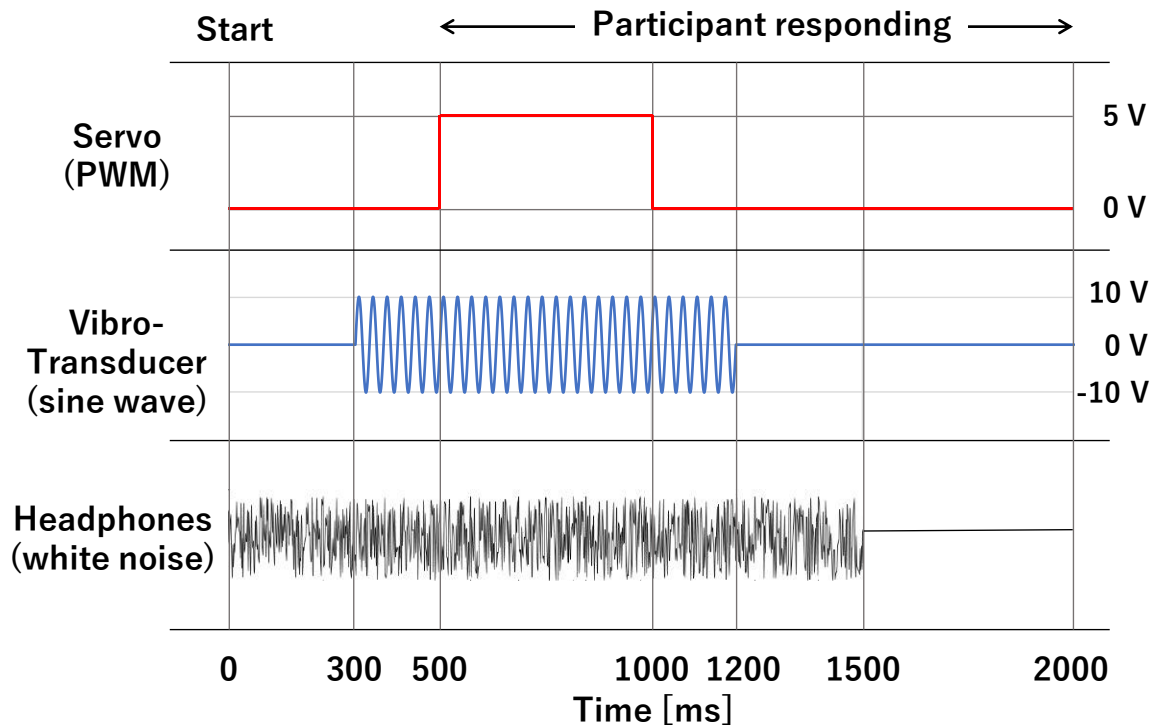


Fig. 4.11. Timing chart of source signals

(3) Experimental results

Fig. 4.12 illustrates the normalized correspondence-relation map between the dent points on the ball-type interface and touch points on the participant's hand. Although the hand size of participants varied widely, each dent point was perceived with almost the same corresponding touch point on the finger or of the palm. Interestingly, almost all participants reported that they had thought touch points 5, 6, and 7 were nearer to the wrist than actual points. Fig. 4.13 shows the mean correct answer rates corresponding to each dent point with respect to the four vibration frequencies ($n = 14$). "0 Hz" means the case where no vibration was given. The results of one-way ANOVA were as follows:

0 Hz and 250 Hz showed no significant differences by dent point (0Hz: $F_{7,104} = 1.813$, $p = 0.092$, 250Hz: $F_{7,104} = 1.283$, $p = 0.266$).

30Hz and 80Hz showed significant differences by dent point (30Hz: $F_{7,104} = 7.045$, $p < 0.01$, 80Hz: $F_{7,104} = 4.469$, $p < 0.01$). The confusion matrices in Fig. 4.14 show the identification rates of the applied dent point as well as the percentage of confusion with other dent points.



Fig. 4.12. Normalized correspondence-relation map between dent points on the ball-type device and touch points on participant's hand.

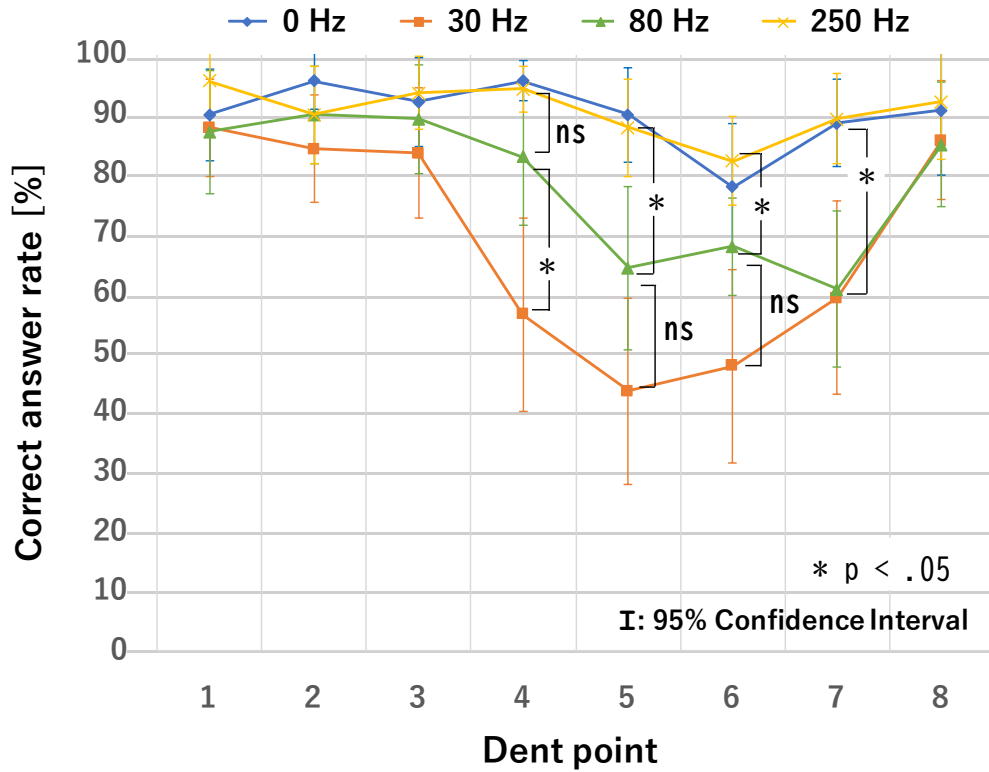


Fig. 4.13. Mean correct answer rate corresponding to each dented point with respect to four vibration frequencies

0Hz	1	2	3	4	5	6	7	8	30Hz	1	2	3	4	5	6	7	8
1	90.0	7.1	0.0	0.0	0.0	0.0	0.0	2.9	1	87.9	2.1	1.4	0.0	1.4	0.7	2.9	3.6
2	0.0	95.7	4.3	0.0	0.0	0.0	0.0	0.0	2	6.4	84.3	5.7	0.0	0.0	0.0	0.7	2.9
3	0.0	0.0	92.1	7.9	0.0	0.0	0.0	0.0	3	2.1	1.4	83.6	5.0	0.7	3.6	1.4	2.1
4	0.0	0.0	0.7	95.7	3.6	0.0	0.0	0.0	4	2.1	0.7	10.0	56.4	11.4	6.4	4.3	8.6
5	0.0	0.7	0.0	1.4	90.0	7.9	0.0	0.0	5	5.0	6.4	5.0	2.9	43.6	20.7	10.7	5.7
6	0.0	0.0	0.0	0.0	7.1	77.9	15.0	0.0	6	3.6	6.4	7.1	3.6	6.4	47.9	16.4	8.6
7	0.0	0.0	0.0	0.0	0.7	5.7	88.6	5.0	7	5.0	1.4	3.6	0.7	4.3	9.3	59.3	16.4
8	0.0	0.0	0.0	0.0	0.7	0.0	8.6	90.7	8	3.6	0.0	2.1	0.0	1.4	0.7	6.4	85.7

(a) (b)

80Hz	1	2	3	4	5	6	7	8	250Hz	1	2	3	4	5	6	7	8
1	87.1	4.3	1.4	1.4	0.0	0.0	2.1	3.6	1	95.7	1.4	0.0	0.0	0.0	0.0	0.0	2.9
2	5.0	90.0	3.6	0.0	0.0	0.7	0.7	0.0	2	2.1	90.0	7.9	0.0	0.0	0.0	0.0	0.0
3	0.7	2.9	89.3	5.7	0.0	0.7	0.0	0.7	3	0.0	0.7	93.6	5.7	0.0	0.0	0.0	0.0
4	0.0	1.4	3.6	82.9	9.3	2.1	0.0	0.7	4	0.0	0.0	2.1	94.3	3.6	0.0	0.0	0.0
5	2.1	2.1	5.0	2.1	64.3	18.6	2.1	3.6	5	0.0	0.0	0.7	0.7	87.9	10.0	0.7	0.0
6	2.1	2.1	4.3	1.4	6.4	67.9	15.0	0.7	6	0.0	0.0	0.0	0.7	4.3	82.1	12.1	0.7
7	0.7	4.3	0.0	2.1	1.4	14.3	60.7	16.4	7	0.0	0.0	0.0	0.0	0.0	2.1	89.3	8.6
8	2.9	1.4	0.0	0.0	0.7	1.4	8.6	85.0	8	0.0	0.0	0.7	0.7	0.0	0.0	6.4	92.1

(c) (d)

Fig. 4.14. Confusion matrices for different pedestal vibration frequencies. (a) 0 Hz: no vibration, (b) 30 Hz, (c) 80 Hz, and (d) 250 Hz.

4.2.4. Discussion

(1) Potential of proposed haptic interface

The average recognition rates for the condition of 0 and 250 Hz were almost over 80% (Fig. 4.13). In addition, one participant recorded 100% accuracy regardless of dent points with 0 and 250 Hz pedestal vibration. Therefore, this interface has the potential to present the point of an impact force with continuous vibrotactile information. The average recognition rate for each frequency was over 80% for dent points 1, 2, 3, and 8, which correspond to the participant's index finger, middle finger, ring finger, and thumb, respectively. These results indicate that fingers are more sensitive to pressure sensation than the palm. Moreover, participant's fingers might have used a kind of kinesthetic sense to detect dent stimuli because the displacement (at least 3 mm) of the dent points were sufficient to move finger joints. In particular, dent point 4 corresponds to the little finger, and the mean recognition rate with 30 Hz vibration was less than 60%.

We believe the reasons for this is that participants hardly used both cutaneous sense of fingertip and kinesthetic sense. This was because most participants touched dent point 4 using the lateral or the near the base of proximal phalanx of the little finger, as shown in Fig. 4.12. The mean recognition

rates for dent points 4, 5, 6, and 7 were less than 60% with 30 Hz vibration. These dent points were touched by the corresponding palm areas of the participants (Fig. 4.12). According to the confusion matrices (Fig. 4.14), dent point 5 was mostly misperceived as being point 6, point 6 was mostly misperceived as point 7, and point 7 was mostly misperceived as point 8. In the next subsection, we discuss possible reasons to explain these misrecognitions from the viewpoint of vibrotactile masking.

(2) Masking effect between vibration and pressure sensation

Tanaka et al. [52] discussed the phenomenon that a vibration sensation of a fingertip can be masked by applying the same frequency as another vibration (50 Hz) to the forearm of the user. Yem et al. [53] reported only pressure sensation in a fingertip remained when they applied mechanical vibration to the palm along with the electrical stimulation to the fingertip. We assumed that reduced pressure sensations produced by denting a surface is perceived independently from vibrotactile sensations even on the palm areas. Agreeing with this assumption, it was possible to discriminate a dented point with 250 Hz vibration when each dent points were at least 30 mm from apart.

However, the participants could not locate the dent point on the palm with 30 Hz vibration. Most participants reported that they could perceive whether the surface was dented, but could not locate it. From the viewpoint of the mechanoreceptors of the human hand, 30 Hz is the resonant frequency of FA-I, and is in the range of that of SA-I. The 250 Hz vibration frequency is the resonant frequency of FA-II [6]. Consequently, the following hypothesis could be raised; Mechanoreceptors FA-I and SA-I in the fingers and thenar were masked by the 30 Hz palm vibration and FA-II distinguished the irregular signal of acceleration from the signal reflecting the dent. This hypothesis corresponds to the findings in previous studies [7][8].

Mechanoreceptors FA-II and SA-II have comparatively large receptive fields; therefore, we expected 30 mm distance between two denting points might be short for mechanoreceptors FA-II and SA-II in palm region. This explains why the participants thought touch points 5, 6, and 7 were farther from the center of the palm than the actual points. We also assumed that SA-I might be robust for detecting changes in pressure by the dent; however, about 120 dB (reference value: 10^{-6} m/s²) masking vibration (Fig. 4.9) is thought to be strong to overcome.

We plan to investigate detectable parameters (e.g. displacement, contact area, texture, etc.) of a pressure sensation on the palm that can overcome the vibro-tactile masking effect.

4.2.5. Conclusion

In this section, we proposed a ball-type haptic interface system that presents both impact vibration and the impact points to display the hit event with the direction. The impact vibration is presented using one vibro-transducer, and the impact points are presented by depressing one of eight points on a ball surface that users can grasp with one hand. We conducted an experiment to clarify the perceptual characteristics when an impact point was along with intense vibration of three different frequencies (30, 80, 250 Hz). The results indicate that most participants could detect the dent point of eight directions with 250 Hz pedestal vibration. Therefore, our proposal interface system has the potential to present the impact point with impact vibrations. We also found that the mean correct answer rate decreased to approximately 40 percent with 30 Hz vibration compared to 250 Hz, especially in the palm. This reveals a significant masking effect between vibration and pressure sensation on the palm. For further improvement, we intend to clarify the possibility of displaying impact force direction by the device and apply the system to televised sporting events.

4.3 Method to evoke the sense of self-attribution with particular object in visual content

4.3.1. Problems and background

As described in Chapter 1, the interactive media such as video games and tele-existence are suitable for adding haptic sensation according to user operation. The haptic feedback accompanying the user's operation is naturally recognized that the target of presented haptic stimulus is the user. On the other hand, when presenting haptic information in passive media such as TVs and movies, it is not easy to specify the object, which generates the haptic stimulus.

Fig. 4.15 shows a scene where boxer on the right side hits the boxer on the left side in a boxing game. In the prior approach, the impact presented on the haptic device held in the hand is the impact on the right side, and when presenting the impact on the left side, the haptic sensation should be applied to the punched part of user's body such as the face. However, selective stimulations of all haptic sensations on the select part of body is not practicable in general use.

In video production, some methodologies have been accumulated for many years that encourage viewers to empathize or to imply gaze. Angle of view or focus of camera are key factors that can implicitly indicate the main object in the scene to viewers. On the other hand, haptic perception is a sensation that is highly to be perceived relate to ourselves because the body is directly stimulated. For this reason, haptic media may change the video production methodologies that have been cultivated so far. In particular, production processes using high-definition video systems with a wide field of view, such as 8K Super Hi-Vision or 360 degrees content in VR systems. Therefore, the need for haptic designers to appropriately attach haptic information is pointed out [12].



Fig. 4.15. Example scene image of viewing a live boxing game with haptic information.

4.3.2. Sense of self-attribution

Self-attribution is a sense that we feel the viewing object as ourselves [54]. It is known that in the process of generating a sense of self-attribution, the recognition of the accompanying relationship between the visually recognized movement of the object (visual movement) and the self's movement is greatly affected [55]. Saito et al. revealed that the consistency between visual and predictive image is dominant in the process of self-affiliation during active movement [56].

The process of producing a sense of self-attribution to the object in the outside world is discussed using two concepts by Gallagher: sense of agency (SoA) and sense of ownership (SoO). Argelaguet et al. have shown that visual appearance affects the occurrence of self-attribution in VR environments [54]. In the research, the virtual hand that moves in synchronization with the operator's hand presented in the VR space evokes strong ownership when it looks closer to the real body. On the other hand, when the virtual hand looks closer to a symbolic representation such as a sphere, the operation was possible to perform well, and the evaluation value of the agency was higher than that of the realistic virtual hand condition [57].

4.3.3. Producing "touched" feeling to evoke the sense of self-attribution

In this section, it is verified that we might control the sense of self-attribution to which object the user feels to belong by producing the "touched" feeling in a visual content. For the preliminary experiment, we improved the four types of Hapto-ball used in Section 4.1 to have a built-in optical mouse function as shown in Fig. 4.16.

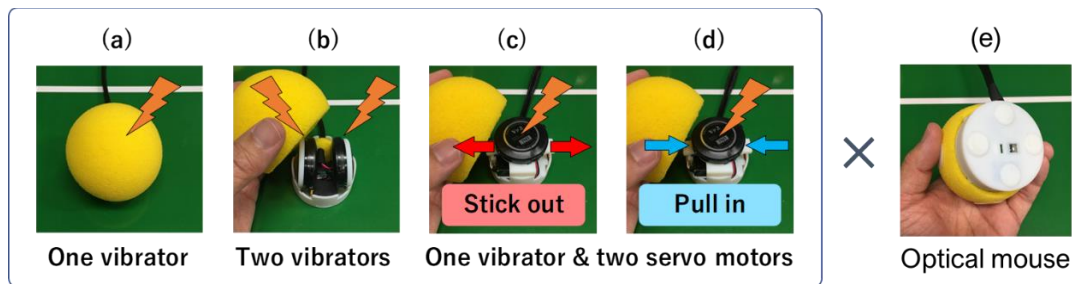


Fig. 4.16. Four types of Hapto-ball with default optical mouse function (e) and built-in one vibrator (a), two vibrators (b), one vibrator and two servo motors (c)(d).

4.3.4. Preliminary experiment

In this experiment, participants were asked to sit on a chair in front of the experimental apparatus and grasp a Hapto-ball in their right hand. They were also asked to wear noise-canceling headphones producing white noise during an experimental sequence. This time, participants asked to watch a 27inch LCD monitor in front of them during the task. Twenty-four right-handed participants (20s – 50s) took part in the experiment.

Fig. 4.17 shows the experimental conditions. Participants were asked to move Hapto-ball to the

right and left so as to move the virtual ball “A” or “B” until two balls bump into each other at least three times. When the virtual balls bumped into each other, the Hapto-ball presented one of seven haptic sensations (Hb1, Hb2L, Hb2R, Hb3L, Hb3R, Hb4L, and Hb4R) at the impact. Hb1 means impact vibration stimuli using the device showed in Fig. 4.16a. Hb2L/R mean impact vibration stimuli side L/R respectively. Hb3L/R mean impact vibration with convex stimuli on the side L/R respectively. Hb4L/R indicate impact vibration with dent stimuli on the side L/R respectively.

We hypothesized that the black stretch line between two virtual balls makes the visual scene ambiguous and may cause a figure-ground perceptual illusion. As shown in Fig. 4.17, We prepared four scenarios depend on movable virtual ball and presence or absence of the linkage between two balls.

- (A) “A” bump into the resting ball “B”.
- (B) “B” bump into the resting ball “A”.
- (A’) “A” bump into the resting ball “B” which linked to “A” with a black stretch line.
- (B’) “B” bump into the resting ball “A” which linked to “B” with a black stretch line.

Then the participants were asked to verbally respond the question “Which virtual ball are you holding now?” with the two alternatives “A” or “B” based on their intuitive feelings. Each participant performed 96 trials (4 scenarios × 7 conditions × 3 times) in pseudo random order. Informed consent was obtained from all individual participants included in this study.

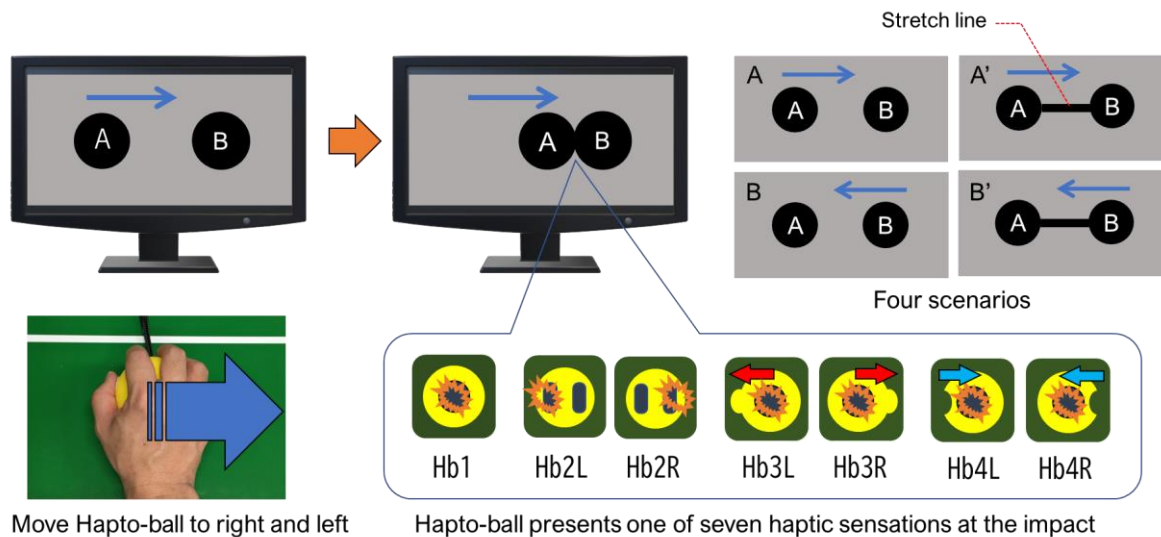


Fig. 4.17. Experimental conditions.

4.3.5. Results and Discussion

Fig. 4.18 shows the mean proportion of each responses related to each of the haptic stimulus patterns. We found that the sense of self-attribution could be overwritten by the haptic cues which might conflict to the prediction from the hand movement. In other words, it is suggested that the appropriate haptic cues can control the sense of self-attribution not only for the passive visual content but also for the interactive content. This effect is remarkable especially when the two virtual balls were linked via an imaginary stretch line (see Fig. 4.18 Hb4R at scenario A' and Hb4L at scenario B'). This method has a possibility to control the visibility of an ambiguous visual image.

It is known that in the process of generating a sense of self-attribution, the recognition of the accompanying relationship between the visually recognized movement of the object (visual movement) and the self's movement is greatly affected [59]. However, our proposed method evokes the sense of self-attribution to the object which is not operated. This method has a possibility to control the visibility of an ambiguous visual image.

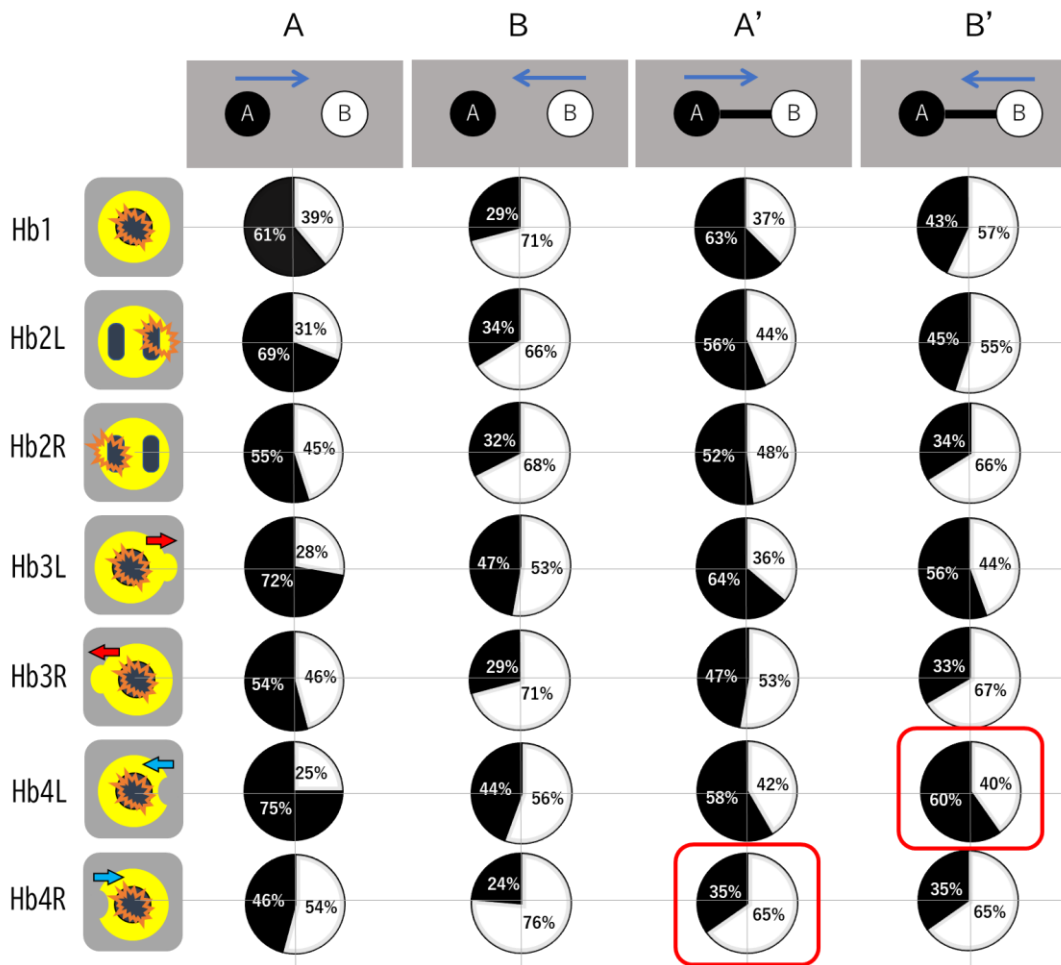


Fig. 4.18. Mean proportion of each response (“A” or “B”) related to the haptic stimulus pattern.

4.4 Conclusion

We developed a grasping-type haptic device that converts contact timing between objects in a movie scene into haptic stimulation. We clarified that this method can present the direction of an impact more intuitively compared to the condition of vibration alone. Then, the masking effect when simultaneously presenting a concave stimulus and a vibration stimulus to the palm was verified from the relationship with the spatial resolution of the haptic sense of the palm, and the problems were clarified. In addition, our proposed method for simultaneously presenting vibration and concave stimuli can be applied to a method of explicitly presenting the target object. This is a factor that greatly affects the sense of self-attribution which is one of the issues when applying haptic stimuli to visual media. In the last chapter, we will show some application systems to apply our findings in the service-oriented universal media.

Chapter 5

Applications and feedback from field tests

In this chapter, we describe some useful application systems of our two proposed haptic presentation methods and feedback from users in the field trials.

5.1 Haptic display system to transmit shape and hardness distribution of remote object

Fig. 5.1 shows the concept image of a demo system that transmit haptic information along with visual image. This system transmits the shape and hardness distribution data of a real object using the noncontact hardness-sensing system [17] and the prototype multipoint force-feedback haptic system [33] described in Section 2.2.

Fig. 5.2. shows the appearance of this demo system that presents the shape and hardness distributions with a reflection type spatial image display (ASKANET ASKA3D plate). This haptic display system virtually reproduces the remote object using the real object image, 3D shape data, and hardness distribution data measured with the noncontact hardness sensing device (Fig. 1.9).

First, a 3D shape is generated from point cloud data with polygons that are interpolated between adjacent points. Then, the image data are pasted as texture according to the unevenness of the 3D surface. The reproduced image of the virtual object is displayed on the visual display in Fig. 5.2b and projected in the mid-air. When the finger pad of a user reaches the position of the image projected in the mid-air, the reaction force is presented at the haptic stimulation point on the finger pad (Fig. 5.2a).

The reaction force is calculated every 1 ms according to the spatial coordinates of the fingertip, 3D shape data, and hardness distribution data. As described in section 2.2, the multipoint force feedback display presents three degrees of freedom of haptic stimuli independently to multiple points on the finger pad. In this application, three haptic stimulation points with a diameter of 4 mm were placed on the finger pad (Fig. 5.2a).

In the real world, when the finger pad applies force to an object, the object is deformed according to the degree of penetration of the finger pad, and the visual deformation at this time also affects the user's recognition of hardness. To reproduce this effect, the deformation of the virtual object according to the hardness and penetration depth of the finger is visually feedback in the reproduced image. In the exhibition [58], the actual measured object is placed next to the haptic display to experience the haptic sensation with the reproduced virtual object.

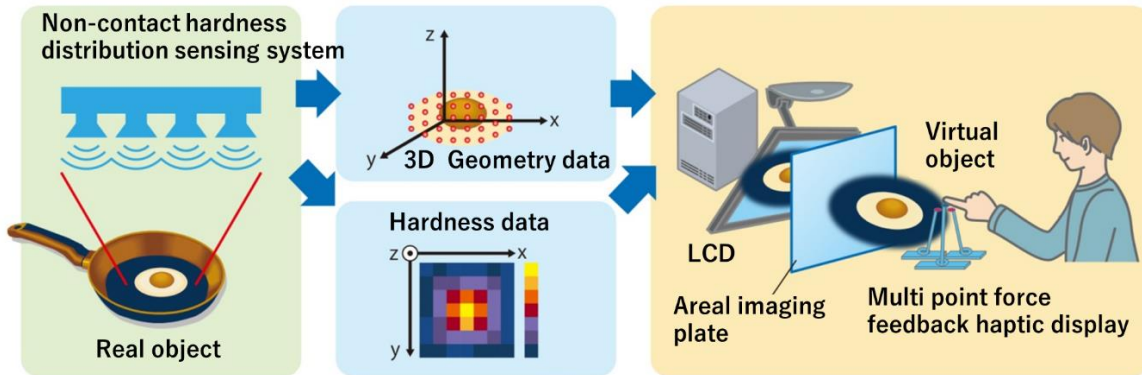


Fig. 5.1. Demo system transmitting shape and hardness of real object

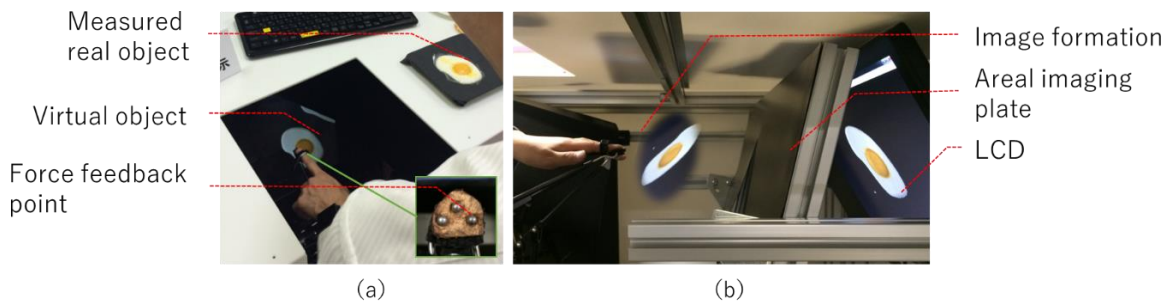


Fig. 5.2. (a) appearance of the multipoint force feedback haptic display, (b) interior of the haptic display that presents the shape and hardness distribution in mid-air. Since displayed image cannot be photographed from side, dummy image is superimposed at imaging position.

Ten visually impaired participants touched the reproduced object without notifying the target object being reproduced. Seven out of them found that it was egg sunny-side up and answered that the yolk was softer than the white. On the other hand, the remaining three visually impaired participants said that it would be better if the entire body should be uniformly hard when they want to know three-dimensional shape of the object. In addition, all of them pointed out that the one finger exploration is unnatural to recognize the shape and hardness of an object without visual image. This is one of the reasons why we developed the GraspForm-type haptic device GraspForm described in Chapter 3.

Fig. 5.3. shows again the appearance of the GraspForm and application system. In this case, most of users interested in the shape of carapace, however, they could not recognize that the object was a turtle without any hints by audio descriptions. It is known that recognizing the shape only by haptic sensation is difficult even when touching with bare hands. Therefore, we focus on the information that can only be conveyed by haptic sense for all people regardless of whether there was a visual

disability. In other words, shape, hardness, and impact sensation are not substitute information for vision. This is an important design guideline for providing services that can be enjoyed not only by the visually impaired users but also the sighted people.

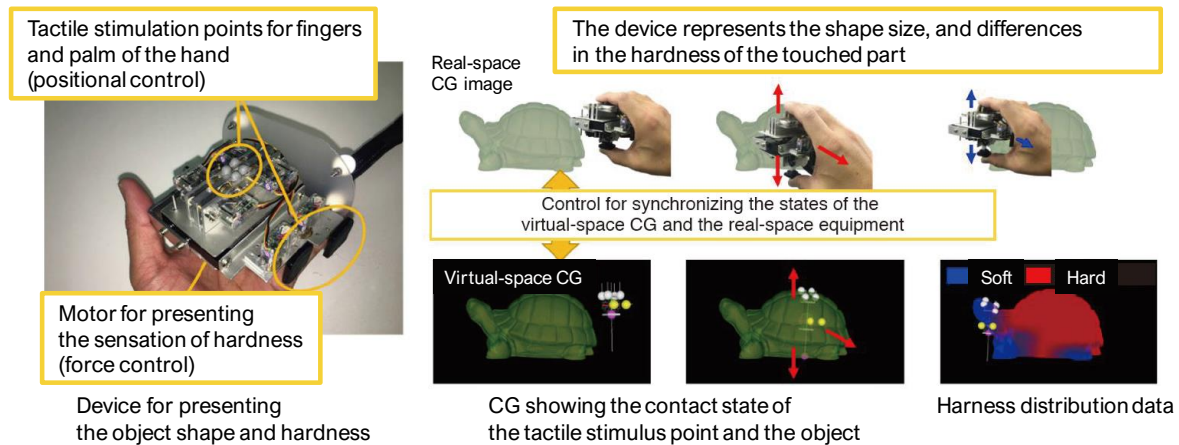


Fig. 5.3. Appearance of the Grasping-type haptic device and application system

5.2 Haptic interface system for physically experiencing sports games

5.2.1. Haptic applications for televised sporting events

There are several methods for adding haptic sensation to broadcast media. “Touch TV” [56] is well-conceived method for adding interactivity and engaging the viewer in the programmed experience. Directional cues are vital to the creation of compelling haptic stimuli, they use a combination of 2DoF remote control and couch-shaker to display powerful impacts such as a goal shot in a football game. “Vibration Soccer” [60] renders live football games on mobile phones through vibration. It uses coding information, but a goal event and the team in possession of the ball, can be rendered. One issue with these methods is the difficulty of installing sensors on rackets, balls, or other equipment used in regular matches. As a solution, “VibroTracker” [61] can measure vibrations produced by a table tennis paddle in real time with high precision and without contact. Okubo et al. [62] developed an object-tracking system that does not require dedicated sensor cameras and that can track a ball in a video from several broadcast cameras. Yoshida et al. [63] proposed a method that estimates racket-grip vibration from tennis video using a neural network. These technologies are powerful for generating haptic applications and contents in real time. Our proposed interface system uses ball tracking technology to estimate the intensity and direction of a player’s impact force.

In this research, we have developed a ball-type haptic display that uses beach volleyball 3D tracking data recorded by the object tracking system to provide a more-active way to enjoy sports

games. This article gives an overview of the interface and reports on the results of experiments with eight visually impaired participants.

5.2.2. Ball-type haptic device

Figure 5.3 shows external and internal views of the ball-type haptic device and examples of using the haptic devices for sports games [64]. The device is covered with a 90-mm sponge ball with a polyurethane surface, and it contains a vibration device (ACOUVE Vp4), an active speaker (SONY SRS-X11), and a Qi wireless charging adapter (MS Solutions LEPLUS). The device connects to a PC by Bluetooth wireless and vibrates based on the left or right audio signal from the PC. In this research, we prototyped two devices, colored blue for the left channel and yellow for the right channel, corresponding to the colors of the team uniforms in the beach volleyball game.

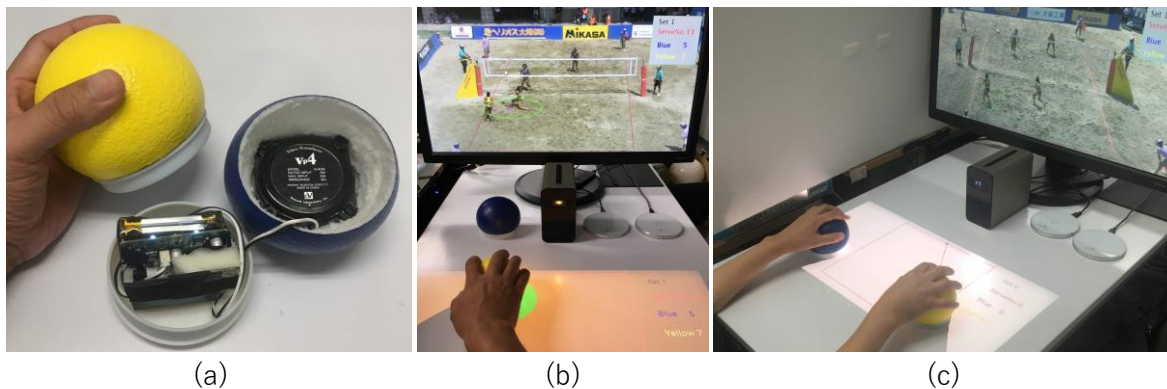


Fig. 5.3. (a) External and internal views of the ball-type device. (b), (c) Examples of using the haptic interface for sports events.

5.2.3. Application demo system overview

A schematic diagram of the demo system is shown in Fig. 5.4. The left half of the figure shows the object tracking system [62]. This system analyzes video from four cameras placed around the court, recording the 3D position of the ball in each frame of the video in CSV format. Game event data (points, serving team, court changes, etc.) were also recorded manually as the game proceeded. As a typical example, the Olympic Data Feed (ODF) [65] provides real-time data for the Olympics and Paralympics. Our interface is composed of the elements on the right half of Fig. 5.4. The control PC (Apple Macbook Pro OS X) receives the data recorded by the object tracking system. Changes in the acceleration of the volley ball are computed from the position data and used to detect events such as when players hit the ball. Pre-set simulated audio signals based on these events, such as a received sound, are sent to the devices via Bluetooth communication. The ball-type devices present the received audio signals as vibrations, and these devices also play them back as sounds. An Xperia

Touch (SONY G1109 Android 7.0), which is a smart device with an LCD projector supporting touch operations on the projection surface, is connected to the control PC by Wi-Fi. The positions of the two devices on the table are sent to the control PC. The control PC outputs vibration signal on the right channel when the ball is in the area covered by the yellow device, and the PC outputs to the left channel when the ball is not in that area.

For video output, the control PC selects and displays the camera image. The location of the ball is also projected onto the court surface along with computer graphics indicating the area currently covered by the device, which is overlaid on the game video and shown on an arbitrary LCD display. The Xperia Touch draws the current ball position and area currently covered by the device over computer graphics of the court surface and projects it onto the table with a 23-inch image size.

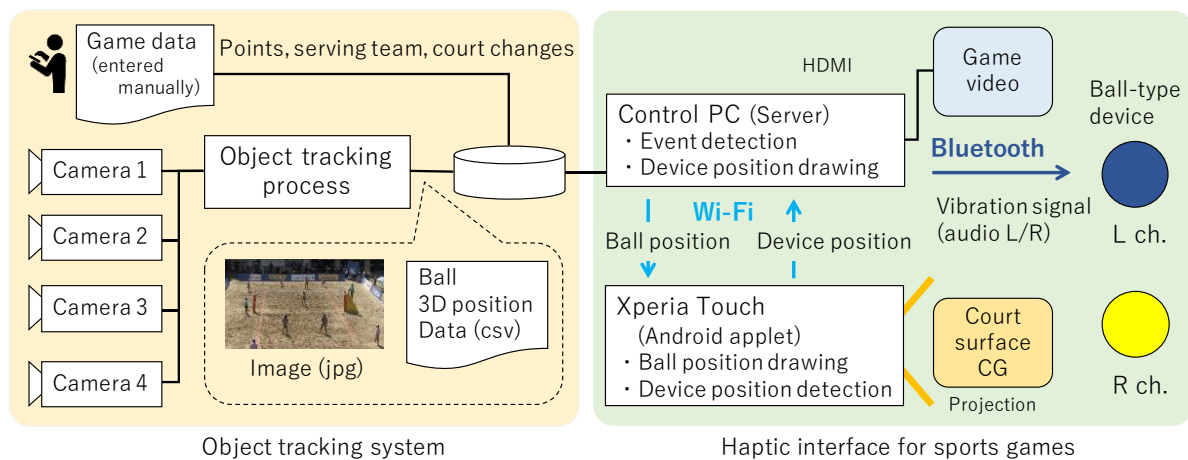


Fig. 5.4. Schematic diagram of object tracking system and haptic interface for sports games.

5.2.4. Evaluation by visually impaired users

For the most passive case, we evaluated the degree to which participants with visual disabilities could understand the state of the game and enjoy it.

(1) Method

By maximizing the area covered by each device, we configured the system so that the yellow device would always vibrate for strikes by the yellow team and so that the blue device would vibrate for strikes by the blue team. Participants placed their hands on the devices resting on the table while the beach volleyball game playing back (Fig. 5.3c).

Experiments were conducted under the following two conditions. Single-hand conditions were enabled so that strikes by the yellow team were perceived as vibrations in the right hand and so that strikes by the blue team were perceived audibly. Two-hand conditions were enabled so that strikes by the yellow team were perceived as vibrations in the right hand and so that strikes by the blue team

were perceived as vibrations in the left hand. The plays from ten serves in a real beach volleyball game are as shown in Table 5.1 for the experimental stimulus. For example, for serve number 1, the yellow team served, and the blue team played a conventional attack by receiving, setting, and attacking. However, the ball went out of the court on the yellow team side, so the yellow team scored the point. In this case, the audio information presented was the referee's first whistle (to start the serve), the color of the serving team, the impact sounds (the same for the serve, receive, set, and attack), the referee's second whistle (for the point), and cheering on the side of the team that got the point.

Under each of the experimental conditions, participants would verbally express the game state after each ball. Then, after completing all trials, they gave a five-grade subjective evaluation of each condition in terms of the enjoyment of the game. There were eight visually impaired participants aged 40 to 69 (four totally blind, four with low vision), and each participant performed 20 trials (10 plays \times 2 conditions).

Table 5.1. Ten ball game states used as stimulus

Serve no.	Scoring team	Game state (Y: Yellow, B: Blue)
1	Yellow	Serve(Y), Receive(B), Set(B), Attack(B), Out of yellow court
2	Yellow	Serve(Y), Receive miss(B), Set miss(B), In the blue court
3	Blue	Serve(Y), Receive(B), Set(B), Attack(B), In the yellow court
4	Yellow	Serve(B), Receive(Y), Set(Y), Attack(Y), Blue blocks, out.
5	Blue	Serve(Y), Receive(B), Set(B), Attack(B), In the yellow court
6	Yellow	Serve(Y), Receive miss(B), Set miss(B), Blue faults with 4 hits
7	Blue	Serve(Y), Receive(B), Set(B), Attack(B), Yellow receives to out
8	Blue	Serve(B), Receive miss(Y)
9	Yellow	Serve(B), Receive(Y), Set(Y), Attack(Y), In the blue court
10	Blue	Serve(Y), Receive(B), Set(B), Attack(B), In the Yellow court

(2) Results

Fig. 5.5 shows the correct answer rates for the scoring team color and the game state. For the game state, the answers completely matching the state shown in Table 5.1 were deemed correct. For example, answers for serve number 1, when the blue attack went into the net or when the third hit for blue was out on the blue side, were incorrect. Fig. 5.6 and Fig. 5.7 show the subjective evaluation value in ease of understanding of state and enjoyment of the match under single and two-hand conditions.

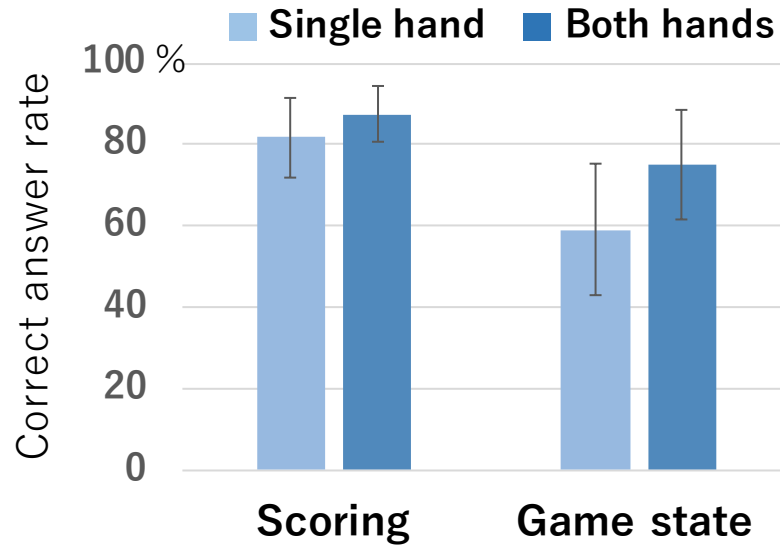


Fig. 5.5. Scoring team and game state correct answer rates.

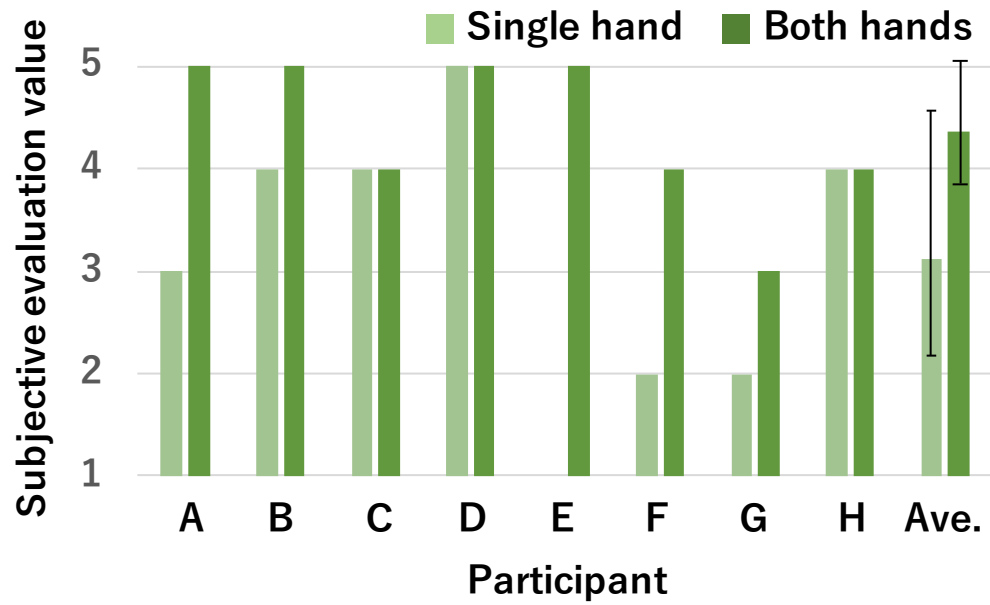


Fig. 5.6. Subjective evaluation results for ease in understanding state of the match.

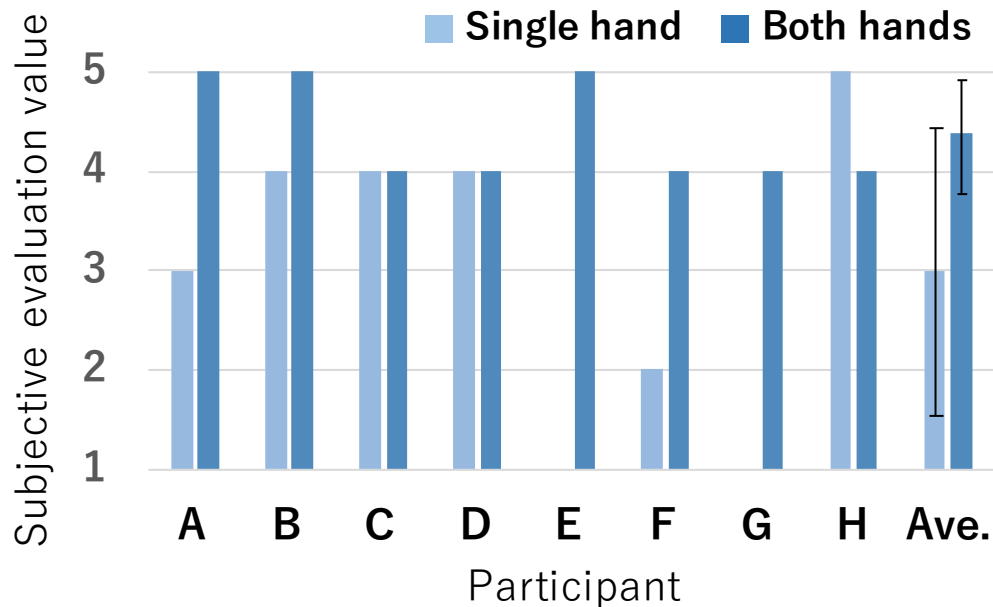


Fig. 5.7. Subjective evaluation results for enjoyment of the match.

(3) Discussion

The correct answer rates were higher under two-hand conditions for both the scoring team and the game state (Fig. 5.5). Enjoyment was also evaluated more highly for the two-hand conditions (Fig. 5.7). The experiments had no sound recorded at the venue and no announcer commentary of the game state or other explanation, so participants had to determine the game state from the simulated sound signals of player strikes and cheering and the vibration stimulus. All of the participants answered that they had to concentrate to follow the game state by just listening, and this prevented them from enjoying the game.

The results suggest that under two-hand conditions, subjects understood the game conditions in Table 5.1 at a level of approximately 70% and were able to enjoy watching the game. All participants reported that the intervals between two strikes helped to understand situations such as attacks, sets, and missed receptions. This fact indicates that they understood when the vibration of the next strike occurred, and until then they could only imagine what was happening after the strike. Thus, this understanding at least lags from that gained by visual information as shown in Fig. 5.8.

To enjoy the sense of presence and impact of the game at the same time as sighted people, each of the hits—receptions, volleys, and attacks—need to be presented with a corresponding vibration. Many of the participants also reported that it was enjoyable to have a visceral impression of the intensity of an attack. The uncertainty states from the participant responses and their introspection were as follows.

- Which side of the court did the ball go out on?
- Did it hit the net or was it out?
- Did the ball hit the sand in the court or was it out?

Most participants responded that some additional information, such as vibrations for contacting the net or of the ball hitting the sand would help. When designing this system, we hypothesized that presenting only the strikes by one of the teams would increase empathy for that team and make it easier to understand the state of the game by fixing the subjective viewpoint. However, our results showed that all, but one participant found that watching with the two-hand conditions made it easier to understand the offense, defense, and developments in the game, which increased their sense of presence. We also received comments that it would be effective for people with hearing impairment and that it could also help convey the game state to deaf-blind people. In the future, we will evaluate cases with sighted viewers moving the ball-type device while watching a game and continue making improvements so that most people can have even more enjoyment from watching sports.

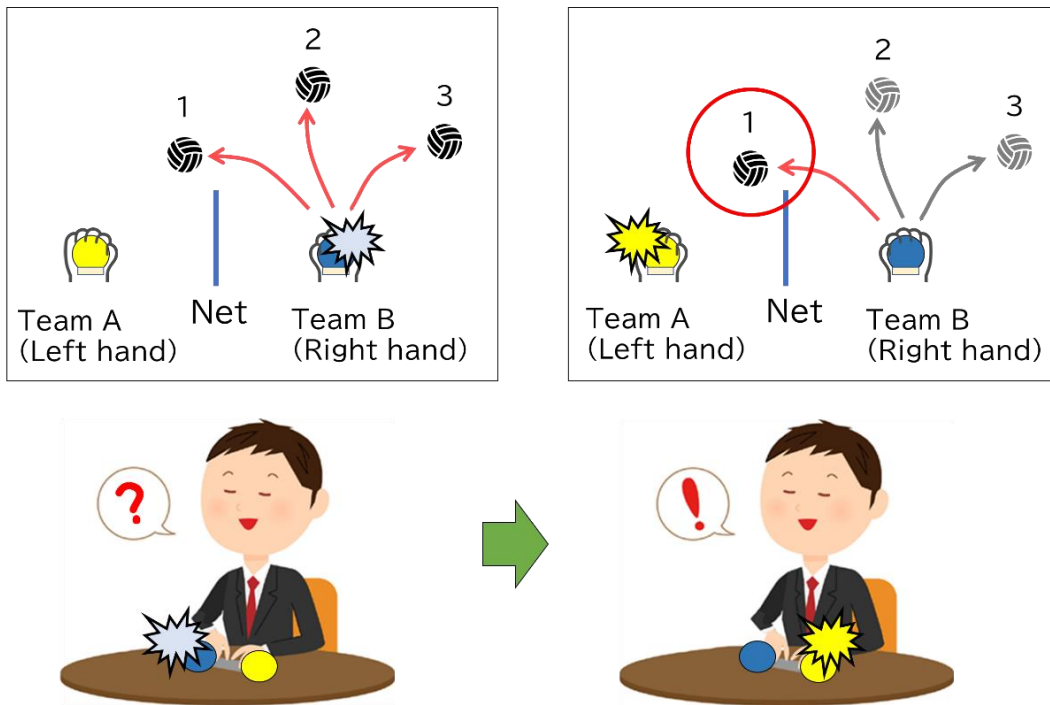


Fig. 5.8. Schematic image of a recognizing process of a visually impaired user without directional haptic cue.

5.2.5. Application system using haptic devices for presenting impact directions

Fig. 5.9 shows an example application user interface [66] to present the impact information using our proposed grasping-type haptic devices described in Chapter 3. We use a side view video image (1920× 1080 pixels, 30 fps) of a volley ball game to estimate the acceleration of the real ball in the video using an object tracking system (Fig. 5.9a). In this system, six haptic devices are placed on a wooden table that represents the floor of the volley ball court (Fig. 5.9b). Users can choose to experience actions of the team they are rooting for. The haptic devices present both impact vibration and impact direction depend on the estimated acceleration at each impact timing.

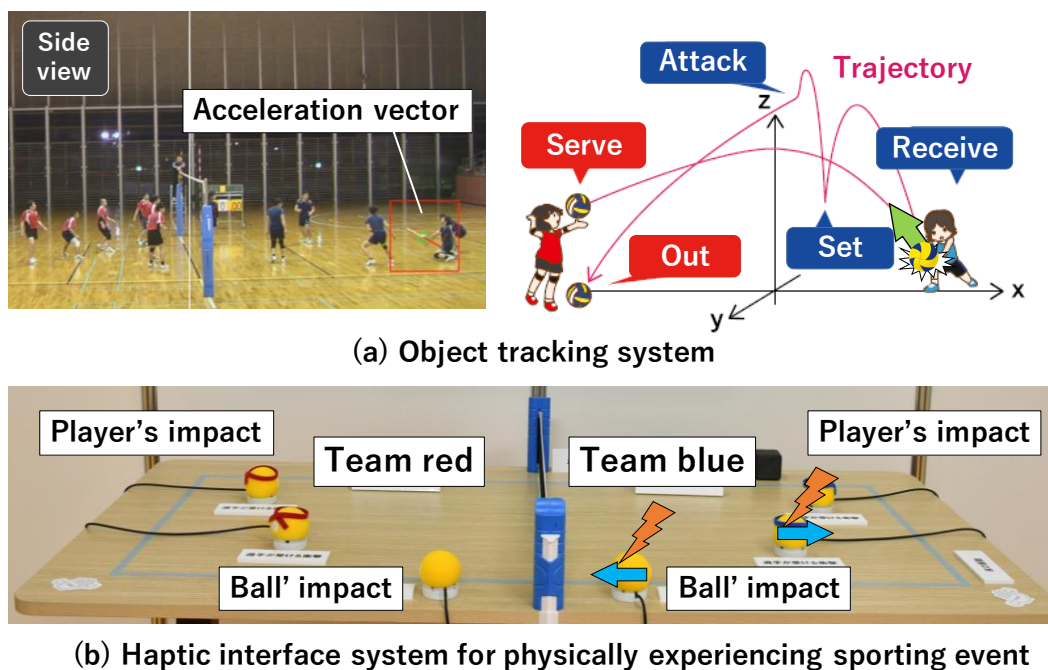


Fig. 5.9. (a) Object tracking system. (b) Haptic interface system providing the action in volley ball games.

5.2.6. Discussion for presenting impact direction effectively to expand visual media

Our proposed haptic devices have the potential to present both impact vibration and impact points. In this section, we describe two methods for presenting impact sensations effectively for televised sporting events.

(1) 2-D Information for visually impaired users

In some cases, haptic information is helpful for intuitive expression of game situations at sporting

event that are difficult to convey in words for the visually impaired. Fig. 5.10 shows an example application image to convey a critical situation of curling games for visually impaired users. From the top view of the curling court, vision-based object tracking system detects the red stone as the target object which is nearest to the center of the circle. In this case, the visually impaired supporters of the red team will want to know the intensity and the direction of the yellow stone's attack. The haptic device can display the impact points with vibrations that represent the direction and intensity of the impact. We assumed that this intuitive haptic information will enhance the thrill of the situation and assist to enjoy high-context tactics of the games not only for the visually impaired but also for all supporters.

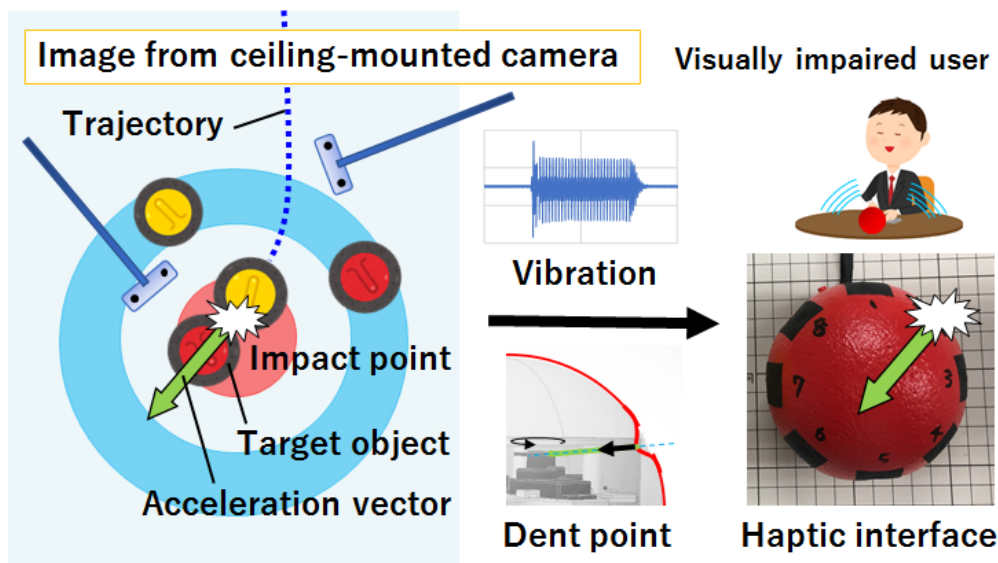


Fig. 5.10. Application image to convey a scene of curling games to visually impaired users.

(2) Presenting method for converting 3-D information to 2-D directions

As shown in Fig. 5.9b, the impact side of the volley-ball's impact is opposite to the player's impact side because there is a relationship based on the action-reaction forces. Fig. 5.11 shows an example application image to present the 3-D impact vector information using our proposed haptic device. It is important to ensure the consistency between the direction cue of the haptic device and the actual 3-D information. We assume that the top view image displayed on the table plays a role to present the correspondence between the haptic directional cue and multi-angle camera image on the TV screens in front of the viewers as shown Fig. 5.11. This kind of fixed coordinate system is helpful for the visually impaired users and the special needs to experience the first-person perspective of one viewer's favorite player.

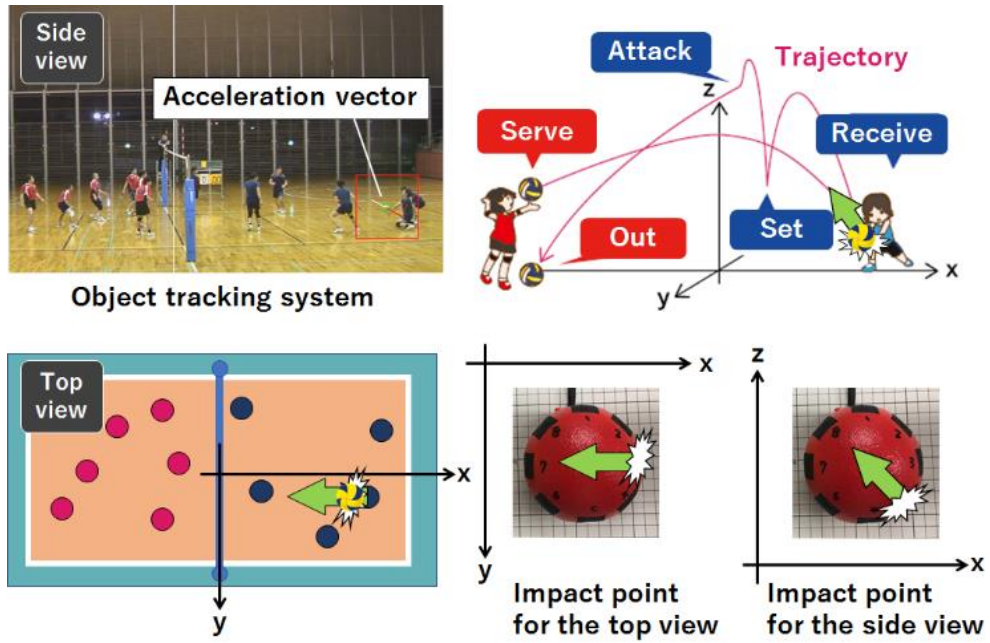


Fig. 5.11. Application image to present the impact vector of volleyball.

Chapter 6

Conclusion

6.1 Summary of results

In this thesis, we propose two methods for adding haptic information to visual media provided by broadcasting and communications and providing universal information services that anyone can use. We first propose a method for conveying the shape, size, and the differences of partial hardness/softness of a 3D object. We then propose a method for directly converting the timing, magnitude, and direction of impact between moving objects into haptic stimulation. These two methods are not only useful for visually impaired individuals but can also be applied to improving realism through AR/VR technology.

In Chapter 2, we present the basic design, prototyping, and a preliminary evaluation revealing requirements relevant to the number of haptic stimulation points on a finger pad necessary for recognizing 3D shapes. To improve the ease of tactilely exploring contours of 3D object, we constructed a prototype system that can provide force feedback with 3-DoFs to each of the five points on a finger pad. The results of evaluation indicate that the ease of recognizing edges improved significantly with two or more haptic stimulation points, and the most easily explore condition was four haptic stimulation points.

In Chapter 3, we describe the concept and evaluation results of grasping-type haptic devices to present 3D shape and hardness distributions of an object. We developed a grasping-type haptic device based on the requirements from the preliminary findings. This device presents four haptic stimuli on a finger pad of the index finger, two points on the palm, and one point on the thumb. As an experimental result, the difference in the side surfaces of the 3D shapes could be identified and the effectiveness was clarified. In addition, we developed a PWM control method for the actuator output in accordance with the hardness data set for each voxel of a CG object. The results of an experiment comparing the difference between the hardness presented on the haptic device and that of a real spring suggests that the user can sufficiently distinguish the difference in relative hardness.

In Chapter 4, we present a method for transmitting the timing and impact of haptic sensation when moving objects come into contact. We developed a grasping-type haptic device that converts contact timing between objects in a movie scene into haptic stimulation. The impact vibration is presented using one vibro-transducer, and the impact points are presented by depressing one of eight points on a device surface that users can grasp with one hand. We clarified that this method can present the direction of an impact more intuitively compared to the condition of vibration alone. Then, we conducted an experiment to clarify the perceptual characteristics when an impact point was along with intense vibration of three different frequencies (30, 80, 250 Hz). The results indicate that most participants could detect the dent point of eight directions with 250 Hz pedestal vibration. Therefore,

our proposal interface system has the potential to present the impact point with impact vibrations. We also found that the mean correct answer rate decreased to approximately 40 percent with 30 Hz vibration compared to 250 Hz, especially in the palm. This reveals a significant masking effect between vibration and pressure sensation on the palm. We also argue that concave haptic stimuli can be applied to control the sense of self-attribution. Our proposed method for simultaneously presenting vibration and concave stimuli can be applied to a method of explicitly presenting the target object. This is a factor that greatly affects the sense of self-attribution which is one of the issues when applying haptic stimuli to visual media.

In Chapter V, we describe some useful application systems of our proposed methods. We have studied viewing styles for enjoying sports events and have developed a haptic interface system utilizing a ball-type device. This interface system is able to associate tactile information, simulated using vibration, with real video of games such as volleyball using 3D ball location data obtained from video with object tracking technology. We then evaluated how much people with visual disabilities could understand the state of a game and enjoy it. The results suggested that participants were able to understand the state of the game about 70% of the time and enjoy it using two devices to perceive strikes by each team with the left and right hands even without visual and audio descriptions. In addition, through the field test, visually impaired users pointed out the enjoyment of the feeling that they can know the shape, hardness, impact timing and impact intensity at the same time as a sighted people.

6.2 Design guidelines of haptic devices to expand visual media

Haptic sensation is caused by interaction between the human skin and the surface of an object. Active (to be precise, the sensation with active movement is mainly called haptics) and passive haptic sensations are perceived at various parts of the whole body. For this reason, it is not realistic to develop a haptic device that can be used for all kinds of content. In this study, the development of haptic device was carried out with the aim of presenting the shape, hardness, and impact with a single grasping-type haptic device. At present, we have come to the conclusion that it is reasonable to design dedicated haptic device according to the information to be presented. However, I believe that grasping-type haptic device will be able to use for general purpose to expand visual media in the future. Another aspect for realizing universal haptic information services, visually impaired people are said to be more sensitive to haptic sensations than sighted people. However, except for the identification of Braille and symbolic vibration meanings, haptic sensations of the shape, hardness, and impact that is perceived on a daily life are considered to equivalent to that of a sighted person.

As my conclusion, haptic information that expands visual media should not be as a special substitute of vision for people with visual disabilities but presents new information that cannot be known even by sighted people with conventional media. Through the series of research described above, we propose the following basic design guidelines for developing a haptic device that presents the shape, hardness, and impact of objects to expand visual media and provides universal service.

- Present at least 4 stimulation points at a fingertip with a control frequency of 60 Hz or more.
- Relative differences within the object should be expressed rather than absolute hardness.
- Present the direction of impact to create a sense of self- belonging to a specific object.
- The device can be held or released at any time as user like.

6.3 Conclusion and future perspective

We have developed a haptic device that can present the 3D shape and hardness of a virtual object in real space towards implementing a universal information device. Basic experiments with the device revealed that users are able to understand the shape and hardness of virtual objects even without visual information. We also developed a grasping-type haptic device that converts contact timing between objects in a movie scene into haptic stimulation. We clarified that this method can present the direction of an impact more intuitively compared to the condition of vibration alone. In addition, our proposed method for simultaneously presenting vibration and concave stimuli can be applied to a method of explicitly presenting the target object. This is a factor that greatly affects the sense of self-attribution which is one of the issues when applying haptic stimuli to visual media.

In conclusion, we clarified some guidelines of haptic technology that contributes to the expansion of visual media to universal service. we focus on the information that can only be conveyed by haptic sense for all people regardless of whether there was a visual disability. In other words, shape, hardness, and impact sensation are not substitute information for visual information. This is an important design guideline for providing services that can be enjoyed not only by the visually impaired users but also the sighted people. If the haptic information can be transmitted as one more sense that complements vision and audio, such new media can convey the material, hardness/softness, warmth, and so forth to the viewers. It is also possible to touch information of the target that a person with visual impairment could not know before. Furthermore, it will be possible to provide powerful and realistic feeling by conveying movements and impacts of content, such as that of dramas and sports.

On the other hand, the cognitive mechanism based on human haptic sensation is still unclear. In this study, issues that should be further investigated in cognitive sciences and technical approaches are clarified. In the future, we expect that our results will contribute to the realization of an information environment that is also useful to people with visual and hearing impairments in addition to providing a sense of reality and realism as one of the VR technologies.

Acknowledgement

My research life has become very enjoyable and fulfilling thanks to the following great people. First of all, I would like to sincerely appreciate the mentorship of Professor Hiroyuki Shinoda. I was impressed by Prof. Shinoda's overwhelming knowledge, depth of insight, and the willingness to create the future of haptic technologies, and I desired to conduct haptic research in the Shinoda-Makino Laboratory. He always welcomed me and gave constructive instructions. I also appreciate Prof. Shinichi Warisawa, Prof. Akinao Nose, Associate Prof. Michiaki Inomoto, and Associate Prof. Yasutoshi Makino who are in charge of reviewing this thesis and gave me many valuable instructions and sincere critical questions during the review process.

Toru Ifukube, emeritus professor who had been the research advisor of our institute gave a lot of instructions to provide methods for universal broadcasting services. Associate Professor Yasutoshi Makino and Assistant Professor Masahiro Fujiwara always gave me essential and unique suggestions at laboratory meetings. They are also the members of a joint research project between Shinoda-Makino Laboratory and NHK Science and Technology Research Laboratories. Thanks to them, we were able to realize three-dimensional shape and hardness distribution transmission system exhibited at the NHK STRL open house 2014. I also thank to Yasuaki Monnai, Akihito Noda, Keisuke Hasegawa, Tatsuma Sakurai, Akimasa Okada, Seki Inoue, Yuichi Masuda, Takaaki Kamigaki, Mitsuru Ito, Takuro Furumoto, and all Shinoda-Makino Laboratory members for treating me friendly and discussing sincerely.

I also appreciate to all my colleagues in NHK Science and Technology Research Laboratories. Thanks to Kenji Murase, Makiko Azuma, Toshihiro Shimizu, and Satoru Kondo who are the co-authors of each paper that forms the basis of this doctoral thesis. Special thanks to Tadahiro Sakai who had been the leader in tactile research at NHK STRL. I was taught a lot from his passion and philosophy for realizing a human-centric information barrier-free environment. In addition, I would like to thank all researchers who gave me valuable advices at academic societies. All results in this thesis are supported by the large number of participants who cooperated in our psychophysical experiments. Yoshihiro Watanabe and Takaaki Takahashi provided technical support in the development of our haptic devices. I genuinely thank again all the people who supported me.

Finally, I want to thank my family, Anna and Naomi. This research would not have been possible without their special cooperation and assistance in my life.

Bibliography

- [1] R. Fielding (ed.), "A Technological History of Motion Pictures and Television, " University of California Press, pp.76–83, 1967.
- [2] S. Tachi, "Tele-existence (1) Design and Evaluation of a Visual Display with Sensation of Presence, " Proc. of the 5th Symposium on Theory and Practice of Robots and Manipulators (RomanSy 84), 2451254, CISM-IToMM, Udine, Italy, 1984.
- [3] Jones, L. A., & Lederman, S. J., "Human hand function", Oxford University Press, 2006.
- [4] A.B. Vallbo and R. S. Johansson, "Properties of Cutaneous Mechanoreceptors in the Human Hand Related to Touch Sensation," *Human Neurobiology* 3, pp.3-14, 1984.
- [5] R. S. Johansson and A. B. Vallbo, " Tactile sensory coding in the glabrous skin of the human hand, " *Trends in Neurosciences*, Vol. 6, pp. 27-32, 1983.
- [6] S. J. Bolanowski, G. A. Gescheider, R. T. Verrillo and C. M. Checkosky "Four Channels Mediate the Mechanical Aspects of Touch," *J. Acoust. Soc. Amer.*, vol. 84, pp.1680{1694, 1988.
- [7] W.H. Talbot, I. Darian-Smith, H.H. Kornhuber and V.B. Mountcastle: "The Sense of Flutter-Vibration: Comparison of the human Capability with Response Patterns of Mechanoreceptive Afferents from the Monkey Hand," *J. Neurophysiology*, 31, pp.301-335, 1969.
- [8] A.W. Freeman and K.O. Johnson: " A Model Accounting for Effects of Vibratory Amplitude on Responses of Cutaneous Mechanoreceptors in Macaque Monkey," *J. Physiol.*, 323, pp.43-64, 1982.
- [9] Lackner, J.R., "Some proprioceptive influences on the perceptual representation of body shape and orientation," *Brain*, vol.111, no.2, pp.281-297, 1988.
- [10] A. Lecuyer, S. Coquillart, A Kheddar, P. Richard and P. Coiffet: Pseudo-haptic feedback, "Can isometric input devices simulate force feedback ?", *Proceedings IEEE Virtual Reality 2000*, 2000.
- [11] Y. Ban, T. Kajinami, T. Narumi, T. Tanikawa and M. Hirose, "Modifying an identified curved surface shape using pseudo-haptic effect," *2012 IEEE Haptics Symposium*, pp. 211-216, 2012.
- [12] S. Tachi, K. Minamizawa, M. Furukawa, C. L. Frenando, "Haptic Media Construction and Utilization of Human-harmonized 'Tangible' Information Environment", *Proceedings of the 23rd International Conference on Artificial Reality and Telexistence*, 145-150, 2013.
- [13] TELEXISTENCE, [Online]. Available: <https://tx-inc.com/en/index/>.
- [14] AVATAR XPRIZE, [Online]. Available: <https://avatar.xprize.org/prizes/avatar/>.
- [15] H. Shinoda, "Intelligence in Human Skins, " *System, control and information*, vol. 46, no. 1, pp. 28-34, 2002.
- [16] K. Hisatomi, M. Katayama, K. Tomiyama, Y. Iwadate, "3D Archive System for Traditional Performing Arts", *International Journal of Computer Vision*, vol.94, no.1, 2011, p.78-88.
- [17] M. Fujiwara and H. Shinoda, "Coaxial noncontact surface compliance distribution measurement for muscle contraction sensing", *Proc. 2014 IEEE Haptics Symposium (HAPTICS)*, 2014, pp.385-389.
- [18] H. Iwata, H. Yano, F. Nakaizumi, R. Kawamura, "Project FEELEX: Adding Haptic Surface to Graphics", In *Proceedings of the 28th Annual Conference on Computer Graphics and Interactive Techniques (SIGGRAPH '01)*, pp.469-476, 2001.
- [19] I. Poupyrev, T. Nashida, S. Maruyama, J. Rekimoto, Y. Yamaji, "Lumen: Interactive Visual and Shape Display for Calm Computing", In *ACM SIGGRAPH 2004 Emerging Technologies (SIGGRAPH '04)*, p.17, 2004.

- [20] S. Follmer, D. Leithinger, A. Olwal, A. Hogge, H. Ishii, "inFORM: Dynamic Physical Affordances and Constraints Through Shape and Object Actuation", In Proceedings of the 26th Annual ACM Symposium on User Interface Software and Technology (UIST'13), pp.417-426, 2013.
- [21] H. Iwata, "Pen-based Haptic Virtual Environment", In Proc. of IEEE VRAIS'93, 1993.
- [22] T. H. Massie and J. K. Salisbury, "The phantom haptic interface: A device for probing virtual objects", In Proceedings of the ASME winter annual meeting, symposium on haptic interfaces for virtual environment and Teleoperator systems, vol. 55, pp.295-300, 1994.
- [23] M. Sato, "A String-based Haptic Interface -SPIDAR-", ISUVR2006, pp.1-5, 2006.
- [24] CyberGrasp, [Online]. Available: <http://www.cyberglovesystems.com/cybergrasp/>.
- [25] Exos, [Online]. Available: <https://exiii.jp/>.
- [26] X. Gu, Y. Zhang, W. Sun, Y. Bian, D. Zhou, P.O. Kristensson, "Dexmo: An Inexpensive and Lightweight Mechanical Exoskeleton for Motion Capture and Force Feedback in VR", In Proceedings of the 2016 CHI Conference on Human Factors in Computing Systems (CHI'16). 2016, pp.1991-1995.
- [27] Nakagaki, L. Vink, J. Counts, D. Windham, D. Leithinger, S. Follmer, H. Ishii, "Materiable: Rendering Dynamic Material Properties in Response to Direct Physical Touch with Shape Changing Interfaces", In Proceedings of the 34th Annual ACM Conference on Human Factors in Computing Systems (CHI '16), pp.2764-2772, 2016.
- [28] M. G. Larson, F. Bengzon, "The Finite Element Method: Theory, Implementation, and Practice", Springer, 2010.
- [29] W. M. Bergmann Tiest and A. M. L. Kappers, "Kinaesthetic and cutaneous contributions to the perception of compressibility," Proceedings of the EuroHaptics 2008, pp. 255-264, 2008.
- [30] K. Fujita and H. Omori, "A new softness display interface by dynamic fingertip contact area control," Proc. 5th World Multiconference on Systemics, Cybernetics and Informatics, 2001, pp.496-504.
- [31] Lederman, S. J., and Klatzky, R. L., "Hand movements: A window into haptic object recognition", Cognitive Psychology, 19, pp.342-368, (1987).
- [32] T. Handa, T. Sakai, and H. Shinoda, "Evaluation of size and shape perception in multi-finger haptic system", In Proc. IEEE World Haptic Conference (WHC'11), pp.523-528, 2011.
- [33] T. Handa, S. Sakai, T. Shimizu, and H. Shinoda, "Recognition of three-dimensional geometry using multipoint force feedback on a fingertip", IEICE Technical Report, HIP, Vol. 112, No. 483, pp. 13-16, 2012.
- [34] Phantom Premium, [Online]. Available: <https://www.3dsystems.com/haptics-devices/3d-systems-phantom-premium/>.
- [35] T. Handa, K. Murase, M. Azuma, T. Shimizu, S. Kondo, and H. Shinoda, "A haptic three-dimensional shape display with three fingers grasping. 24TH IEEE Virtual Reality (IEEE VR2017), pp. 325-326, 2017.
- [36] M. Hirose, K. Hirota, T. Ogi, H. Yano, N. Takehi, M. Saito and M. Nakashige, "HapticGEAR: the Development of a Wearable Force Display System for Immersive Projection Displays," Proc. IEEE Virtual Reality 2001 Conference, pp.123-129, 2001.
- [37] T. Handa, M. Azuma, T. Shimizu and S. Kondo: "GraspForm: Shape and Hardness Rendering on Handheld Device Toward Universal Interface for 3D Haptic TV," Adjunct Proc. ACM UIST '17 (2017)
- [38] T. Handa, "Development of a Haptic Device that Presents Information on Three-dimensional Shape and Hardness of a Virtual Object by Grasping and Moving", ITE Journal, Vol. 73, No.1, pp.161.166, 2019.
- [39] H. Benko, C. Holz, M. Sinclair, E. Ofek, "NormalTouch and TextureTouch: High-fidelity 3D Haptic Shape Rendering on Handheld Virtual Reality Controllers", Proc. of ACM UIST '16, 2016.
- [40] S. Choi, K. J. Kuchenbecker, "Vibrotactile display: Perception technology and applications", Proc. IEEE, vol. PP, no. 99, pp. 1-12, 2012.

- [41] T. Handa, M. Azuma, T. Shimizu, and S. Kondo, "A Ball-type Haptic Interface to Enjoy Sports Games", AsiaHaptics2018, D1A16, 2018.
- [42] K in VR: <http://www.ntt.co.jp/activity/jp/innovation/> last accessed 2019/4/26.
- [43] Mizushina, Y., Fujiwara, W., Sudou, T., Fernando, C. L., Minamizawa, K., and Tachi, S.: Interactive instant replay: sharing sports experience using 360-degrees spherical images and haptic sensation based on the coupled body motion. Proceedings of the 6th Augmented Human International Conference, pp. 227-228 (2015).
- [44] L. A. Jones, M. Nakamura, B. Lockyer, "Development of a tactile vest", Haptic Interfaces for Virtual Environment and Teleoperator Systems, pp. 82-89, 2004.
- [45] A. Cosgun, E. A. Sisbot, H. I. Christensen, "Evaluation of rotational and directional vibration patterns on a tactile belt for guiding visually impaired people", Haptics Symposium (HAPTICS). IEEE, 2014.
- [46] S. Paneels, M. Anastassova, S. Strachan, S. Van, S. Sivacoumarane, C. Bolzmacher, "What's around me? Multi-actuator haptic feedback on the wrist", Proc. World Haptics Conf. (WHC), pp. 407-412, Apr. 2013.
- [47] S. Kim, B. Son, Y. Lee, H. Choi, W. Lee, and J. Park, "A Two-DOF Impact Actuator for Haptic Interaction", AsiaHaptics2018, D1A12, 2018.
- [48] T. Amemiya, H. Sugiyama, "Navigation in eight cardinal directions with pseudo-attraction force for the visually impaired", In Systems Man and Cybernetics 2009. SMC 2009. IEEE International Conference on, pp. 27-32, 2009.
- [49] M. Antolini, M. Bordegoni, U. Cugini, "A haptic direction indicator using the gyro effect", Proc. IEEE World Haptics Conference, pp. 251-256, 2011.
- [50] Guinan, A.L.; Koslover, R.L.; Caswell, N.A.; Provancher W.R.: "Bimanual skin stretch feedback embedded within a game controller," 2012 Haptics Symposium, Vancouver, B.C., Canada, March 4-7, 2012, pp. 255-260.
- [51] M. Azuma, T. Handa, T. Shimizu, S. Kondo, "Development of Vibration Cube to Convey Information by Haptic Stimuli," in 25th International Display Workshop, pp. 128-130, ITE, Sendai (2017).
- [52] Y. Tanaka, S. Matsuoka, W.M.B. Tiest, A.M.L. Kappers, K. Minamizawa and A. Sano, "Frequency-specific masking effect by vibrotactile stimulation to the forearm," in Eurohaptics'16, 2016.
- [53] V. Yem, H. Kajimoto, "Masking of Electrical Vibration Sensation Using Mechanical Vibration for Presentation of Pressure Sensation." IEEE World Haptics Conference 2017, June 6-9, 2017.
- [54] Brozzoli, C., Gentile, G. and Ehrsson, H.H., "That's near my hand! Parietal and premotor coding of hand-centered space contributes to localization and self-attribution of the hand. Journal of Neuroscience, 32 (42), 14573-14582. 2012.
- [55] K. Watanabe, F. Higuchi, M. Inami, and T. Igarashi, "CursorCamouflage: Multiple Dummy Cursors as a Defense Against Shoulder Surfing," in SIGGRAPH Asia 2012 Emerging Technologies, ser. SA, 2012, pp. 61-62, 2012.
- [56] H. Saito, and K. Fukuchi, "A Study of the Process of Self-Attribution in Active Rotation Manipulation," Transactions of the Virtual Reality Society of Japan (TVRSJ), Vol. 22, No. 1, pp.81-90, 2017.
- [57] Argelaguet, F., Trico, M., Hoyet, L. and Lecuyer, A., The Role of Interaction in Virtual Embodiment. Effects of the Virtual Hand Representation; In Proc. of IEEE VR 2016, pp.3-10, 2016.
- [58] NHK STRL, OPEN HOUSE 2014, [Online].
Available: https://www.nhk.or.jp/strl/open2014/tenji/tenji15/index_e.html
- [59] S. O'Modhrain, I. Oakley, "Touch TV: Adding feeling to broadcast media", Proc. Eur. Conf. Interactive Television: From Viewers to Actors, pp. 41-47, 2003.
- [60] S. ur Rehman, Jiong Sun, Li Liu, Haibo Li, "Turn Your Mobile Into the Ball: Rendering Live Football Game Using Vibration", IEEE Transactions on Multimedia, v.10 n.6, p.1022-1033, October 2008.

- [61]Miyashita, L., Zou, Y., and Ishikawa, M.: VibroTracker: A Vibrotactile Sensor Tracking Objects, SIGGRAPH 2013, Emerging Technologies, Anaheim, California, USA, 21-25 (2013).
- [62]Okubo, H., Takahashi, M., Kano, M., Ikeya, K., Mishina, T.: Prototyping of Live Sports Graphics System Equipped with Object Tracking Function - Real-time 3D Ball Tracking Utilizing Multiple PTZ Cameras -, ITE Technical Report, Vol. 41, No. 26, ME2017-85, pp. 9-12 (2017).
- [63]Kentaro Yoshida, Yuuki Horiuchi, Tomohiro Ichiyama, Seki Inoue, Yasutoshi Makino, and Hiroyuki Shinoda: Estimation of Racket Grip Vibration from Tennis Video Using Neural Network, IEEE Haptics Symposium 2018, WiP Poster B5 (Work-in-Progress Papers), 25-28 March, San Francisco, California, USA, 2018.
- [64]T. Handa, M. Azuma, T. Shimizu, and S. Kondo, "A Ball-type Haptic Interface to Enjoy Sports Games," AsiaHaptics2018, D1A16, 2018.
- [65]International Olympic Committee: Olympic Data Feed, [Online].
Available: <http://odf.olympictech.org/>.
- [66]NHK STRL, OPEN HOUSE 2019, [Online].
Available: https://www.nhk.or.jp/strl/open2019/tenji/19_e.html

Publications

Journal papers

1. T. Handa, "Development of a Haptic Device that Presents Information on Three-dimensional Shape and Hardness of a Virtual Object by Grasping and Moving," ITE Journal, Vol. 73, No.1, pp.161-166, 2019. (in Japanese)

Refereed conference papers

1. T. Handa, M. Azuma, T. Shimizu, S. Kondo, M. Fujiwara, Y. Makino, and H. Shinoda, "Ball-type Haptic Interface to Present Impact Points with Vibrations for Televised Ball-based Sporting Event," In 2019 IEEE World Haptics Conference (WHC), pp. 85-90, IEEE, 2019.
2. T. Handa, M. Azuma, T. Shimizu, and S. Kondo, "A Ball-type Haptic Interface to Enjoy Sports Games," AsiaHaptics2018, D1A16, 2018.
3. T. Handa, M. Azuma, T. Shimizu and S. Kondo, "GraspForm: Shape and Hardness Rendering on Handheld Device Toward Universal Interface for 3D Haptic TV," Adjunct Proc. ACM UIST '17, 2017.
4. T. Handa, K. Murase, M. Azuma, T. Shimizu, S. Kondo, and H. Shinoda, "A haptic three-dimensional shape display with three fingers grasping," 24TH IEEE Virtual Reality (IEEE VR2017), pp. 325-326, 2017.
5. T. Handa, T. Sakai, and H. Shinoda, "Evaluation of size and shape perception in multi-finger haptic system", In 2011 IEEE World Haptic Conference (WHC), pp.523-528, 2011.

Domestic presentations

1. 半田拓也, 東真希子, 清水俊宏, 近藤悟, "スポーツ中継を能動的に楽しむためのボール型ハプティックインターフェースの開発,"第 23 回日本バーチャルリアリティ学会大会論文,21A-5, 2018.
2. 半田拓也, 東真希子, 清水俊宏, 近藤悟, "仮想物体を空間に提示する触覚インターフェースにおける空間位置検出方式の評価,"電気学会研究会資料, 知覚情, PI-18-31, pp.35-38, 2018.
3. 半田拓也, 東真希子, 清水俊宏, 近藤悟, "空中ハプティックインターフェースにおける空間位置検出方式の評価,"映像情報メディア学会冬季大会講演予稿集, 21C-3, 2017.
4. 半田拓也, 東真希子, 清水俊宏, 近藤悟, "物体の形状と硬さを空間に提示するハプティックデバイスの開発," 第 22 回日本バーチャルリアリティ学会大会論文集, 3D1-02, 2017.
5. 半田拓也, 藤原正浩, 坂井忠裕, 清水俊宏, 牧野泰才, 篠田裕之, "物体の形状と硬さ分布の触覚伝達システムの開発," 映像情報メディア学会年次大会講演予稿集, 22-3, 2014.

6. 半田拓也, 坂井忠裕, 清水俊宏, 篠田裕之, “指先への多点分布力覚提示による立体稜線の触察動作の評価,” 電子情報通信学会技術研究報告, 福祉情報工学, vol.113, no.347, WIT2013-61, pp.5-9, 2013.

Demonstrations

1. World Congress of Science & Factual Producers 2019, "Haptic Interfaces for Physically Experiencing Sports Games, " December 2019.
2. T. Handa, M. Azuma, T. Shimizu, S. Kondo, M. Fujiwara, Y. Makino, and H. Shinoda, "Ball-type Haptic Display to Present Impact Points with Vibrations for Televised Ball-based Sporting Event, " 2019 IEEE World Haptics Conference (WHC). July 2019.
3. T. Handa, M. Azuma, T. Shimizu, and S. Kondo, "A Ball-type Haptic Interface to Enjoy Sports Games," AsiaHaptics2018, D1A16, 2018.
4. NHK STRL OPEN HOUSE 2019, “Haptic Interfaces for Physically Experiencing Sports Games – Creating a universal service for sports programs –, " May 2019.
[Online]. Available: https://www.nhk.or.jp/strl/open2019/tenji/19_e.html
5. NHK STRL OPEN HOUSE 2016, "Haptic Presentation Technology for Conveying 3D Shapes of Object – Making Tactile TV a reality, " May 2016.
[Online]. Available: https://www.nhk.or.jp/strl/open2016/tenji/c5_e.html
6. NHK STRL OPEN HOUSE 2015, "Let’s see if you can touch it!, " May 2015.
[Online]. Available: https://www.nhk.or.jp/strl/open2015/en/tenji_t2.html
7. NHK STRL OPEN HOUSE 2014, "Tactile Presentation Technology to convey 2D & 3D information – Towards the introduction of Tactile TV, " May 2014.
[Online]. Available: https://www.nhk.or.jp/strl/open2014/tenji/tenji15/index_e.html

Appendix A

Summary of experimental results using a multi-finger haptic system

This document provides summary of experimental results using a multi-finger haptic system. The multi-finger haptic system is an experimental environment to evaluate the haptic perception of size and shape of a virtual object. The experiment below was conducted as a pilot test to propose the multi-point force feedback method described in Chapter II.

A.1. Multi-finger haptic system

The system architecture and a screenshot of the control software are shown in Fig. A.1, where the user is grasping a virtual object with three fingers (thumb, index finger, and middle finger) and the palm of the right hand. The positional relationships between the PHANToMs [34] and the virtual objects in the multi-finger haptic system are shown in Fig. A.2. The four PHANToMs were arranged as shown in Fig. A.2 and were calibrated to ensure that the coordinate systems of the PHANToMs were aligned. The virtual object was placed so that its upper edge was 22 cm above the desktop, and each participant sat in a chair and performed the haptic exploration with elbows on the desk.

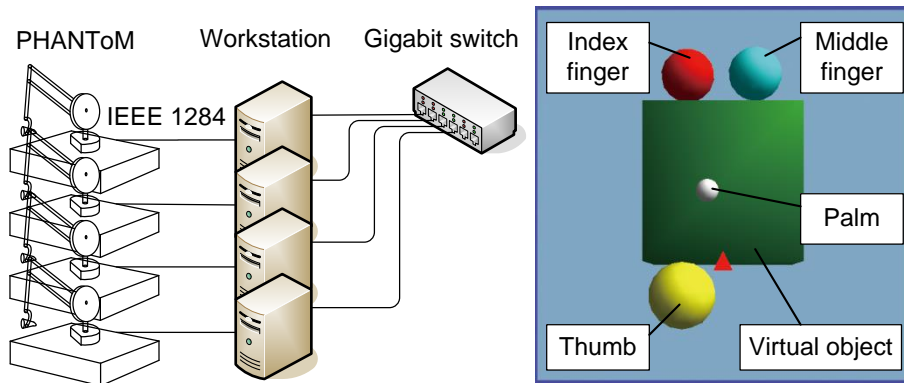


Fig. A.1. System architecture and a screen shot of control software.

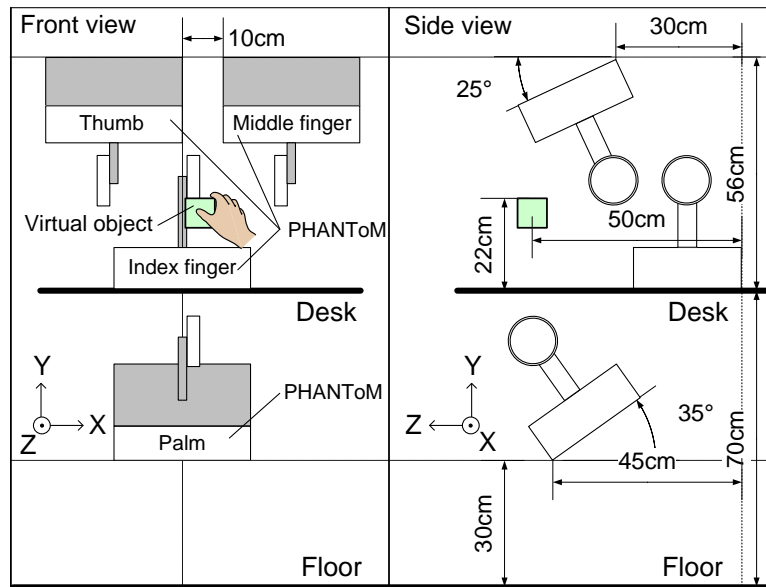


Fig. A.2. Arrangement of PHANToMs and presentation position of virtual object.

The size relationships between the finger and palm attachments and the virtual object are shown in Fig. A.3, when the virtual object is a cube. We configured the thimble-plus-gimbals and palm attachments we used in the PHANToM mount as shown in Fig. A.3. Fig. A.3 shows a situation as seen from the upper surface and the right-side surface when the user is grasping the cube with the right hand, with the front surface grasped by the thumb and the far surface grasped by the index and middle fingers. The attachment for the palm is provided with a 10-mm diameter steel sphere at the same position as the center of the gimbal mechanism, linked by magnetic force to a disk of a diameter of 20 mm and a thickness of 5 mm. Once the thimbles had been placed on the fingers they were covered with a thin cloth glove and the palm attachment was mounted by a strap on the palm near the base of the index and middle fingers.

Before the experiments, we used a virtual cube of the same size presented over the same position as a real cube and adjusted the sizes of the virtual pointers so that the positions of the inner side surfaces of the thimbles felt like they matched the surfaces of the object exactly. Therefore, the physical size of each virtual object means the distance between the inner side surfaces of the thimbles. With the palm attachment too, we adjusted the surface that fits on the palm so that it matched the surface of the object. After adjusting the size of the visual pointers, we presented a cube having edges of 60 mm, and measured the distances between the inner sides of the thimbles in real space over each of the X, Y, and Z surfaces, using vernier calipers. By repeating this measurement and calibration process, we confirmed that the ultimate presentation measurement error was within 1 mm for one PHANToM and within 2 mm for each combination of two PHANToMs.

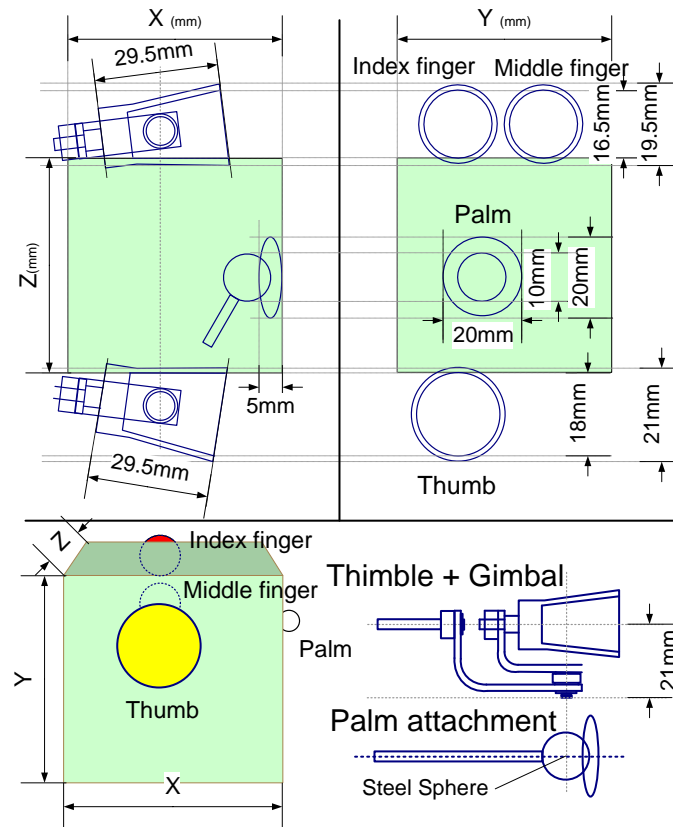


Fig. A.3. Size relationship between virtual object and thimbles.

A.2. Shape perception experiment

A.2.1. Method

We implemented a function that generates an attractive force corresponding to distance, between the object surface and the virtual pointers. We adjusted the magnitude of the attractive force to a level at which the participants were not aware of it during preliminary experiments, and confirmed that the force with which a virtual pointer separates from an object surface in the normal direction after being in contact with that surface has a measured value approximately 0.8 N.

From the shapes that the participants depicted orally and in drawings, we evaluated the extent of perception of shape characteristics due to the presence or absence of the attractive force and the reaction force to the palm. We used four shapes and two dummies having characteristics such as tapers, cones, and curves, as shown in Fig. A.4. We presented these stimuli at random under the five conditions shown in Fig. A.4. During the experiments, we presented the presence or absence of the attractive force and the reaction force to the palm by software switching, with the apparatus always being mounted on the three fingers and a palm of the right hand of the participant. The participants did not know there were six types of stimuli, but were instructed that there were various different sizes and shapes, including subtle differences.

Each participant was instructed to touch the virtual object with the right hand for one minute, and afterwards to draw the shape that he or she imagined. Features that could not be drawn were added verbally. There were ten participants, including two visually impaired people. The participants gave their written consent to the experimental protocol that had been approved by the institutional review board at NHK STRL. Fig. A.5 shows an experimental environment.

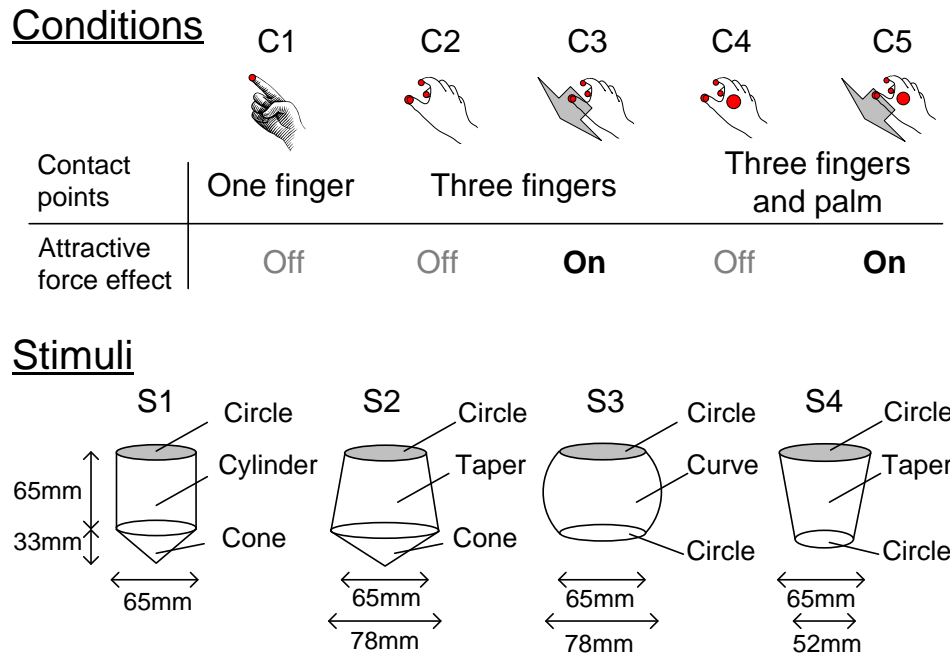


Fig. A.4. Experimental conditions and stimuli configurations.



Fig. A.5. Experimental environment.

A.2.2. Results

The results showed a tendency towards differences between visually-impaired people using their dominant hands, sighted people using their dominant hands, and sighted people using their non-dominant hands. The sketch results for each combination of stimulus shape and condition of participant G (sighted person, using dominant hand), and participant J (sighted person, using non-dominant hand) are shown in Figs. A.6 and A.7, by way of example.

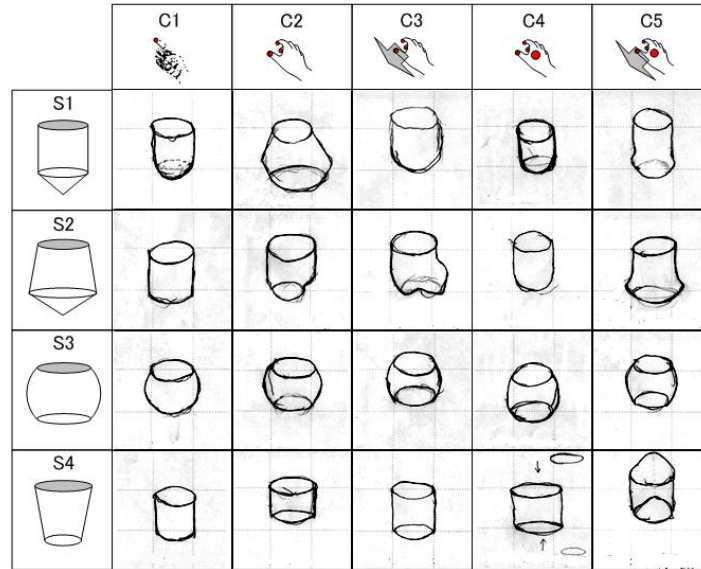


Fig. A.6. Sketch results of participant G (sighted person, using dominant hand, 40's male).

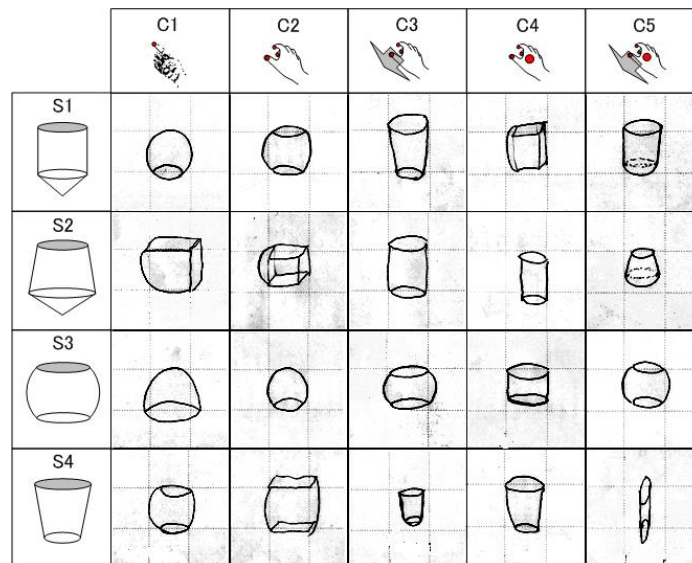


Fig. A.7. Sketch results of a participant (sighted person, using non-dominant hand, 30's male).

A.2.3. Discussion

From observation of the experimental situation, we saw that the haptic exploration of visually-impaired people had very little deviation at the corners of the objects. One reason is thought to be the way in which they are more used to haptic exploration by feeling around unknown shapes, in comparison with sighted people. Tapers and curves have been difficult to perceive with a point-contact type of haptic device, but the results of these experiments are considered to demonstrate that it would be possible to comprehend the features of tapers and curves, if haptic exploration can be done with no deviation from the object surfaces, even with a point-contact type of haptic device.

We see from Figs. A.6 and A.7 that sighted people using their non-dominant hands mostly found it difficult to perceive shapes under conditions with no attractive forces. In these experiments, the perception of object shapes was improved using attractive forces, particularly with sighted people using their non-dominant hands (such as at S2-C5, S3-C3, and S3-C5 in Fig. A.7). However, even sighted people using their dominant hands were unable to completely comprehend the shape characteristics of the stimuli by attractive force alone.

S2-C3 and S2-C5 in Fig. A.6 are examples of shape misperceptions due to attractive force. It is highly possible that the degree to which the attractive forces facilitate the haptic exploration of the edges of an object imparts the feeling that sizes are perceived to be larger when perceiving features with a single finger. It is thought that the sensory illusion of size by a single finger has a large effect when using one finger to perceive features while grasping the object. Conversely, it is thought that it would be possible to enable improved comprehension of small features that are difficult to perceive, by controlling the magnitude of the attractive forces.

S4-C4 and C5 in Fig. A.6 are examples of shape misperception due to the force feedback on the palm. We find that there is a feeling of distortion, particularly with cylindrical shapes that are oval or triangular. Our hypothesis is that users feel that the object does not exist at locations where the object slips away, which increases with the number of places at which force feedback is applied, such as on the number of fingers and the palm. In the future, we intend to verify this hypothesis while improving the range of reaction force and the degrees of freedom of the palm.

A.3. Conclusion

We have prototyped a multi-finger haptic system with the objective of clarifying the necessary conditions for a presentation method that can use haptic means to transmit the size and shape of a three-dimensional object more accurately and evaluated the perception of shape. In the experiment, we evaluated the influence of the presence or absence of the force feedback on the palm and an attractive force from the virtual object on the perception of shape. The results suggested that this attractive force reduced the deviation of the fingers at the edges of the objects. This is mainly effective in perceiving tapering and curvature. However, in some cases, features were emphasized excessively, and misperception could occur. On the other hand, the effect of the force feedback on the palm remained unclear. In the future, we intend to clarify these perception phenomena and further investigate the necessary conditions for presentation devices.

Appendix B

User documentation of GraspForm system

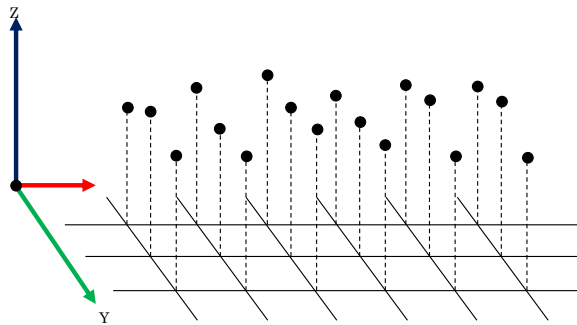
This document provides summary of user documentation for the current version of the GraspForm system described in Chapter III.

B.1. Basic processes and algorithms

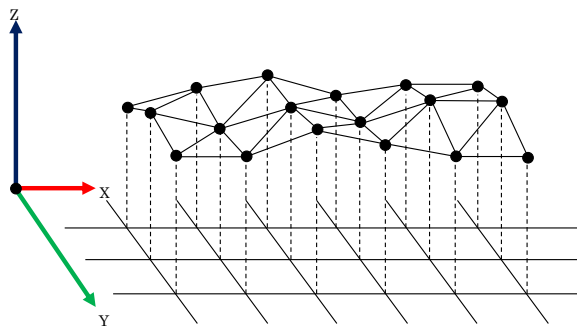
B.1.1. Polygon data construction from point cloud

GraspForm system using following three steps algorithm for constructing polygon data from point cloud data provided by three-dimensional digitizer in CSV format.

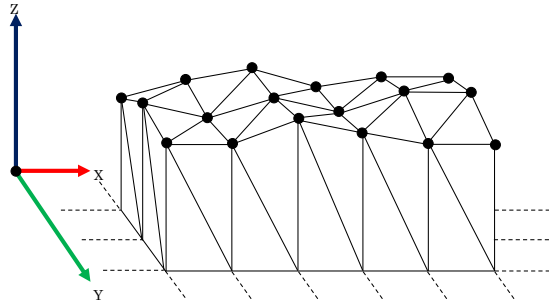
- (1) Load point cloud data from CSV file.



- (2) Construct the top surface polygon data by concluding each vertex of the point cloud to triangle.



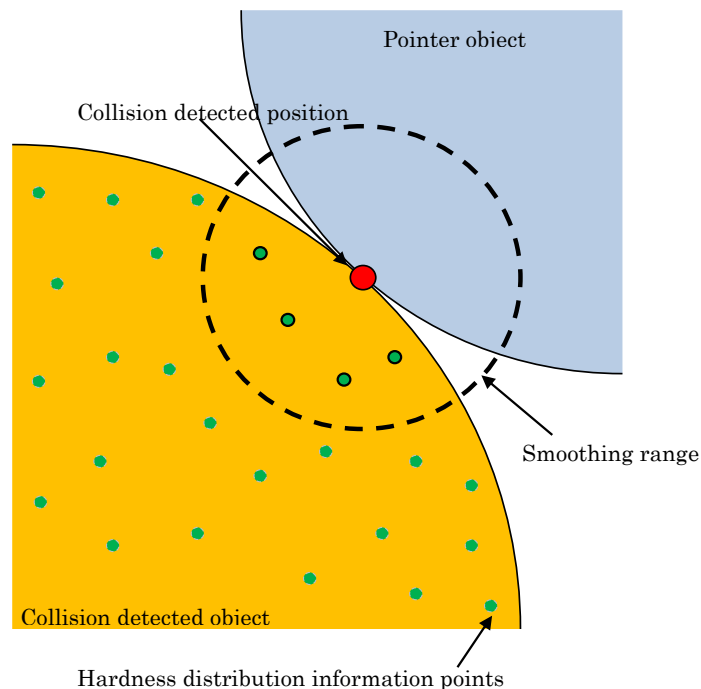
(3) Construct side and bottom surfaces polygon data.



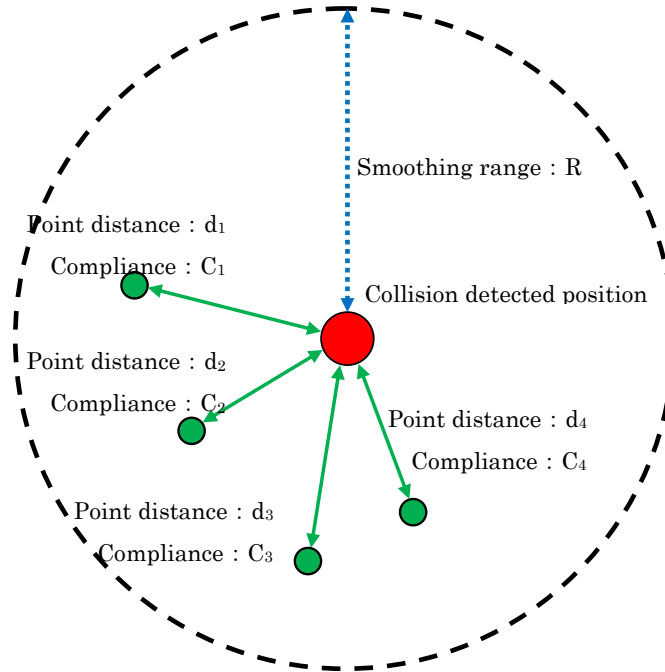
B.1.2. Calculation of hardness in the collision point

Perform collision detection. Gather the hardness distributions points which exist within the smoothing range from collision detection point if collision detected with an object having hardness distribution information. Use the nearest exist hardness point value as the compliance value if hardness distribution points do not present within smoothing range. Interpolate the compliance value as given in smoothing process if many hardness distribution points exist within smoothing range. Smoothing process for hardness calculation at the collision point as follows.

(1) Suppose collision is detected between a pointer object and the scene object as given in the following figure.



- (2) Gather hardness distribution data points with in the smoothing range from collision detected position.



- (3) Interpolate the hardness value C_{smooth} using point distance d_i and compliance C_i of point group gathered in the above process (W_i : distance weight, CW_i : Weighted compliance value).

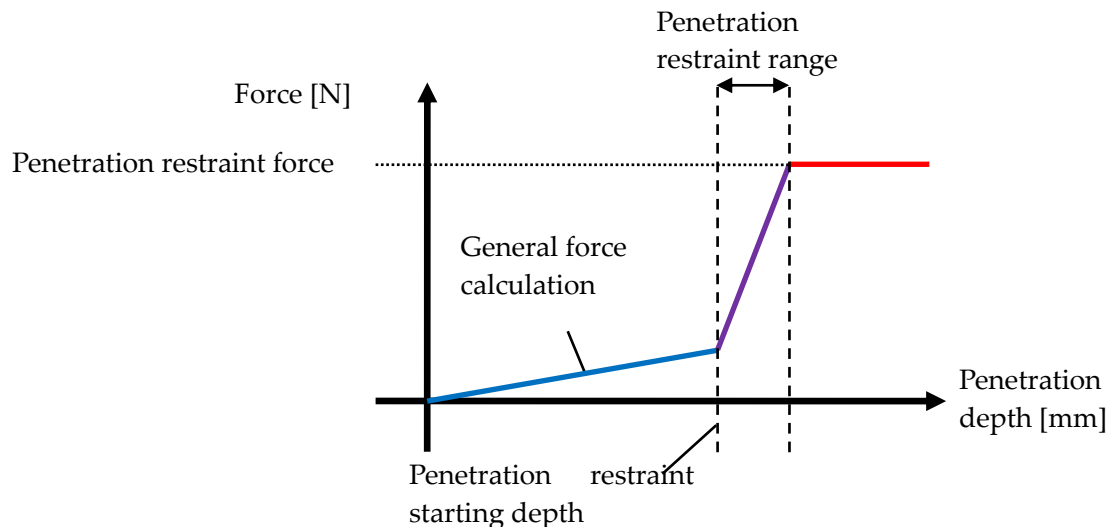
$$W_i = \frac{(R - d_i)}{R}$$

$$CW_i = C_i W_i$$

$$C_{smooth} = \frac{\sum_i^n CW_i}{\sum_i^n W_i}$$

B.1.3. Penetration restrain force generation function

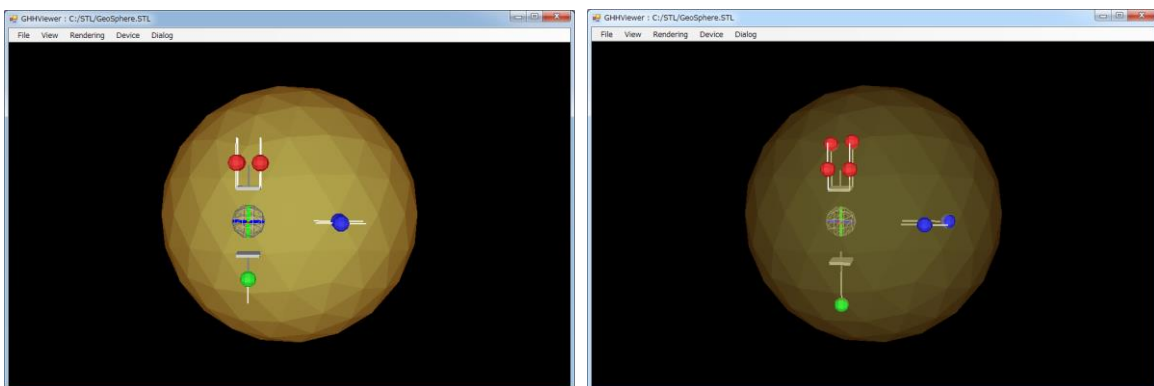
When the hardness parameter is too small, the power generated to force feedback device will be very low even if the penetrated depth is too large which may feel as slipping through. Therefore, this penetration restrain force generation function is to avoid the extreme penetration by generating a large force when penetration depth is increased regardless of hardness parameter as described in the following graph.



B.2. User's manual of GraspForm control software

B.2.1. Virtual scene viewer

In the scene graph, the position, posture, structure and state of the stimulation points of the GraspForm device in addition to the virtual object. The following right figure shows a state in which the displacement calculated from the interference between the virtual object and the stimulation point.

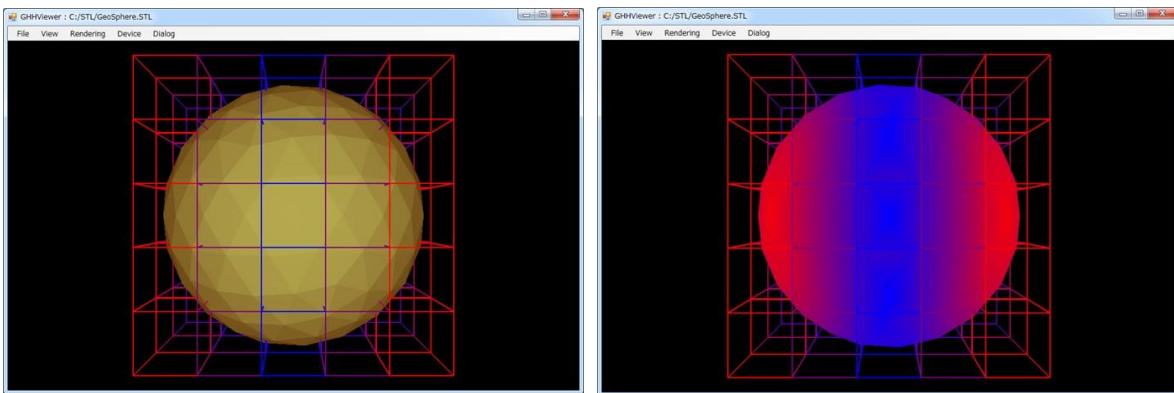


B.2.2. Hardness distribution data

Hardness distribution data express the hardness distribution at each position of the virtual object. Hardness can be set for each voxel containing the virtual object in the local coordinate system. The file format of the hardness distribution data is described below.

- File format: ASCII
- First line: parameters x, y, z of a matrix.
- Second and subsequent lines: compliance value of each voxels.

It is desirable that the hardness data of each surface position in the virtual object change smoothly, however, the input hardness distribution data is represented as discrete data. Therefore, this software calculates the interpolated value by three-dimensional linear interpolation using the hardness data of adjacent voxels. The following figure shows the visualization of hardness distribution data. Blue voxels indicate soft and red voxels indicate hard.

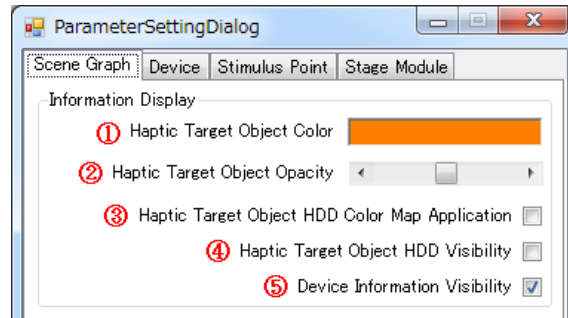


B.2.3. Parameter setting dialog

The dialog for setting the parameters of the object and device for simulation is described below. The parameters that can be set for each tab, such as scene graph, device, stimulus point, and stage module are categorized in the dialog.

(1) Scene Graph tab

- ① Haptic Target Object Color box
Color of the virtual object can be set. The color setting dialog is displayed by clicking the mouse.
- ② Haptic Target Object Opacity slider
Opacity of the virtual object can be set.
- ③ Haptic Target Object HDD (Hard Distribution Data) Color Map Application check box
Color map corresponding to the value of the HDD for the virtual object can be set.
- ④ Haptic Target Object HDD Visibility check box
Visibility of the HDD of the virtual object can be set.
- ⑤ Device Information Visibility check box
Visibility of GraspForm device information such as stimulation points, movable range of the stage module.

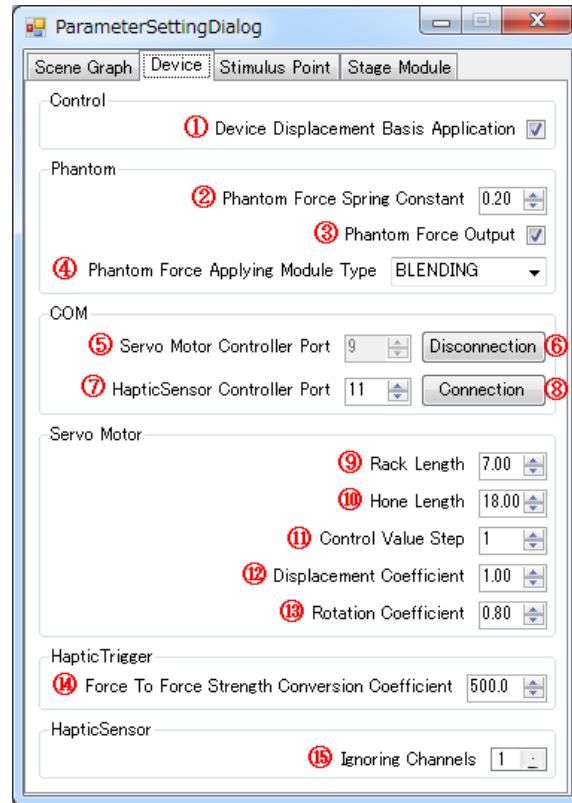


(2) Device tab

- ① Device Displacement Basis Application check box
Whether to apply the device displacement reference can be set.
- ② Phantom Force Spring Constant spin
Spring constant for Phantom force calculation can be set.
- ③ Phantom Force Output check box
Enable/disable force output of Phantom.
- ④ Phantom Force Applying Module Type drop-down list box
Select the type of module to which the Phantom force applies.
- ⑤ Servo Motor Controller Port spin
COM port number for connecting the servo motor controller can be specified.
- ⑥ Servo Motor Controller connect/disconnect button
Connection and disconnection with the servo motor controller can be set. The button changes depending on the connection status.
- ⑦ Haptic Sensor Controller Port spin
COM port number for connecting to the sensor controller can be specified.
- ⑧ Haptic Sensor Controller connect/disconnect button
Connection and disconnection with the sensor controller can be set. The button changes depending on the connection status.
- ⑨ Rack Length spin
Rack length of the servo motor corresponding to the stimulation point can be set.
- ⑩ Hone Length spin
Horn length of the servo motor corresponding to the base module can be set.
- ⑪ Control Value Step spin
Step of the set value for the servo motor can be set.
- ⑫ Displacement Coefficient spin
Coefficient to be multiplied by the displacement of the servo motor can be set.
- ⑬ Rotation Coefficient spin
Coefficient to be multiplied by the rotation of the servo motor corresponding to the base module can be set.
- ⑭ Force to Force Strength Conversion Coefficient spin
Coefficient for converting the force value of Phantom to the force intensity value for HapticTrigger can be set.

⑮ Ignoring Channels spin

You can check the channel number of the sensor for which data acquisition is disabled.



(3) Stimulus Point tab

① Operation Target Stimulus Point Number spin

Select the stimulus point number to set the parameter below. The selected stimulus point flashes in the scene graph with the current setting color and its complementary color.

② Stimulus Point Device Type text box

The device type corresponding to the selected stimulus point is displayed.

③ Position X/Y/Z spin

Location of the selected stimulus point can be set.

④ Displacement Direction X/Y/Z spin

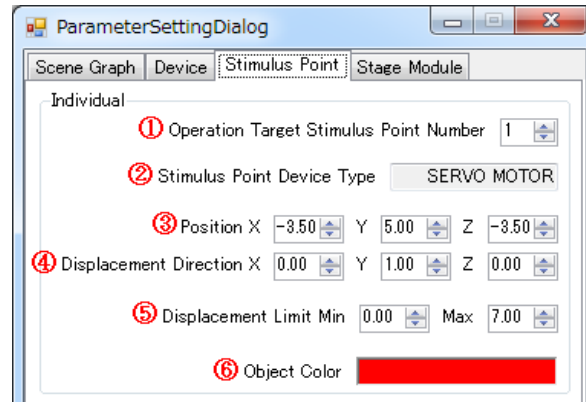
Displacement direction of the selected stimulus point can be set.

⑤ Displacement Limit Min/Max spin

Minimum/Maximum displacement value of the selected stimulus point can be set.

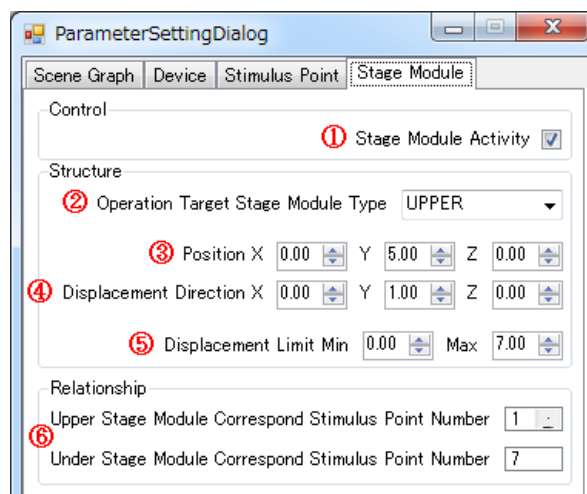
⑥ Object Color box

Color of the currently selected stimulus point can be set. The color setting dialog is displayed by clicking the mouse.



(4) Stage Module tab

- ① Stage Module Activity check box
Whether to enable the operation of the stage module can be selected.
- ② Operation Target Stage Module drop-down list box
In the dialog, you can select the stimulus point group of the parameter to be set. Items that be selected are UPPER and UNDER.
- ③ Position X/Y/Z spin
Position of the selected stage module can be set.
- ④ Displacement Direction X/Y/Z spin
Orientation of the selected stage module can be set.
- ⑤ Displacement Limit Min/Max spin
Minimum/Maximum displacement value of the selected stage module can be set.
- ⑥ Upper/Under Stage Module Correspond Stimulus Point Number spin
Stimulus point numbers corresponding to the upper and under stage modules are listed.



B.2.4. Sensor data displaying dialog

The dialog for displaying the sensor data of the GraspForm device is described below. This dialog shows the pressure and temperature data obtained from haptic sensors.

- ① Haptic Sensor channel number
Displays the sensor channel number.
- ② Force X/Y/Z value
Displays the pressure vector obtained from the sensor. The unit is [N].
- ③ Temperature value
Displays the row data of the temperature value obtained from the sensor. The unit is [V].

The screenshot shows a window titled "SensorDataDisplayDialog" with a table of sensor data. The table has 8 rows, one for each haptic sensor. Each row contains the sensor name, force X, Y, and Z values, and the temperature value. Red circles with numbers 1, 2, and 3 are placed above the first, second, and third columns respectively, corresponding to the legend items.

Haptic Sensor	Force X	Y	Z	Temperature
Haptic Sensor 1	-	-	-	-
Haptic Sensor 2	-0.005	0.001	0.002	1.652
Haptic Sensor 3	-0.018	-0.004	-0.004	1.648
Haptic Sensor 4	-0.027	0.000	0.021	1.645
Haptic Sensor 5	-	-	-	-
Haptic Sensor 6	0.004	0.001	-0.003	1.652
Haptic Sensor 7	0.034	0.013	-0.009	1.639
Haptic Sensor 8	-0.005	0.005	0.003	1.652

